ROLE OF ADENOSINE A1 RECEPTORS IN NATIVE CORONARY ATHEROSCLEROSIS, IN-STENT STENOSIS, AND CORONARY BLOOD FLOW REGULATION IN METABOLIC SYNDROME AND EXERCISE

Xin Long

Submitted to the faculty of the University Graduate School
in partial fulfillment of the requirements
for the degree
Doctor of Philosophy
in the Department of Cellular and Integrative Physiology,
Indiana University

February 2010

Accepted by the Faculty of Indiana University, in partial fulfillment of the requirements for the degree of Doctor of Philosophy.

_____

Michael S. Sturek, PhD, Chair

_____

Robert V. Considine, PhD

Doctoral Committee

_____

Susan J. Gunst, PhD

December 10, 2009

_____

B. Paul Herring, PhD

_____

Johnathan D. Tune, PhD

DEDICATION

To my super supportive parents, my insightful big brother, and my dearest husband Jun.

ACKNOWLEDGEMENTS

To my advisor, Dr. Michael Sturek - Thank you for encouraging me to always look forward in the days of rain and snow. Thanks for your insightful guidance and great patience all the way along. I am deeply inspired by your enthusiasm towards work and research. You are a wonderful role model for me.

To my committee members, Dr. Robert V. Considine, Dr. Susan J. Gunst, Dr. B. Paul Herring, and Dr. Johnathan D. Tune - Your guidance has been invaluable. Thank you for your patient helps in the past 4 years.

To my warm-hearted friends, Dr. Liguo Zhang, Zachary P. Neeb, James W. Wenzel, Dr. Rui Duan, Dr. Rong Zhao, Hong Fang, Sixin Jiang, Jie Liang, Dr. Min Zhang, Emily Blue, Ryan Widau - Thank you for always being there in support of me and helping me. To all my lab coworkers, Dr. Pamela G. Lloyd, Zachary P. Neeb, James W. Wenzel, James P. Byrd, Dr. Mouhamad Alloosh, Kimberly Pohle, Dr. Ian Bratz, Dr. Eric A. Mokelke and etc. - We are a big great team. Thanks for your help all the time. I could not have done my work without you all.

To my parents, my brother, and my husband - Thank you for your selfless love and endless support. Thanks for always having faith in me. To all the people who helped me and encouraged me - Thank you all for being part of my life.

ABSTRACT

Xin Long

ROLE OF ADENOSINE A1 RECEPTORS IN NATIVE CORONARY ATHEROSCLEROSIS, IN-STENT STENOSIS, AND CORONARY BLOOD FLOW REGULATION IN METABOLIC SYNDROME AND EXERCISE

Adenosine is widely thought to elicit coronary vasodilation and attenuate smooth muscle cell (SMC) proliferation, thereby providing cardioprotection. We cloned the porcine adenosine A1 receptor (A1R) subtype and found that it paradoxically stimulated proliferation of cultured coronary SMC by the extracellular signal-regulated protein kinases 1 and 2 (ERK1/2) signaling pathways, thus suggesting A1R dysregulation could play a role in coronary artery disease (CAD), restenosis, and regulation of coronary blood flow (CBF). We utilized the Ossabaw swine model of metabolic syndrome (MetS) to test the hypothesis that A1R activation contributes to development of CAD, in-stent stenosis, and CBF regulation. Swine were fed standard chow (Lean) or excess calorie atherogenic diet for over 20 weeks, which elicited MetS characteristics and coronary atherosclerosis compared to Lean. We observed increased A1R in native CAD in MetS, which was reversed by exercise training, and upregulation of A1R expression and A1R-ERK1/2 activation in an in vitro organ culture model of CAD. Intracoronary stent deployment followed by different durations of recovery showed A1R upregulation occurred before maximal in-stent stenosis in

vivo. More importantly, selective A1R antagonism with 8-cyclopentyl-1, 3-dipropylxanthine (DPCPX)-eluting stents decreased coronary ERK1/2 activation and reduced in-stent stenosis comparable to Taxus® (paclitaxel-eluting stents). A1R antagonism potentiated vasodilatory effects of some vasodilators other than adenosine in porcine coronary microcirculation under basal conditions. Short-term exercise training around stenting prevented stent-induced microvascular dysfunction and attenuated native atheroma in the genetically lean Yucatan swine. Conclusions: A1R upregulation and activation contributes to coronary in-stent stenosis in vivo in MetS, plays a role in the development of coronary atherosclerosis in vitro, and might involve in CBF dysregulation in dyslipidemia and stenting. Exercise training decreased A1R expression in atherosclerosis, reduced native atheroma, and prevented stent-induced microvascular dysfunction. Selective pharmacological antagonism of A1R holds promise for treatment of CAD.

Michael S. Sturek, PhD, Chair

TABLE OF CONTENTS

LIST OF TABLES

LIST OF FIGURES

LIST OF ABBREVIATIONS

ANOVA	One-way analysis of variance	IVGTT	Intravenous glucose tolerance test
APV	Average peak velocity	IVUS	Intravascular ultrasound
AR	Adenosine receptors	JNK	c-Jun-N-terminal kinase
CAD	Coronary artery disease	K_{ATP}	ATP-dependent K^+ channel
CBF	Coronary blood flow	LAD	Left anterior descending coronary artery
CCPA	2-chloro-N(6)-cyclopentyladenosine	LDL	Low density lipoprotein
CFR	Coronary flow reserve	MAP	Mean arterial pressure
CFX	Left circumflex coronary artery	MAPK	Mitogen-activated protein kinase
CSA	Cross sectional area	MetS	Metabolic syndrome (also group code)
CVR	Coronary vascular resistance	MR	Mineralocorticoid receptor
DES	Drug-eluting stent	NADPH	Nicotinamide adenine dinucleotide phosphate

DMPX	3,7-dimethyl-1-propargylxanthine	NCEP	National Cholesterol Education Program
DPCPX	8-cyclopentyl-1, 3-dipropylxanthine	NO	Nitric Oxide
EC	Endothelial cells	PCNA	Proliferating cell nuclear antigen
EDTA	Ethylenediaminetetraacetic acid	PKA	cAMP-dependent protein kinase
ERK1/2	Extracellular signal-regulated protein kinases 1 and 2	RAAS	Renin-angiotensin-aldosterone system
ET	Endothelin	RC	Right coronary artery
HDL	High-density lipoprotein	RT-PCR	Reverse transcription-polymerase chain reaction
HR	Heart rate	SBP	Systolic blood pressure
ICAM	Intercellular adhesion molecule	SMC	Smooth muscle cells
IGF	Insulin-like growth factor	TG	Triglyceride

CHAPTER 1. INTRODUCTION

1.1. Coronary anatomy and coronary artery disease

The left main, circumflex, left anterior descending, and right coronary arteries are the main epicardial coronary arteries branching from aortic ostium (Figure 1.1A). The coronary vascular wall is divided by internal and external elastic laminae into three different layers: intima, media, and adventitia (Figure 1.1B). The intima is lumenal to the internal elastic lamina and includes the inner cellular lining of the vascular wall, i.e. endothelium. Media is bounded by internal and external elastic lamina and mainly composed of smooth muscle cells (SMCs) often separated by collagen and elastin fibers in the large epicardial conduit arteries. Outside of the external elastic lamina is adventitia, comprised of connective tissue matrix, which is largely elastic fiber proteins, proteoglycans, and collagen, which is synthesized and deposited by SMCs [1].

Microvascular and macrovascular disorders are the two main categories of coronary artery disease (CAD) in our research focus.

Microvessels are usually defined as small vessels with diameter less than 100 μm [2]. Microvascular dysfunction is mediated by endothelium dependent or independent mechanisms. Endothelium-dependent dysfunction is primarily attributable to an increase in endothelin-1 (ET-1) [3], a reduction in nitric oxide (NO)

synthase [4] or responsiveness to NO [5], or a mixture of these factors. Endothelium-independent dysfunction includes impairment of smooth muscle relaxation [6].

Bradykinin (BK), a vasoactive peptide, is an endothelium-dependent vasodilator. BK interacts with BK type 2 receptors on the endothelial cell surface, increasing NO generation via endothelial NO synthase (eNOS) activation, thus mediating vasodilation [7]. The endothelium-independent coronary vasodilators include dipyridamole, papaverine, and adenosine (see section 1.5) [6]. In porcine coronary circulation and human forearm circulation, adenosine-induced vasodilation was mainly in NO-independent manner [8].

Atherosclerosis, a disease of the conduit arteries, is responsible for about 50% of all mortalities [1, 9]. Atherosclerotic lesions are initiated from fatty streaks and progress to intermediate lesions and eventually to fibrous plaques [1, 9]. Fatty streaks are mainly composed of subendothelial lipid-scavenging macrophages (foam cells) with minimal SMC infiltration. Intermediate lesions are composed primarily of SMCs and macrophages, while fibrous plaques are comprised of SMCs in dominance, macrophages, and T lymphocytes [1]. Fibrous plaques usually have a fibrous cap of collagen and elastin and often enclose a lipid-rich necrotic core [9]. A thin fibrous cap is one of the defining features of unstable plaque. Figure 1.2 and Figure 1.3 show many of these features. Figure 1.2 shows Masson's trichrome stain for collagen used to assess changes in atherosclerosis [10, 11]. Comparison between healthy, early stage, and advanced

stage atherosclerotic artery segment reveals that collagen deposition and foam cell infiltration increases as lesion progresses, lumen size decreases consequently. Stary classified atherosclerosis into eight different stages [12]. All Stary stages of atherosclerosis are displayed in the Ossabaw miniature swine model of MetS and CAD [13]. Figure 1.3A shows Picrosirius red staining as another index of collagen and elastin. This atherosclerotic lesion shows a thin fibrous cap and lipid core characteristic of unstable or vulnerable plaque [1, 14]. Intense Verhoeff-van Gieson staining (Figure 1.3B) shows extensive elastin beyond the typical single layer internal elastic lamina and many layers deep into the media layer interspersed between SMC. This is further reinforced by immunostaining for smooth muscle a actin (Figure 1.3D). The inflamed feature of the lesion is shown by extensive scavenger receptor immunostaining (Figure 1.3C), which is a marker for macrophages.

Atherosclerosis develops over decades in humans, having its origin in childhood during which the process is typically entirely benign without any symptoms [9, 15]. When the conduit coronary diameter stenosis reaches >50% (usually ~70-80%), angina pectoris can arise due to insufficient coronary oxygen supply, especially with increased oxygen demands like exercise or emotional stress [9]. Even worse, myocardial infarction could happen in case of an acute coronary artery occlusion due to thrombus formation from rupture of vulnerable plaque [9].

1.2. Treatments for coronary artery disease and restenosis – exercise, drugs, angioplasty and stents

A number of medicines can be used to help relieve angina pectoris, like nitroglycerin, beta-blockers, and calcium channel blockers [16]. However, blood flow-limiting atherosclerotic lesions cannot be treated effectively by pharmacological agents alone. First line therapy for flow-limiting coronary atherosclerotic lesions includes angioplasty and stent placement [17], as shown in Figure 1.4.

The benefits of exercise training exist in patients with coronary atherosclerosis [18-23] as well as the population undergoing percutaneous coronary revascularization [22, 24-26]. It was shown that long-term exercise training of pigs attenuated conduit artery neointimal proliferation after balloon angioplasty [27]; however, microvascular effects were not determined. Further, the effects of plasma cholesterol and exercise on in-stent stenosis, conduit atherosclerosis, and microvascular dysfunction after coronary stenting have not been studied. Those facts led to the first hypotheis in this thesis that short-term exercise training prevents micro- and macrovascular disease in porcine model of hypercholesterolemia and coronary artery disease.

1.3. Metabolic syndrome

Atherosclerosis is increased 2-4-fold in metabolic syndrome (MetS) [28-33], which complicates treatment for coronary atherosclerosis. Metabolic syndrome

(MetS) is a cluster of metabolic disturbances, and is defined by National Cholesterol Education Program (NCEP) Adult Treatment Panel-III as the concurrence of any three of the following abnormalities: central obesity, dyslipidemia, hypertension, impaired glucose tolerance, and insulin resistance [34]. Insulin resistance and dyslipidemia are considered key attributes to the pathophysiology of MetS [35].

MetS is pervasive, with approximately 44% of the U.S. population over age 50 meeting the NCEP criteria [36]. Importantly, MetS indicates increased risk of atherosclerotic cardiovascular disease as well as type 2 diabetes mellitus [28-33, 37]. Additionally, hyperinsulinemic MetS patients have increased restenosis after percutaneous coronary interventions [38-41]. Dyslipidemia is usually defined as the combination of dyslipoproteinemia and hypertriglyceridemia [42]. We found that increased FFA are not the main cause for CAD in MetS (data not shown), consistent with report that FFA are not the cause in MetS and diabetes [43]. Instead, the research done in our lab suggests LDL gram-years as a great predictor for CAD severity in MetS (data not shown). The increased risk for CAD, type 2 diabetes, and restenosis in MetS demands therapeutic attention for those at high risk. The fundamental approach includes weight reduction and exercise training; however, pharmacological approaches are highly effective and have much greater patient compliance [35]. Our preliminary data indicated that plasma aldosterone was upregulated in MetS, which put aldosterone in our research focuses.

1.4. Renin-angiotensin-aldosterone system

Activation of the renin-angiotensin-aldosterone system (RAAS) and subsequent elevations in aldosterone are often seen in MetS [44]. Both contribute to endothelial dysfunction and CAD by altered insulin/insulin-like growth factor-1 signaling pathways, reactive oxygen species formation, and other signaling [44]. Aldosterone, the endogenous mineralocorticoid in humans, was first isolated in 1953 as the last discovered steroid hormones [45], which include estrogen, androgen, progesterone and glucocorticoids [46]. Aldosterone production, mediated by the zona glomerulosa of the adrenal gland, increases in response to angiotensin II or high dietary potassium.

Aldosterone attenuates endothelial nitric oxide synthesis, promotes SMC proliferation, inflammation and fibrosis, and increase oxidative stress partially through activation of nicotinamide adenine dinucleotide phosphate (NADPH) oxidase [44, 47, 48]. Interestingly, aldosterone increases neointimal formation after ballon injury [48] and aldosterone antagonism has been shown to suppress neointimal proliferation after coronary stenting [49]. Despite those exciting findings, the cellular and molecular mechanisms underlying the proatherogenic effects of aldosterone remain elusive to us.

1.5. Adenosine and adenosine receptors

Under stress conditions, such as hypoxia, depressed cellular energy state leads to acute increase and release of adenosine from the cell [50]. Two main

cellular events are responsible for the production of adenosine, the hydrolysis of AMP to adenosine by 5" nucleotidase and the catabolism of S-adenosylhomocysteine [50]. Adenosine activates plasmalemmal adenosine receptors to regulate various functions. Adenosine receptors (ARs) are members of the G protein-coupled receptor family and four AR subtypes have been cloned: A1R, A2AR, A2BR, and A3R [51]. The discrimination of A2Rs into two subtypes was based on agonist binding affinity (high affinity-A2AR; low affinity-A2BR). All AR subtypes are distinctly distributed throughout the body. Various AR agonists and antagonists are listed in Table 1.1 [51].

AR activation regulates a diverse set of physiological functions, including cardiac rate and contractility, smooth muscle tone, sedation, release of neurotransmitters, platelet function, lipolysis, renal function, white blood cell function, and cellular proliferation [50]. Figure 1.5 shows our model of AR actions on coronary SMCs. A2A/BR were shown to mediate the vasodilatory effect of adenosine [52-54]. Since the A1R inhibit and A2R stimulate adenylyl cyclase [51], A1R antagonism could positively modulate the coronary vasodilaton in the microcirculation. The second main hypothesis in the thesis is that A1R antagonism potentiates coronary vasodilation in healthy Ossabaw swine.

Coronary stenting was shown to mechanically damage vascular cells in the target conduit artery segment [55] and induce downstream microvascular dysfunction [56-60]. The mechanisms for microvascular dysfunction associated with

stenting remain unclear to us. Dyslipidemic patients displayed impaired AR-mediated coronary flow reserve [60, 61]. ARs may be responsible for the dysregulated adenosine-induced coronary flow in dyslipidemia. The third main hypothesis in the thesis is that stent deployment in coronary arteries elicits microvascular dysfunction in dyslipidemic swine, and A1R and/or A2A/BR might contribute to the changes.

SMCs are typically characterized as either contractile or synthetic based on the distribution of myosin filaments and the massive formation of secretary protein apparatus [1]. Contractile SMCs respond robustly to vasoconstrictors and vasodilators and largely mediate tone. In contrast, synthetic SMCs are primarily responsive to growth factors and are largely responsible for synthesis of extracellular matrix [1, 14]. Phenotypic switching of SMCs from contractile to synthetic phenotype is a pivotal event in atherosclerosis [1, 9, 62-64].

In aortic SMC, adenosine was found antimitogenic via the A2BR [65-68]. Our laboratory made the novel observation that the A1R mediated mitogenic effects of adenosine on porcine coronary artery SMC via activation of the extracellular signal-regulated protein kinases (ERK), the c-Jun-N-terminal kinases (JNK), PI3K-AKT signaling pathways [65, 69]. In addition, A1R mRNA was shown upregulated in stented vs. non-stented porcine coronary segments [70], thus suggesting A1R could play a role in CAD.

Since increased plasma aldosterone is a hallmark of “obesity hypertension” [71], which is a key component of MetS, aldosterone is important in the “metabolic syndrome milieu” that drives CAD in MetS. Both aldosterone and A1R regulate vascular SMC proliferation via similar signaling pathways in vitro [65, 69, 72, 73]. Glucocorticoid receptor activation stimulated A1R gene expression in cells [74, 75] and rat brain [76]. Mineralocorticoid and glucocorticoid receptors are very similar in sequence and structural organization [77], therefore MR activation by aldosterone could potentially regulate A1R expression, thereby contributing to coronary atherosclerosis.

Exercise training of patients in coronary atherosclerosis elicits beneficial effects [18-23]. However, the underlying mechanisms are unknown. It is possible that exercise acts on systemic aldosterone and A1R in coronary artery to improve coronary atherosclerosis in MetS. The fourth main hypothesis in the thesis is that aldosterone regulation of A1R contributes to coronary atherosclerosis in MetS, and is mitigated by short-term exercise training.

Although DES have substantially decreased restenosis vs. bare metal stents [78, 79], caution must be taken with current DES in human patients because of possible late stent thrombosis caused by the endothelial cytotoxicity of the eluted agents [80-85]. To ensure the recovery of proper endothelial function, the ideal DES agent should inhibit proliferation of vascular SMCs while not preventing the restoration of endothelial cells.

In-stent restenosis (re-blockage of the stenotic artery segment) occurs in up to 40% of lesions after percutaneous coronary intervention [16]. The abnormal growth and migration of vascular SMCs play major roles in restenosis after stenting [9, 62-64], which shares similar pathogenesis as coronary atherosclerosis. Based on the aforementioned facts, the fifth main hypothesis in the thesis is that A1R-ERK1/2 signaling contributes to the development of coronary in-stent stenosis in MetS.

1.6. Ossabaw swine model of MetS and CAD

Several animal models recapitulate MetS [86-91]; however, none are able to fully reproduce symptoms of MetS and CAD observed in humans. Swine are quite similar to humans in many ways, e.g. lipids metabolism, docine and sedentary behaviors. Swine coronary arteries are also similar to humans in size, anatomical structure, and flow dynamics [92, 93], and develop CAD spontaneously [94]. Our group has developed Ossabaw miniature swine as an excellent large humanoid animal model of MetS and CAD. When fed excess calorie atherogenic diet, Ossabaw swine develop MetS, manifesting central obesity, dyslipidemia, hypertension, impaired glucose tolerance [11, 92, 95, 96], and like humans (but different from many other laboratory animal models) develop CAD [11, 92, 95, 97]. Because in-stent neointimal hyperplasia is greater in Ossabaws than in other lean swine breeds (e.g. Yucatan) [92], Ossabaw swine provide a nearly ideal model for study of coronary in-stent stenosis, and presumably, coronary atherosclerosis, especially in the setting of MetS. The profoundly greater in-stent neointimal

hyperplasia is shown in Figure 1.6, which is accompanied by decreased fibrosis of neointima in Ossabaw vs. Yucatan pigs.

The study of efficacy of stents and underlying cellular and molecular events is one of the most compelling reasons for the use of the Ossabaw swine. Figure 1.7 shows the comparison of the size of a relatively small conduit coronary artery of the pig vs. the mouse. The 2 mm pig conduit artery completely dwarfs the largest conduit artery in the mouse, which is the tiny speck in the center of the pig artery. It is completely impossible to stent any mouse coronary artery because the stent struts themselves are 100 μm thick.

1.7. Major hypotheses tested in the thesis

1. Short-term exercise training prevents micro- and macrovascular disease in porcine model of hypercholesterolemia and coronary artery disease.
2. A1R antagonism potentiates coronary vasodilation in healthy Ossabaw swine in basal condition.
3. Stent deployment in coronary arteries elicits microvascular dysfunction in dyslipidemic swine, and A1R and/or A2A/BR might contribute to the changes.
4. Aldosterone regulation of A1R contributes to coronary atherosclerosis in metabolic syndrome, and is mitigated by short-term exercise training.
5. A1R-ERK1/2 signaling contributes to the development of coronary in-stent stenosis in metabolic syndrome.

1.8. Figure legends

Figure 1.1. Coronary artery anatomy and arterial wall structure

A Circumflex coronary (CFX), left anterior descending artery (LAD), and right coronary (RC) are the main epicardial conduit coronary arteries in swine. **B** Representative histology image of Verhoeff-Van Gieson (VVG) stain in right coronary segments from healthy Ossabaw miniature swine. VVG stained for elastin in brown at internal elastic lamina (IEL) and external elastic lamina (EEL), thus differentiates intima (I, within IEL) and media (M, between IEL and EEL) from adventitia (A, beyond EEL); lumen (L) is center of each artery.

Figure 1.2. Progression of atherosclerosis in MetS

Masson's trichrome stain for collagen was used to assess changes in atherosclerosis. A. Healthy artery segment in Lean. Collagen predominates in the adventitia as shown by the blue staining. B. Early stage atherosclerosis in MetS, with collagen deposition in media separating smooth muscle cells (red) and neointima. C. Advanced stage atherosclerosis in MetS. Lumen size decreases dramastically, collagen deposition increases, but smooth muscle and foam cell infiltration predominate in neointima. D. Magnification of the lesion in C. a - adventitia, b - external elastic lamina, c - media, d - internal elastic lamina, e - lumen, f - neointima, g - foam cells.

Figure 1.3. Cellular composition of complex coronary artery lesion in MetS (Courtesy of J.R. Turk, Amgen, Thousand Oaks, CA). Immunohistochemistry of left circumflex coronary atherosclerotic lesion in MetS. Picrosirius red stains for collagen and elastin; thin fibrous cap shown by arrow. Verhoeff-van Gieson (VVG) stains for elastin. Immunostain for scavenger receptor; arrow shows presence in neointima and fibrous cap. D Immunostain for smooth muscle actin (arrow); absence in neointima and fibrous cap is consistent with unstable (vulnerable) plaque.

Figure 1.4. Coronary atherosclerosis and stent deployment

A. Angiogram of left anterior oblique view with the arrow pointing to the stenotic lesion in LAD. B. An expanded bare metal stent over an inflated balloon. C, D. Representative intravascular ultrasound (IVUS) images of a stenotic lesion (intima) before (C) and right (D) after stent deployment. E. IVUS image showing in-stent stenosis 4 weeks after stent deployment in a lean pig. The yellow dotted lines indicate the location of the stent struts, blue dashed lines indicate the current lumen border, and area in between those lines were in-stent hyperplasia (Modified from Z.P. Neeb's thesis with permission).

Figure 1.5. Model of AR actions on SMC

Adenosine induces vasodilatory effect in coronary SMC via activation of A2AR. In aortic SMC, adenosine induces anti-mitogenic effect via interation with A2BR. A1R mediates a novel mitogenic effect of adenosine in coronary SMC. There are no conclusions yet regarding the role of A3R.

Figure 1.6. Ossabaw has greater coronary in-stent neointima (NEO)

Comparison of Mason's trichrome staining for collagen in in-stent segments between Yucatan and Ossabaw. A-adventitia, L-lumen, M-media, Neo-neointima, S-stent strut occupied the area before sectioning.

Figure 1.7. Size comparison between porcine (above) and murine (center) epicardial conduit coronary artery

Verhoeff-van Gieson staining for elastin. Arrows point to internal elastic lamina (IEL). Neointima (NEO) is the thin layer luminal to IEL. Thickness of stent struts used clinically in humans is the entire lumen diameter of the mouse coronary artery.

1.9. Figures

Figure 1.1. Coronary artery anatomy and healthy arterial wall structure

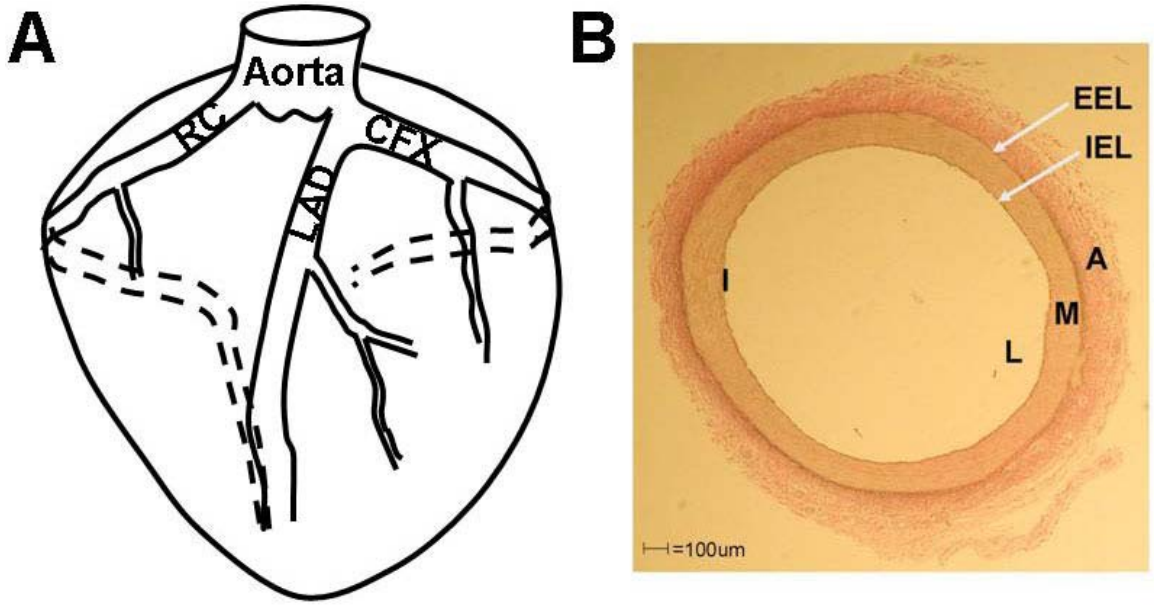

Figure 1.2. Progression of atherosclerosis in MetS

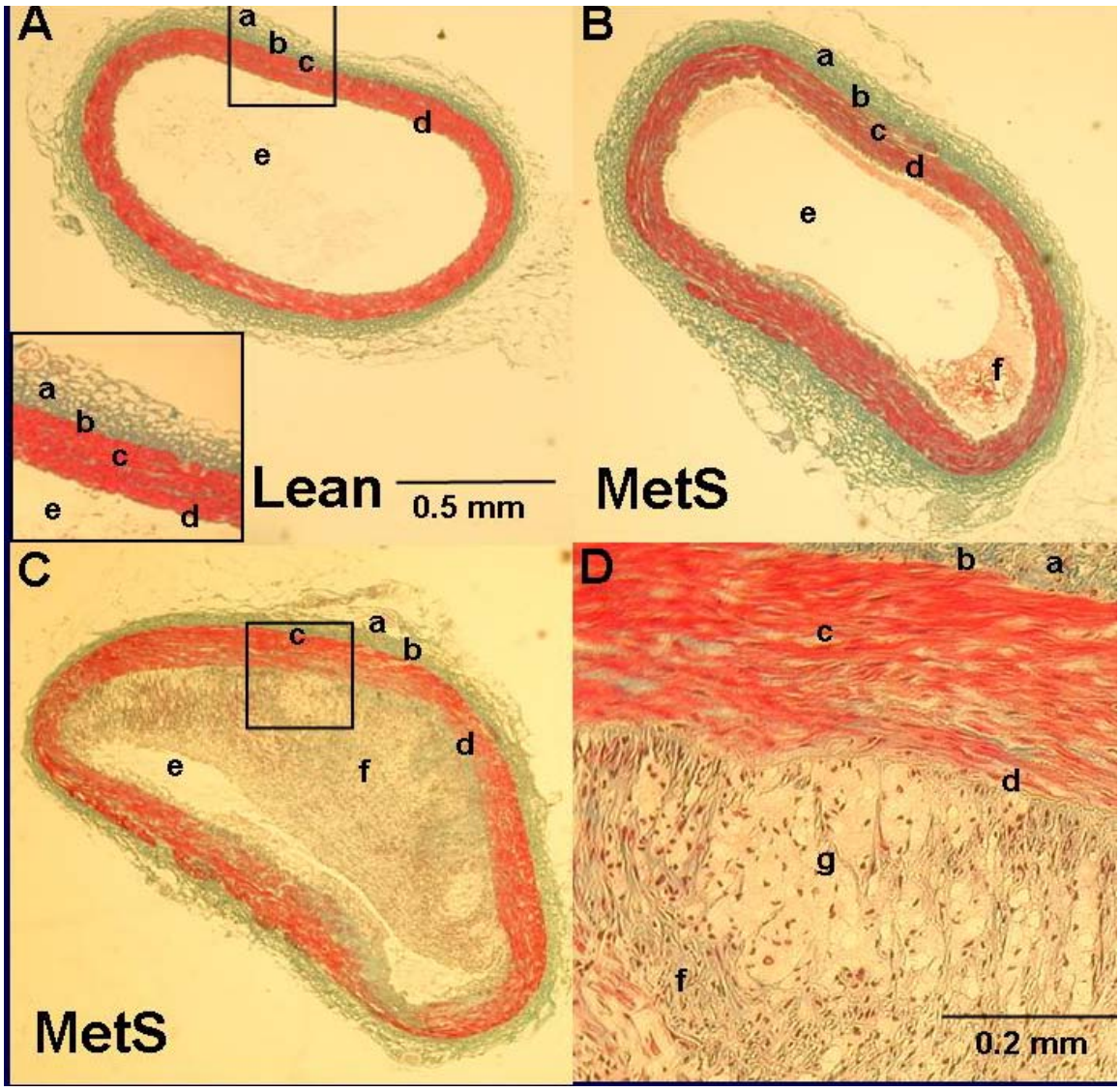

Figure 1.3. Cellular composition of complex coronary artery lesion in MetS

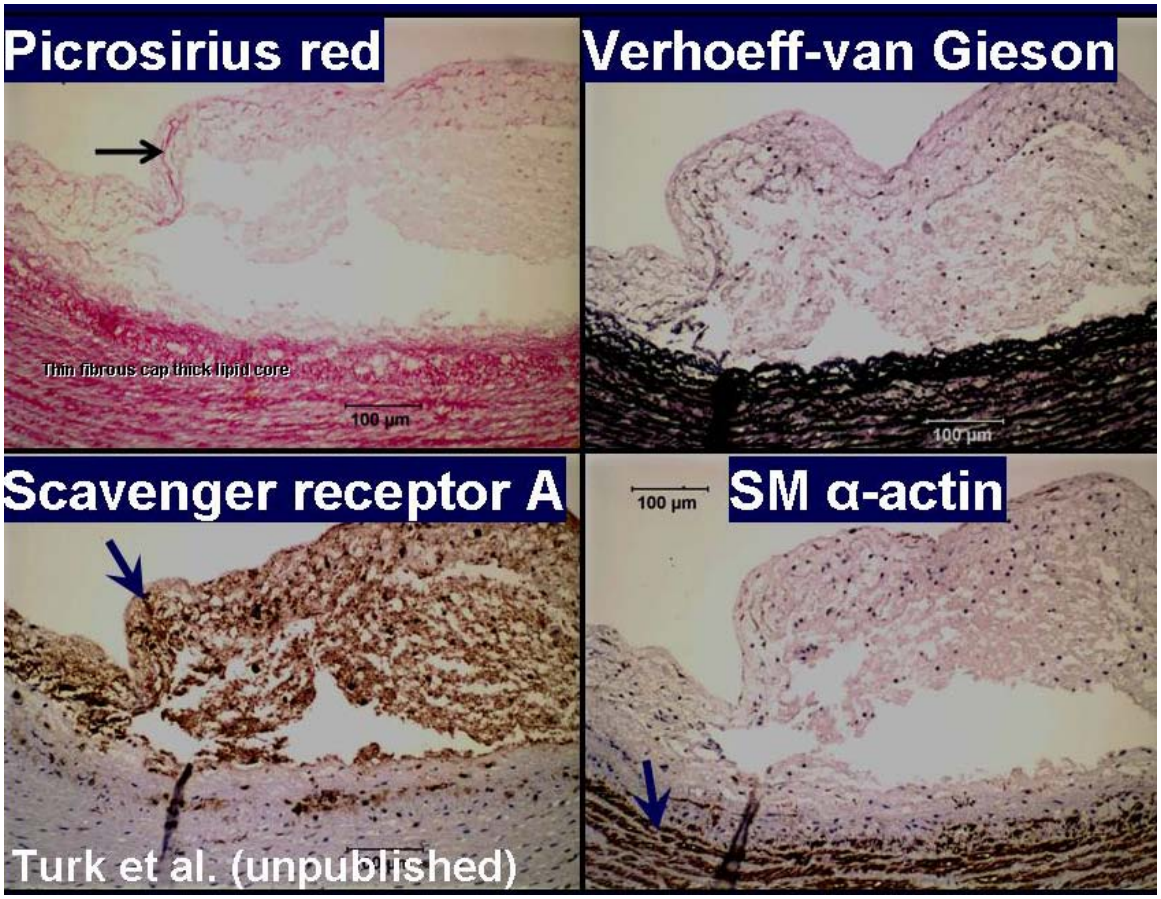

Figure 1.4. Coronary atherosclerosis and stent deployment

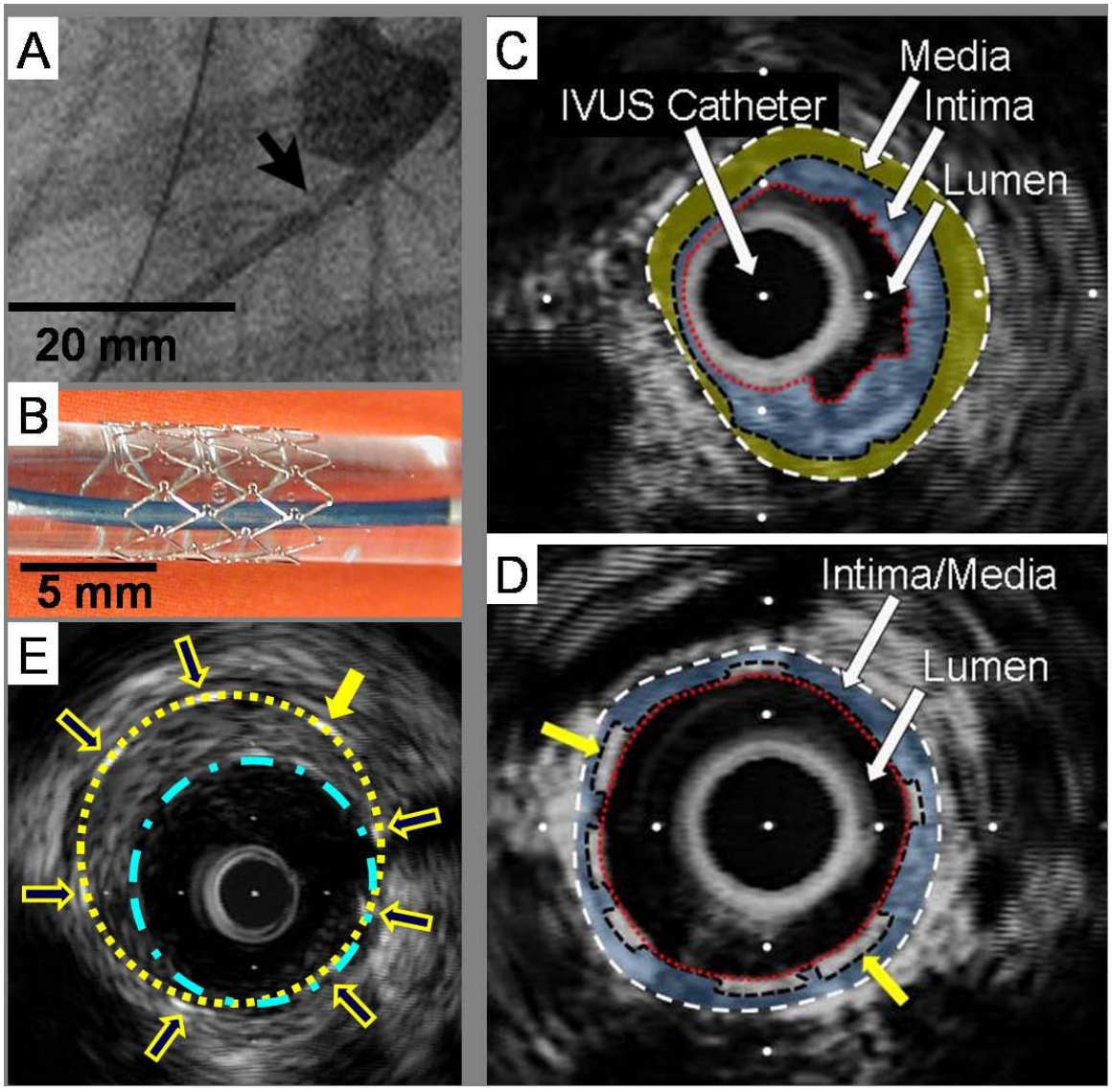

Figure 1.5. Model of AR actions on SMC

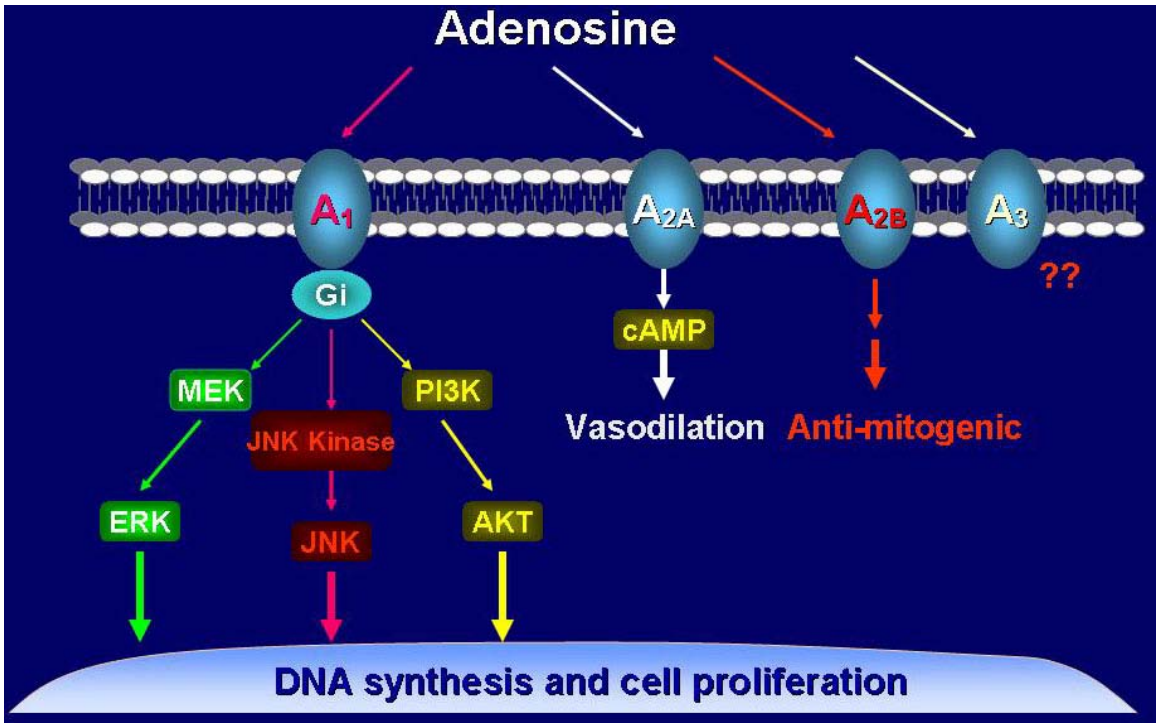

Figure 1.6. Ossabaw has greater coronary in-stent neointima (NEO)

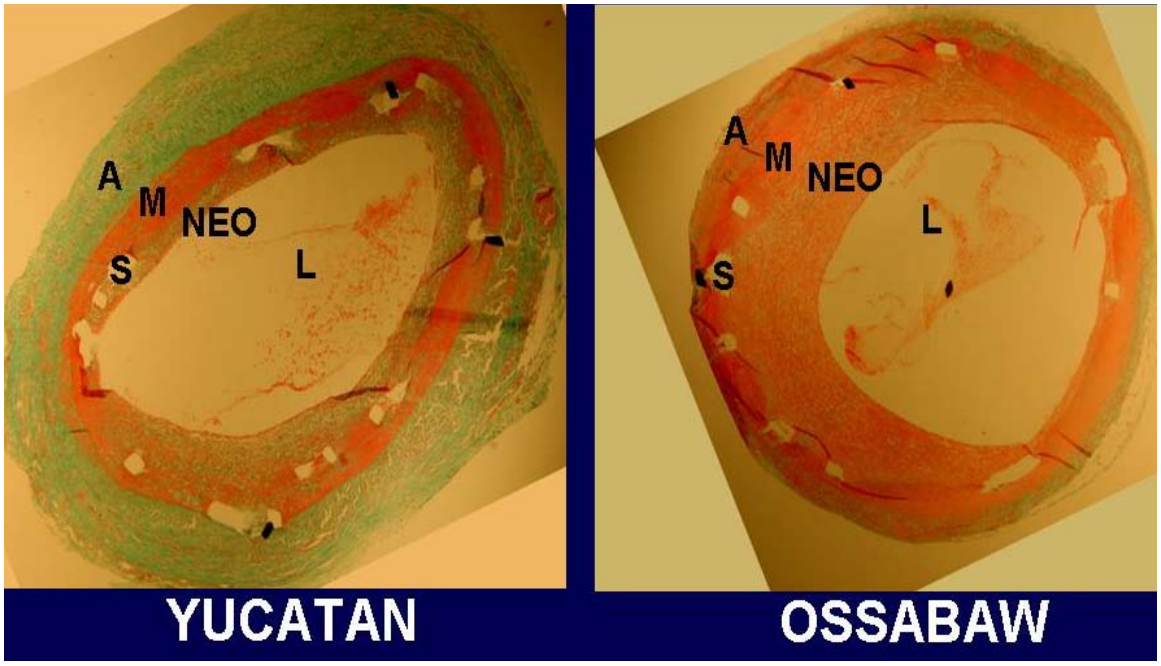

Figure 1.7. Size comparison between porcine (above) and murine (center) epicardial coronary artery

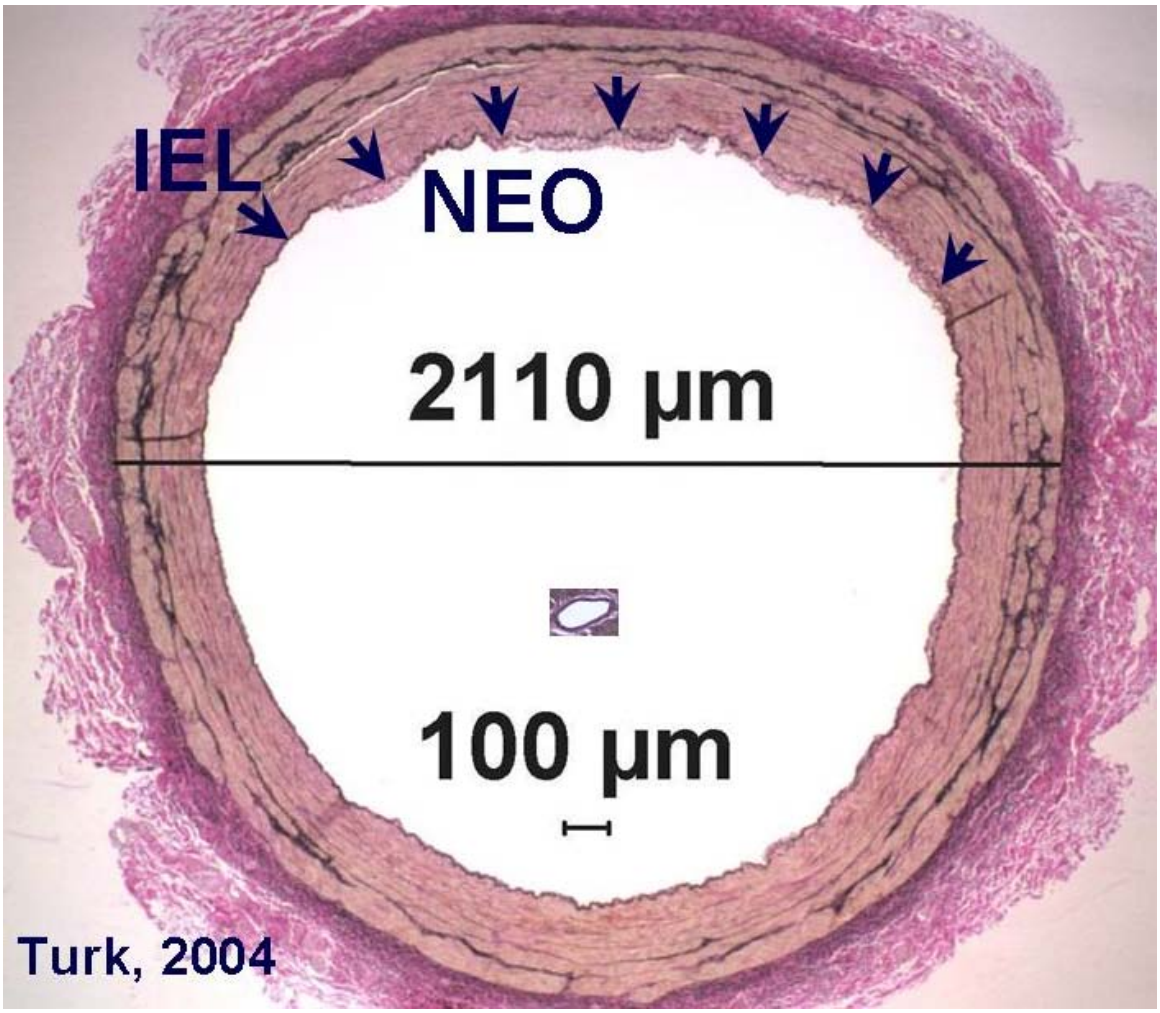

1.10. Table

Receptor	cAMP	Agonist	Antagonist	G protein
A1	↓	ADO, NECA, RPIA, PD81723, CCPA	DPCPX, 1,2-DPA rolofylline	Gi
A2A	↑	ADO, NECA, CV1808, CGS21680	DMPX, ZM241385 SCH58261	Gs
A2B	↑	ADO, NECA, CV1808	DMPX, MRS1706 Alloxazine	Gs
A3	↓	ADO, NECA, 2-Cl-IB-MECA	VUF5574 MRS1220	Gi

Table 1.1. Adenosine receptor pharmacology.

ADO, adenosine.

CHAPTER 2. SHORT-TERM EXERCISE TRAINING PREVENTS MICRO- AND MACROVASCULAR DISEASE FOLLOWING CORONARY STENTING

Xin Long[1], Ian N. Bratz[2],

Mouhamad Alloosh[1], Jason M. Edwards[1], Michael Sturek[1]

[1]Department of Cellular & Integrative Physiology

Indiana University School of Medicine, Indianapolis, IN 46202-5120

[2]Department of Integrative Medical Sciences,

Northeastern Ohio University College of Medicine and Pharmacology,

Rootstown, OH 44272

Running head: Coronary stenting and exercise

Corresponding author:

Michael Sturek, PhD, Professor and Chair

Department of Cellular & Integrative Physiology

Indiana University School of Medicine

635 Barnhill Drive, MS 385

Indianapolis, IN 46202-5120

Phone 317-274-7772

FAX 317-274-3318

Email msturek@iupui.edu

2.1. Abstract

The purpose of this study was to determine the effects of exercise training on coronary blood flow and macrovascular atherosclerosis in response to stent deployment. Male Yucatan swine were fed control (control), high fat/cholesterol (hypercholesterolemic), or high fat/cholesterol diet and aerobically exercise trained (hypercholesterolemic exercised) starting after 36 weeks on the diet. All pigs underwent coronary angiography and intravascular ultrasound (IVUS) guided placement of a bare metal stent in the circumflex coronary artery after 40 weeks on diets and 3 weeks later pigs underwent repeat angiography and IVUS and coronary blood flow (CBF) measurement. Average peak velocity (APV) was measured under basal conditions and in response to intracoronary application of the endothelium-independent vasodilator adenosine and the endothelium-dependent vasodilator bradykinin. There was a similar ~8-fold increase in total cholesterol in hypercholesterolemic and hypercholesterolemic exercised groups compared to control. Baseline CBF was increased above control and hypercholesterolemic groups in hypercholesterolemic exercised group ($p<0.05$). At all doses adenosine-induced CBF was impaired in hypercholesterolemic, but preserved in hypercholesterolemic exercised group. Similarly, bradykinin-induced CBF was impaired in hypercholesterolemic vs. control, yet was potentiated in hypercholesterolemic exercised group. Microvessel density was decreased in hypercholesterolemic and preserved in hypercholesterolemic exercised vs. control. Native atheroma in hypercholesterolemic exercised group was lower relative to hypercholesterolemic and control, while in-stent stenosis in

hypercholesterolemic exercised group was not different from hypercholesterolemic group. Stent-induced microvascular dysfunction in hypercholesterolemia may be a result of reduction in microvessel density. This is the first report that short-term exercise training near the time of stenting prevents stent-induced microvascular dysfunction and attenuates native atheroma independent of changes in plasma cholesterol in this porcine model.

Key words: microvessel, restenosis, porcine, hypercholesterolemia, Yucatan swine

2.2. Introduction

Deployment of a stent in a coronary artery in the setting of flow-limiting stable coronary artery disease (CAD) results in initial improvement in functional capacity and quality of life [98]. However, almost half of patients undergoing coronary angioplasty/stenting eventually experience recurrent angina, resulting in a decline in functional capacity and require further medical attention [99]. It has been shown that coronary stenting mechanically damages vascular cells in the target conduit artery segment and endothelium in peri-stent segments [55], and induces downstream microvascular dysfunction that persists for weeks and has been implicated in causing exertional ischemia [56-60]. Camici and Crea [60] termed this phenomenon post-stent “iatrogenic coronary microvascular dysfunction”, which may be due to enhanced alpha-adrenergic constriction [100], chronic impairment of microvascular response [57, 58], or microemboli that may cause

microinfarcts [58, 101] and perhaps more severe rarefaction (microvessel dropout) [102]. In spite of enormous efforts to reduce in-stent stenosis and microvascular dysfunction, there remains significant room for improvement in addressing both of these post-stent procedure complications. This is especially important because drug-eluting stents, which are the main treatment for flow-limiting lesions, cause even greater microvascular dysfunction than bare metal stents [103, 104].

Exercise training of patients with coronary artery disease elicits beneficial effects, including improvement in exercise tolerance, left ventricular function, and reduction in the ischemic response to submaximal workload after exercise training, and increased dilation of conduit and microvessel coronary arteries [18-23]. Most of these studies have shown concomitant changes in plasma cholesterol; specifically, decreased total and low density lipoprotein (LDL) and increased high density lipoprotein (HDL) cholesterol [24-26]. Hambrecht etc. [23] removed the confounding variable of hypercholesterolemia by excluding those patients from their study, thus implying that the beneficial effects of exercise may be due to more direct actions of exercise on the vasculature.

The benefits of exercise training may also extend to the population undergoing percutaneous coronary revascularization [22, 24-26]. Belardinelli etc. [26] found that progression of macrovascular CAD in arterial segments proximal and distal to the angioplasty / stented segment, i.e. peri-stent CAD, was attenuated by exercise training and accompanied by an improved thallium perfusion stress

test that is indicative of increased metabolic vasodilation of the coronary microvasculature. Further, exercise training may be more beneficial and cost-effective than percutaneous coronary intervention in the setting of chronic stable CAD [22]. Fleenor and Bowles [27] showed that long-term exercise training of pigs with normal plasma cholesterol attenuated conduit artery neointimal proliferation elicited by overexpansion injury from balloon angioplasty; however, microvascular effects were not determined. Further, the effects of plasma cholesterol and exercise on in-stent stenosis, peri-stent CAD, and microvascular dysfunction after coronary stenting have not been studied.

The purpose of this study was first to test the hypothesis that stent deployment in coronary arteries of hypercholesterolemic swine would elicit microvascular dysfunction and if short-term exercise training would prevent the microvascular dysfunction and progression of macrovascular CAD after stenting. A second hypothesis tested was whether exercise elicits beneficial effects by acting directly on the vascular wall, rather than indirectly via decreasing plasma risk factors (i.e. cholesterol). The final hypothesis tested was whether a decrease in microvessel density, i.e. rarefaction, occurs after stenting in hypercholesterolemia, and whether exercise training would prevent this.

2.3. Methods

All protocols involving animals were approved by an Institutional Animal Care and Use Committee and complied fully with standards [105, 106]. Nineteen

male Yucatan swine, 52-70 kg, were randomized to 40 weeks of control diet (C, n=8), high fat/cholesterol diet (H, n=8), or high fat/cholesterol diet with short-term exercise training (HX, n=3). H and HX were fed a diet consisting of 46% kcal from fat [107]. The feed base consisted of mini pig chow with supplemental fat kcals from coconut oil (<1% trans fatty acids; Research Diets, Inc., New Brunswick, NJ) and cholesterol (Research Diets, Inc.). Controls were fed a diet consisting of mini pig chow base with 8% kcal from fat.

2.3.1. Exercise Training

Animals randomized to the exercise group began treadmill training 4 weeks prior to initial cardiac catheterization. During the first week of training, the exercise pigs ran on the treadmill at 3 mph (endurance) with 0% grade for 20-30 minutes and at 4 mph (sprint) for 15 minutes. The speed and duration of running were increased progressively over the course of the following 4 weeks. During the 4^{th} through the 7^{th} week of training, a typical 70 minute training session consisted of the following: 1) 5 minute warm-up at 2.5 mph, 2) 15 minute sprint at speeds of 5.5-6 mph, 3) 40-45 minute endurance run at 3.5 mph, and 4) 5 minute cool down at 2 mph. Ranges of running speeds are presented because the exercise training advanced during the course of the week. Following coronary stenting, each animal resumed symptom limited exercise training. This regimen was maintained for three weeks after stenting when the animals returned for repeat cardiac catheterization. Exercise protocols were compliant with guidelines from the American Physiological Society [108].

2.3.2. Submaximal stress test

At weeks 1, 4, and 7 of exercise training the endurance trained animals underwent a submaximal stress test consisting of running on a treadmill at 3.1 MPH, 0% grade for 15 minutes at which point heart rate data were collected.

2.3.3. Stent Procedure

Each animal received antiplatelet therapy with aspirin 325 mg daily starting the day prior to the initial catheterization procedure and continuing through the completion of the study [70, 92, 109]. Each pig was fasted overnight and all animals arrived at the same time of day for procedure. Animals received preanesthesia with intramuscular injections of atropine (0.05 mg/kg), xylazine (2.2 mg/kg), and telazol (6.6 mg/kg). Following intubation, isoflurane (2-4%, with oxygen) was administered to maintain stable systemic hemodynamics and a stable level of anesthesia. Heart rate, blood pressure (tail cuff and aortic), respiratory rate and electrocardiographic data were continuously monitored throughout the procedure. Under sterile conditions, the right femoral artery was exposed with surgical cut-down technique and an 8F vascular introducer sheath was inserted into the femoral artery followed by administration of heparin 200 U/kg. An 8F Amplatz L (sizes 0.75-2.0) guiding catheter (Cordis Corp., Miami, FL) was inserted through the sheath and advanced to engage the left main coronary ostium (Figure 2.1). Blood pressure measurements were recorded directly from the coronary ostium via a pressure transducer connected to the manifold assembly. A 0.014 inch flex tip Doppler Flow-wire (Cardiometrics, Rancho

Cordova, CA) was advanced through the guiding catheter and positioned in the distal left circumflex artery with the aide of angiographic images. A 3.2F, 30 MHz Intravascular Ultrasound (IVUS) catheter (Boston Sci., Sunnyvale, CA) was advanced over the Flow-wire and positioned in the distal left circumflex coronary artery. IVUS interrogation of the left circumflex artery was performed using an automated pullback technique at a rate of 0.5 mm/sec. Images were recorded on videotapes using Sonos Intravascular Imaging System (Hewlett Packard) for subsequent off line analysis. Strict comparison of IVUS and angiographic images were taken to ensure accurate placement of the coronary stent. Following IVUS pullback, the IVUS catheter was removed and the coronary stent (3.0 to 4.0 mm diameter by 8 to 20 mm length, Multi-link Penta Coronary stent system, Guidant Corp., Temecula, CA) catheter was positioned in the left circumflex artery. Coronary stent size was chosen using angiogram and IVUS information to match the recipient artery diameter with stent deployment at optimal inflation pressure. The coronary stent was deployed in the circumflex artery per routine deployment protocol. Repeat angiography was performed and apposition was confirmed by repeat IVUS interrogation. The IVUS catheter, guide catheter and introducer sheath were then removed and the right femoral artery was ligated. The skin was closed in two layers and the animal was allowed to recover from anesthesia. Arrow in Figure 2.1A indicates stent placement was performed after 4 weeks of exercise training in the HX pigs.

2.3.4. Follow up procedure

Follow up cardiac catheterization for coronary blood flow (CBF) analysis of in vivo microvascular function was performed three weeks after initial stent placement. Preanesthesia and vascular access via the left femoral artery was similar to that described above. The left coronary ostium was engaged with the guiding catheter and a Doppler Flow-wire was positioned in the distal circumflex with angiographic guidance [92, 107]. IVUS catheter was then advanced over the Flow-wire and positioned in the distal circumflex for IVUS interrogation via pullback as previously described in the peri-stent and in-stent regions. Following IVUS pullback, the IVUS catheter was removed and the Doppler Flow-wire was repositioned in the left circumflex artery proximal to the coronary stent. Strict comparison of IVUS and angiographic images were taken to ensure accurate placement of the Flow-wire for determination of CBF responses.

Average peak velocity (APV) measured by intracoronary Doppler Flow-wire was recorded continuously throughout the procedure using FloMap (Cardiometrics, Rancho Cordova, CA) for off-line analysis at a later time. The CBF velocity was allowed to reach a steady state (allowing any effects of preanesthesia to resolve) and baseline measurement of APV was obtained. Hyperemia was then induced with bolus doses (3 mL) of the endothelium-independent vasodilator adenosine (3, 1, 0.33, 0.167 µg/kg) given via the guiding catheter into the coronary artery. Peak APV, heart rate and blood pressure were recorded for each adenosine administration. Subsequent doses of adenosine

were administered only after APV had returned to baseline and stabilized, at which time the baseline parameters were again documented followed by the administration of the next adenosine dose. The effect of adenosine typically lasted 15-30 seconds. After completion of the graded adenosine doses we investigated the response to the endothelium-dependent vasodilator bradykinin. The APV was allowed to return to baseline and bradykinin (1, 2, 4 ng/kg) was administered. APV, heart rate and blood pressure were continuously recorded as described above. Because of the prolonged response to bradykinin, hemodynamic and blood flow parameters were tracked for 2 minutes following each bradykinin to ensure return and stabilization of APV to its previous baseline. Subsequent doses of bradykinin were administered only after APV, heart rate and blood pressure returned to baseline and stabilized.

The APVs, heart rates, blood pressures, and vasodilator-induced peak APVs, heart rates, blood pressures were determined from off-line analysis of FloMap recordings. Coronary blood flow (ml/min) was calculated as: APV (cm/sec) × 0.5 × CSA (artery cross sectional area, cm^2) / 60 (sec/minute) [107]. Coronary vascular resistance (CVR, mm Hg/ml/min) was calculated as mean arterial pressure (MAP) divided by CBF. The rate-pressure product (RPP, bpm × mm Hg) was calculated as heart rate (HR, bpm) multiplied by systolic blood pressure (SBP, mm Hg). Vessel cross-sectional area was calculated off-line from recorded IVUS images using the commercially available Sonos Intravascular Imaging software package. End systolic and end diastolic cross sectional areas

were determined for three consecutive cardiac cycles. The average of these six measurements was taken as the cross sectional area to be used in subsequent calculations and analysis.

2.3.5. Lipid analyses

After 18 hours of fasting blood was taken via the anterior vena cava and collected into vacutainers containing 0.117 ml of 15% EDTA and centrifuged in the cold at 4°C for 20 min at 2000 rpm in a Marathon 21000 R centrifuge (Fisher Scientific, Pittsburgh, PA) and frozen at -80°C. Plasma was analyzed for triglycerides, total cholesterol, and high density lipoprotein (HDL) while low density lipoprotein (LDL) was calculated from Friedewald equation: LDL = Total cholesterol - HDL - (triglyceride/5) [95].

For each plasma analysis, all samples for a given subject were analyzed in a single run. Plasma triglyceride and total cholesterol were assayed directly by standard enzymatic kit (Thermo Trace, Melbourne, Australia). HDL was measured by precipitating apolipoprotein B-containing lipoproteins with heparin-$MnCl_2$ [95, 110, 111]. The supernatant was used to assess HDL using the aforementioned total cholesterol kit and method.

2.3.6. Quantification of atherosclerosis and neointima formation and coronary microvessel density

To determine extent of atherosclerosis in the coronary arteries, we performed IVUS catheterization on the left circumflex and left anterior descending arteries. The left anterior descending was not previously interrogated at the time of stent placement, thus the atheroma detected in this "non-stented" artery (Figure 2.1) was considered native, and uninfluenced by potential catheter-related non-specific trauma of the stent procedure. The IVUS data were recorded on videotape for off-line analysis. Degrees of atheroma (percent wall coverage) were measured from IVUS images at one mm intervals. Degrees of atheroma at each interval of the given vessel were summed and divided by (360/mm * length of vessel in mm). This was multiplied by 100 to yield % atheroma to normalize for different lengths of arteries [70, 109]. See Figure 2.1C and Table 2.3.

Verhoeff-van Gieson and Masson's trichrome staining were performed on sections of stented arteries. Though technically very challenging, we obtained several sections for histology per animal per stain. In animals where more than one section was obtained, values were averaged. Neointima formation was determined by obtaining area measurements bounded by the external elastic lamina and internal elastic lamina (tunica media), internal elastic lamina and lumen (neointima) using commercially available software (ImagePro 3.0). The percent stenosis was calculated by dividing the area of the neointima by the area demarcated by the internal elastic lamina × 100. Collagen content in the sections

of the stented arteries was determined by colorimetric analysis [10]. The adventitia, which is composed predominantly of collagen, was used as the reference color template against which the rest of the section was compared.

A small piece (1 × 1 cm^2) of left ventricular myocardium was obtained at sacrifice and preserved in 10% formalin solution. Each piece was embedded in paraffin and sectioned (4 µm) for immunohistochemistry for smooth muscle a-actin. Immediately prior to treatment with antibodies, each section was deparaffinized and treated with an antigen retrieval process. A monoclonal primary antibody to smooth muscle a actin was used as for identifying coronary vessel (1:1000, Sigma Chemical Co., St. Louis, MO), incubated for 1 hour. A biotinylated secondary antibody (Vectastain Elite, Vector Laboratories, Burlingame, CA) was used for the detection process. Stained samples were viewed under a light microscope, and images were captured with Coolpix digital camera. Only coronary arteries with 70-100 µm internal diameters were used and sections of myocardium contained a wide range of microvessels, thus were normalized to cross sectional area. Optical density (OD) of microvessel cross sections were normalized to the average of the control values and expressed as a percentage of control as indicated in the following: (OD each individual vessel)/(average OD of Control vessels) × 100% = OD as a % of Control. Finally, microvessel density was measured by counting the number of microvessels in randomly selected 6.5 mm^2 areas.

2.3.7. Data analysis

Statistical analysis was performed using commercially available software (SPSS version 10, SigmaStat 5.0). Coronary blood flow responses and hemodynamic parameters were compared between groups using repeated measures ANOVA. Vessel cross-sectional area and % degrees atheroma were compared between groups using single factor ANOVA. The Dunnett's T3 multiple comparison test was used for data that were not normally distributed (microvessel density). In all cases, $p < 0.05$ was considered significant.

2.4. Results

High fat/cholesterol diet resulted in approximately 8-fold increase in plasma total cholesterol, greater than 20-fold increase in LDL cholesterol, and a slight but significant increase in HDL cholesterol in H and HX relative to control (Table 2.1). These differences resulted in a 16-fold increase in LDL/HDL ratio in H and HX vs. control. Despite the significant cholesterol response to diet, the experimental design assured that the body weight was not different between groups. Heart rate response was taken during a submaximal treadmill stress test with the pig running at 3.1 mph at 0% grade for 15 minutes. In HX, heart rate response to submaximal stress testing was approximately 25% lower after 7 weeks of training compared to performance on submaximal stress testing completed at the beginning of week 1 (Table 2.1), thus confirming the efficacy of the exercise training regimen. Heart weight, mean arterial pressure, and rate pressure products were not different between groups as shown in Table 2.1.

IVUS interrogation revealed no flow limiting stenosis in the studied vessel. Baseline conduit cross-sectional area was not different between groups and did not change with administration of vasodilators.

As shown in Figure 2.2A, CBF change in response to bradykinin was decreased in H relative to control at 4 ng/kg and increased in HX relative to H at 2 ng/kg ($p<0.05$). Interestingly, adenosine-induced CBF change was substantially attenuated in H relative to control at all doses (Figure 2.2B, $p<0.001$). Short-term exercise training increased the CBF responses to adenosine relative to H at 0.167 and 1.0 µg/kg doses ($p<0.05$).

Coronary vascular resistance is shown in Table 2.2. Baseline CVR was elevated in H relative to control (2.22 ± 0.23 vs. 1.46 ± 0.14 mm Hg/ml/min), whereas short-term exercise training significant reduced baseline CVR (0.96 ± 0.05 mm Hg/ml/min). Adenosine-induced CVR was approximately two times higher in H vs. control at all doses (i.e. 1.60 ± 0.15 vs. 0.88 ± 0.10 mm Hg/ml/min at 0.33 µg/kg). Short-term exercise training preserved the CVR response to adenosine (0.86 ± 0.16 mm Hg/ml/min at 0.33 µg/kg). Similarly, CVR in response to bradykinin administration was approximately 50 to 60% higher in H than control at all doses (i.e. 1.34 ± 0.05 vs. 0.82 ± 0.06 at 4 ng/kg). Similar to adenosine, the impaired response to bradykinin was prevented with exercise training (0.80 ± 0.13 at 4 ng/kg).

In addition to assessment of microvascular function, we investigated the effect of exercise on the macrovascular atheroma along the entire length of the artery that was interrogated by IVUS. Results of IVUS analysis are shown in Table 2.3. The overall macrovascular atheroma in H was almost 2-fold greater than control as shown as circumflex percent degrees atheroma. Remarkably, this response was completely prevented with exercise training. At sacrifice the left anterior descending, which had not been previously accessed, was also interrogated with IVUS to determine the effects of short-term exercise on native atheroma not related to coronary stenting. As shown in Table 2.3 there was significantly higher percent degrees atheroma in left anterior descending of H vs. control, which was completely absent of atheroma. Importantly, exercise reduced LAD atheroma. Note that overall atheroma burden was evident in the CFX in the control group only because of the in-stent stenosis in control contributed substantially to the overall atheroma burden. Finally, to address the effect of hypercholesterolemia and exercise on the in-stent atherosclerotic processes, analyses for neointima formation (percent stenosis) and collagen content were performed on the stented sections of the circumflex artery. We report no statistical difference across groups with respect to percent stenosis (Figure 2.3E). This is in stark contrast to the percent stenosis that was determined 5 mm (Figure 2.3D) and 10 mm (data not shown) proximal to the stent, as H pigs had significantly greater % stenosis in both locations compared to the control and HX groups. In addition, we found significantly higher % collagen in the stented sections of the H animals (21.5 ± 6.8%) compared to the control (0.9 ± 0.3%) or

HX (2.1 ± 0.8%). Taken together, these data suggest that the higher amount of atheroma in the circumflex artery of the H animals was predominantly in the non-stented sections of the interrogated artery, which is strongly supported by the summary comparison data of histology in Figure 2.3D and E.

Finally, Figure 2.4 represents microvessel density in the left ventricular sections obtained from all pigs. Microvessel density was significantly decreased in H compared to control (47% of C). Microvessel density in the HX group was higher than in the H group (80% of C), suggesting that exercise training partially prevented this reduction in microvessel density.

2.5. Discussion

To our knowledge, this is the first study examining the effects of exercise training on microvascular function and macrovascular atheroma after coronary stenting in a model of hypercholesterolemia and CAD. Additionally, we provide evidence that microvascular rarefaction may underlie the blunted stent-induced response and normalized exercise training-induced blood flow responses to adenosine and bradykinin in the coronary microcirculation in hypercholesterolemia. Coronary stenting has been shown to mechanically damage vascular cells in the target conduit artery segment and endothelium in peri-stent segments [55], and induces downstream microvascular dysfunction that persists for weeks and has been implicated in causing exertional ischemia [56-60]. A major finding of this study is bare metal stent deployment in our

hypercholesterolemic swine model results in microvascular dysfunction, as assessed by the decreased CBF response to intracoronary bradykinin and adenosine administration (Figure 2.2). Secondly, short-term exercise training prevented the microvascular dysfunction in response to intracoronary braydkinin and/or adenosine (Figure 2.2A and B). A third major finding was that stenting decreased microvessel density in hypercholesterolemia (Figure 2.4), thus providing a structural mechanism for the in vivo responses to adenosine and bradykinin reported herein. Interestingly, exercise training prevented the reduction in microvessel density (Figure 2.4). These data demonstrate the efficacy of short-term exercise training on preventing early pathophysiological responses to coronary stent deployment. Equally remarkable is that the beneficial effects of exercise were independent of changes in plasma lipids. Taken together, we conclude that exercise may act directly on the vascular wall or other plasma risk factors not measured here to improve microcirculation after stenting in hypercholesterolemia.

Similar effects on endothelium-dependent microvascular dysfunction and CBF have been reported in the setting of hypercholesterolemia alone [3, 112-115]. Possible mechanisms for the hypercholesterolemia-induced endothelium-dependent dysfunction include an increase in endothelin-1 (ET-1) [3], a reduction in nitric oxide (NO) synthase [4] or responsiveness to NO [5]. We did not measure protein levels of ET-1 or NO synthase nor responsiveness to NO in the microvessel preparations in the present study. Furthermore, coronary

interventions can damage vascular cells and induce endothelial dysfunction in arterial segments distal to the angioplasty/stent site [55], with one study suggesting that endothelial dysfunction following coronary interventions is related to inducible ischemia [56]. Importantly, the impaired microvascular function and CBF could also be secondary to direct endothelial cell damage. The present findings of impaired responses to adenosine (largely endothelium-independent vasodilator) suggest that the microvascular dysfunction was not limited solely to a dysfunctional endothelium, but suggests smooth muscle function was also adversely affected. We acknowledge that a component of adenosine-induced relaxation is endothelium-dependent in rat vasculature [116]; however, the effects of adenosine are primarily endothelium-independent pathway and as such is the predominant vasodilatory pathway in porcine coronary artery.

Previous reports have shown beneficial effects of exercise training including improved myocardial perfusion and improved endothelial function [117-119]. However these studies did not involve revascularized patients. More recent studies involving patients undergoing coronary interventions report improvements in functional capacity and quality of life, but report conflicting results regarding recurrent events and re-hospitalizations and these studies did not directly assess microvascular function [25, 26, 120-122]. Hosokawa etc. directly assessed endothelial function in vivo and reported regular exercise training improved endothelial function in non-infarct related coronary arteries following coronary interventions for myocardial infarction [24]. Importantly, that study did not evaluate function of the

culprit artery. Finally, it is important to note that these studies involved long-term exercise training, which contrasts sharply to the short-term (7 weeks) regimen in the present study.

Short-term exercise training resulted in significantly lower native atheroma burden as determined by IVUS interrogation of the left anterior descending (non-intervened vessel) (Table 2.3). These data are consistent with other investigators who have shown that long-term exercise training has beneficial cardioprotective effects with some evidence suggesting that exercise training may delay the progression or even induce regression of CAD [123-125]. Additionally, IVUS interrogation of the circumflex artery revealed that short-term exercise training significantly decreased the macrovascular atheroma response following stenting. This result is noteworthy in light of recent human studies involving long-term exercise training following coronary interventions that did not result in significant differences in restenosis rates [25, 26, 120, 121]. Interestingly, the formation of neointima within the stent was not different across groups; thus, the differences in atheroma burden across groups stem from difference in the non-stented regions. This is noteworthy as little is known regarding the progression of coronary artery disease in a stented vessel proximal and distal to the stent. Because of the increase in collagen content in the H animals in the tunica media, the mechanisms responsible for the alteration in cellular composition in each of these regions warrant additional investigation. Further punctuating these current findings is the fact that coronary stenting is clearly the most widely accepted

treatment option for patients with CAD, yet restenosis still affects 15-25% of patients and often requires repeated interventions even with recent advances in therapy [126, 127]. The exact mechanisms involved in the beneficial effects of short term exercise are still not clearly elucidated but could involve neurohumoral, mechanical, direct or indirect effects on the vascular wall.

Revascularization of an occluded artery with percutaneous angioplasty has been shown to impair conduit and microvascular dilation [55, 56, 58-60, 100, 101]. We investigated one potential underlying mechanism related to microvascular dysfunction response in the present study - the reduction in microvascular density in the hypercholesterolemic swine (Figure 2.4). Since the hyperemic response to adenosine and bradykinin is a result of microvessel vasodilation, it stands to reason that one potential common explanation for a blunted response to both adenosine and bradykinin could be a reduction in number of microvessels per tissue area.

A limitation of our study is the animals did not receive a typical medical regimen that would be considered standard of care for human patients undergoing coronary interventions. Pigs in our study were given daily aspirin and periprocedural heparin, but did not receive Plavix. Further, the pigs did not receive typical lipid lowering agents, by design, which have also been shown to have an ameliorating effect on endothelial dysfunction and even atheroma burden as well as outcomes in patients with CAD [128-133] and our model [10, 134, 135].

Additionally, by design, our study did not address how long the beneficial exercise effect was maintained, nor did it address whether the effect was preserved following cessation of exercise.

The results of this study demonstrate that short-term exercise training preserves endothelium-independent coronary microvascular responses, potentiates endothelium-dependent coronary microvascular function, and significantly diminishes the overall macrovascular atheroma burden after coronary stenting in a porcine model of hypercholesterolemia and CAD. Our results add direct evidence for microvessel dropout (rarefaction), which may explain the parallel CBF responses to endothelium-dependent (bradykinin) and endothelium-independent (adenosine) dilators. Combined with the exercise-induced decrease in macrovascular atheroma burden, these data provide a compelling basis for exercise to ameliorate complications associated with coronary stenting. To our knowledge this is the first study to report such effects associated with peri-procedural short-term exercise training independent of favorable changes in plasma cholesterol. These phenomenal effects of exercise training, if translatable to human clinical medicine, could offer an outstanding adjunct to drug-eluting stent treatment for flow-limiting lesions if exercise can ameliorate the even greater microvascular dysfunction in drug-eluting compared to bare metal stents [103, 104].

2.6. Acknowledgements

We thank Drs. Shawn G. Kaser and Eric A. Mokelke for their excellent technical support and contributions to the manuscript. This work was supported by National Institutes of Health grants RR013223 and HL062552 to M.S., HL052490 to M.H. Laughlin, T32 HL007094 and T32 AR048523; a Translational Research Fellowship from the Indiana University School of Medicine to J.M.E.; and an American Heart Association Predoctoral Fellowship to X.L.

2.7. Figure legends

Figure 2.1. Schematic representation showing placement of coronary stent, positioning of IVUS and Doppler flow-wire in the circumflex artery, and IVUS images

A. For CBF determinations, IVUS and Doppler flow-wire (thin line in CFX) information were collected from a position in the circumflex (CFX) artery proximal to the coronary stent. The full length of the circumflex artery was interrogated with IVUS (thicker solid line in CFX) at stent placement and 3 weeks later. The non-stented left anterior descending (LAD) artery was interrogated with IVUS only at sacrifice and the right coronary (RC) was not interrogated. B. Representative IVUS image of coronary artery with minimal atherosclerosis. Arrows indicate location of lumen and artifact caused by IVUS catheter. C. Image indicating percent degree atheroma calculation. This artery shows 300 degrees of atheroma (wall coverage) of a thin (<0.3 mm) layer of intimal thickening. Degrees of atheroma for an interrogated artery were summed and divided by (360/mm * length of vessel in mm). This was multiplied by 100 to yield % degrees atheroma to normalize for different lengths of arteries [95].

Figure 2.2. Coronary blood flow change in response to vasodilators

Coronary blood flow change in response to intracoronary bolus injection of endothelium-dependent vasodilator bradykinin (A) or endothelium-independent vasodilator adenosine (B) at different doses. Flow signal was measured with an intracoronary flow-wire placed under the guidance of coronary angiogram as

described in methods section. * denotes $p<0.05$, C or HX vs. H (A) or HX vs. H (B); ** denotes $p<0.001$, C vs. H.

Figure 2.3. Percent stenosis in areas 5 mm proximal to stented section and in-stent section in H compared to control and HX.

A. Represents a diagram of the circumflex artery and relative location of the stented section and the sections proximal to the stent. B. Representative image of the method used to calculate intima and media areas in histological section. Arrowheads indicate location of some stent struts and arrows indicate artery luminal border. Internal and external elastic laminas and neointima are identified. C. Representative images of each histological section. Stented sections of the circumflex artery were stained with Verhoeff-van Gieson stain to accentuate the internal and external elastic lamina. Areas of neointima and lumen were quantified to calculate percent stenosis values. D. Summary data for the percent stenosis determined at the location 5 mm proximal to the stent (peri-stent CAD). * denotes $p<0.05$, H vs. C and HX. E. Summary data for the percent stenosis obtained from histological analysis within the stent. There were no significant differences across groups within the stent.

Figure 2.4. Myocardium coronary microvessel density in H, HX, vs. C after stenting

Left ventricular sections obtained from each animal 3-week after stenting were preserved in formalin and stained with an antibody for smooth muscle α actin to

identify arteriolar microvessels. A-C. Representative section of left ventricular tissue from C, H, and HX animal. D. Summary data for the microvessel density obtained from immunohistochemical analysis in the myocardium. * indicates areas of cardiac muscle, arrow indicates coronary microvessels.

2.8. Figures

Figure 2.1. Schematic representation showing placement of coronary stent, positioning of IVUS and Doppler flow-wire in the circumflex artery, and IVUS images

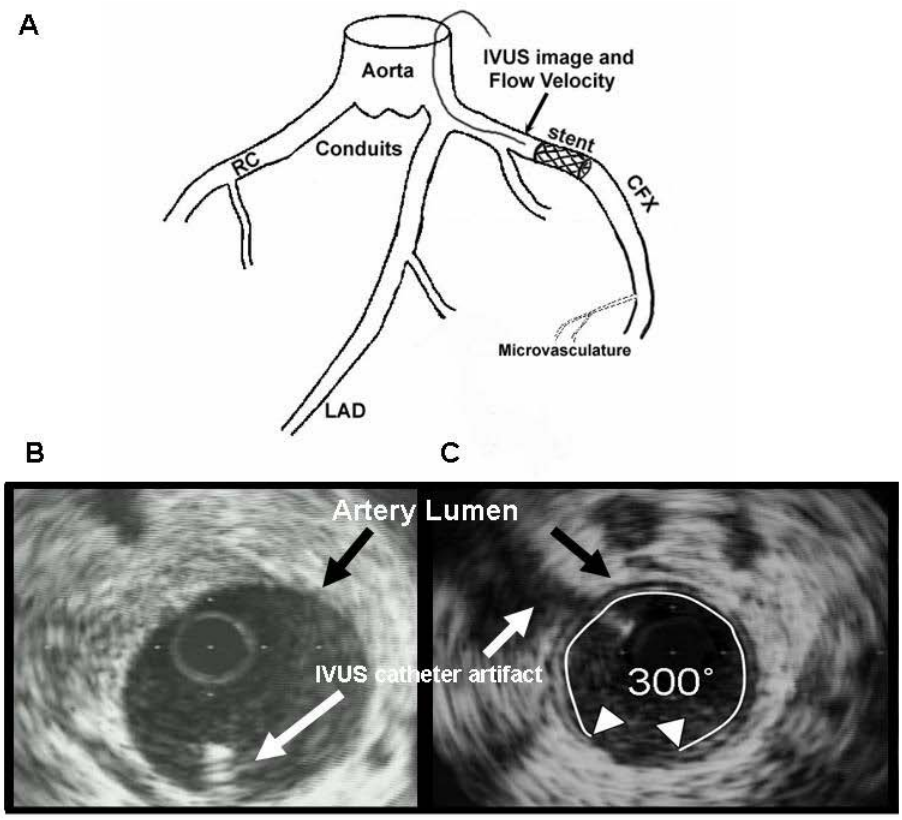

Figure 2.2. Coronary blood flow change in response to vasodilators

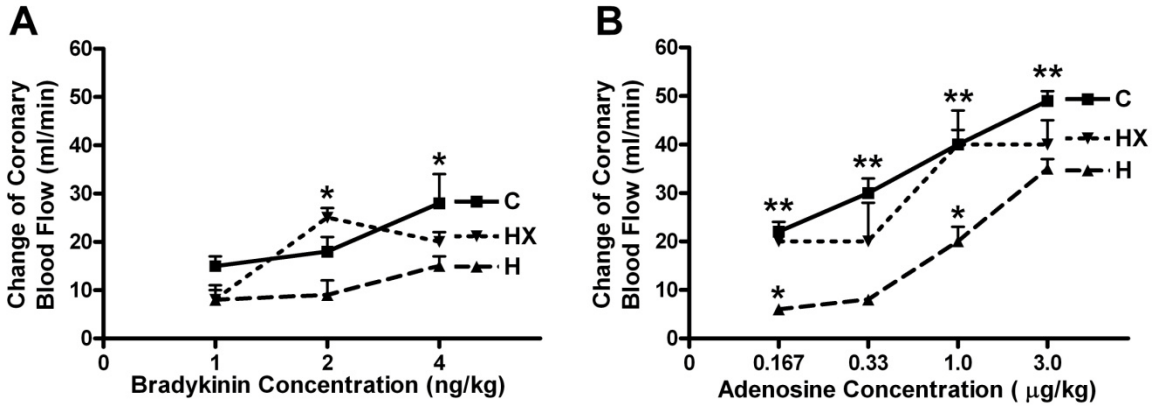

Figure 2.3. Percent stenosis in areas 5 mm proximal to stented section and in-stent section in H compared to control and HX

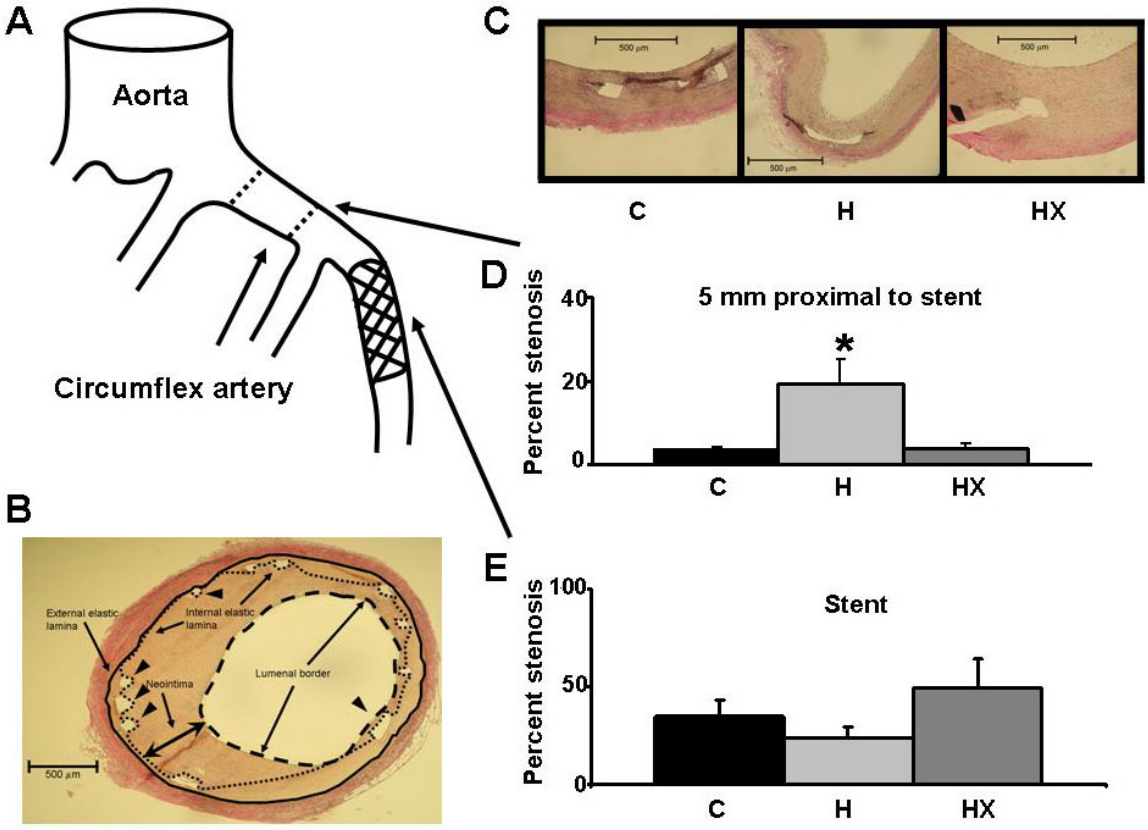

Figure 2.4. Myocardium coronary microvessel density in H, HX, vs. C after stenting

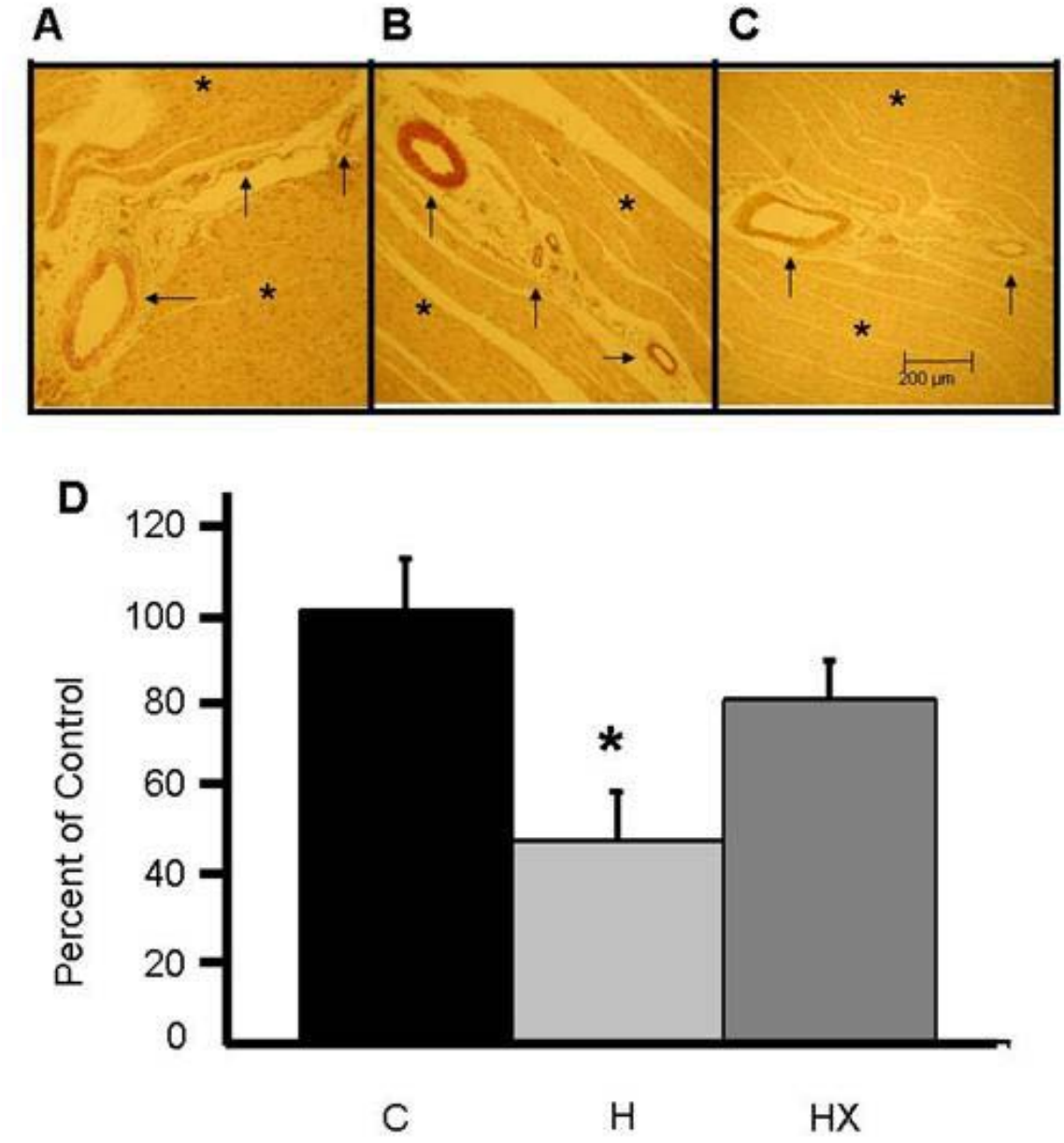

2.9. Tables

Parameter	C	H	HX	Significance
		Phenotypic characteristics		
Weight (kg)	59 ± 2	59 ± 4	58 ± 3	None
Total Cholesterol (mg/dL)	52 ± 4	466 ± 78	393 ± 112	C vs. H, HX
LDL (mg/dL)	14 ± 3	408 ± 72	332 ± 115	C vs. H, HX
HDL (mg/dL)	30 ± 3	51 ± 4	50 ± 8	C vs. H, HX
LDL/HDL	0.53 ± 0.1	7.97 ± 0.8	7.75 ± 3.4	C vs. H, HX
TG (mg/dL)	34 ± 5	41 ± 9	61 ± 34	None
Systolic Blood Pressure (mm Hg)	77 ± 4	76 ± 6	86 ± 6	None
Diastolic Blood Pressure (mm Hg)	50 ± 4	52 ± 6	57 ± 6	None
Heart Rate (bpm)	88 ± 6	77 ± 9	105 ± 9	None
MAP (mm Hg)	59 ± 4	60 ± 6	67± 6	None
RPP (bpm × mm Hg)	6730 ± 580	5800 ± 820	9000 ± 820	None
CSA (mm^2)	12 ± 3	12 ± 2	12 ± 3	None
Heart Weight (g)	235 ± 12	265 ± 18	236 ± 7	None
		Submaximal stress test heart rate (bpm) exercise		
Start exercise training	----	----	200 ± 30	----
Mid exercise training	----	----	160 ± 40	----
End exercise training	----	----	160 ± 10	End < Start

Table 2.1. Phenotypic characteristics of C, H, and HX and adaptations to exercise.

LDL = low-density lipoprotein, HDL = high-density lipoprotein cholesterol, TG = triglycerides, MAP = mean arterial pressure, RPP = rate pressure product, CSA = conduit cross sectional area. Statistical significance at $p<0.05$.

CVR (mmHg/ml/min)	C	H	HX	Significance
Baseline	1.46 ± 0.14	2.22 ± 0.23	0.96 ± 0.05	C vs. H, HX, H vs HX
Adenosine (µg/kg)				
0.167	0.96 ± 0.08	1.80 ± 0.20	0.83 ± 0.03	C vs. H
0.33	0.88 ± 0.10	1.60 ± 0.15	0.86 ± 0.16	C vs. H
1	0.71 ± 0.05	1.18 ± 0.07	0.67 ± 0.03	C vs. H
3	0.58 ± 0.05	0.91 ± 0.13	0.60 ± 0.03	C vs. H
Bradykinin (ng/kg)				
1	1.14 ± 0.08	1.72 ± 0.14	0.86 ± 0.11	C vs. H, HX, H vs HX
2	1.01 ± 0.06	1.71 ± 0.38	0.73 ± 0.15	C vs. H, HX, H vs HX
4	0.82 ± 0.06	1.34 ± 0.05	0.80± 0.13	C vs. H, HX, H vs HX

Table 2.2. Short-term exercise training prevents coronary vascular resistance (CVR) derangements.

Statistical significance at $p<0.05$.

% Degree Atheroma	C	H	HX	Significance
CFX	35.2 ± 5.5	59.5 ± 12.5	23.0 ± 1.1	C vs. H, HX, H vs HX
LAD	0	17.9 ± 2.4	3.9 ± 0.3	C vs. H, HX, H vs HX

Table 2.3. Short-term exercise training prevents overall atheroma burden.

Statistical significance at $p<0.05$.

CHAPTER 3. ADENOSINE RECEPTOR REGULATION OF CORONARY BLOOD FLOW IN OSSABAW MINIATURE SWINE

Xin Long, Eric A. Mokelke, Zachary P. Neeb,

Mouhamad Alloosh, Jason M. Edwards, and Michael Sturek

Department of Cellular & Integrative Physiology

Indiana University School of Medicine, Indianapolis, IN 46202-5120

Running title: Adenosine receptors and coronary blood flow

Corresponding author:

Michael Sturek, Ph.D.

Professor and Chair

Department of Cellular & Integrative Physiology

Indiana University School of Medicine

635 Barnhill Drive, MS 385

Indianapolis, IN 46202-5120

Phone 317-274-7772

FAX 317-274-3318

Email msturek@iupui.edu

3.1. Abstract

Adenosine clearly regulates coronary blood flow; however, contributions of specific adenosine receptor (AR) subtypes (A1R, A2AR, A2BR, A3R) to coronary flow in swine have not been determined. ARs generally decrease (A1R/A3R) or increase (A2A/2BR) cAMP, a major mediator of vasodilation. We hypothesized that A1R antagonism potentiates coronary vasodilation and that coronary stent deployment in dyslipidemic Ossabaw miniature swine elicits impaired vasodilation to adenosine that is associated with increased A1R/A2AR expression. The left main coronary artery was accessed with a guiding catheter allowing intracoronary infusions. Following placement of a flow-wire into the left circumflex coronary artery the responses to bolus infusions of 0.167, 0.33, and 1 μg/kg adenosine were obtained. Steady state infusion of other AR-specific agents utilized a small catheter fed over the flow-wire in lean swine. Flow was increased by the nonselective A2R agonist CV1808 dose-dependently. No other AR subtype-specific agents changed baseline flow, except the highly A1R-selective antagonist DPCPX, which increased baseline flow. The A2R antagonist DMPX and A2AR specific antagonist ZM241385 abolished adenosine-induced flow, while A2BR and A3R antagonism had no effect. Dyslipidemia and stenting decreased adenosine-induced flow ~70%, while A1R, A2AR, and A2BR mRNA were upregulated >5-fold in microvessels distal to the stent. Conclusions: In healthy Ossabaw swine A1R antagonism by DPCPX positively regulated coronary vasodilation under basal conditions. Impaired adenosine-induced flow

after stenting in dyslipidemia is most likely due to altered balance between A1R and A2AR signaling.

3.2. Introduction

Adenosine contributes to maintenance of coronary blood flow, especially during cardiac ischemia [51, 136-138] and is used clinically to elicit maximal vasodilation to diagnose flow-limiting conduit artery stenosis and microvascular dysfunction [139]. Four different subtypes of adenosine receptors (AR) have been cloned and pharmacologically characterized - A1R, A2AR, A2BR, and A3R [51]. All are G-protein coupled and either inhibit (A1R/A3R, Gi/q) or stimulate (A2A/2BR, Gs) adenylyl cyclase [51]. Adenosine predominantly dilates arterioles <100 µm in diameter [138] and the vasodilatory mechanism is not fully understood yet, but involves A2 receptor activation and consequent elevation of cAMP-dependent protein kinase (PKA), resulting in vasodilation mainly via opening of ATP-sensitive K^+ (K_{ATP}) channels [140, 141] and voltage-dependent K^+ (K_v) channels [142, 143]. Since the A1R inhibit and A2R stimulate adenylyl cyclase [51], A1R antagonism could positively modulate coronary vasodilaton. Tawfik etc. [144] provided outstanding evidence for A1R regulation of coronary blood flow in an A1R knockout mouse, but surprisingly studies have not been done on A1R in large animals that more closely mimic human coronary physiology.

Deployment of a stent in a flow-limiting coronary atherosclerotic lesion results in substantial improvement in functional capacity and quality of life.

However, almost one third of patients undergoing coronary stenting eventually experience recurrent angina [99]. It has been shown that coronary stenting induces downstream microvascular dysfunction that persists for weeks and has been implicated in causing exertional ischemia [56-60]. Camici and Crea [60] termed this phenomenon post-stent "iatrogenic coronary microvascular dysfunction", which may be due to enhanced alpha-adrenergic constriction [100], chronic impairment of microvascular response [57, 58], or microemboli that may cause microinfarcts [101]. The mechanisms for microvascular dysfunction associated with stenting remain unclear and deserve careful study. This is especially important because drug-eluting stents, which are the main treatment for flow-limiting coronary lesions, cause even greater microvascular dysfunction than bare metal stents [103, 104].

Dyslipidemic and metabolic syndrome patients displayed impaired adenosine receptor-mediated coronary flow reserve [60, 61], which has been shown convincingly in dyslipidemic swine models by in vivo flow measures [145]. ARs may be responsible for the dysregulated adenosine-induced coronary flow in dyslipidemia. Recently, our lab made a novel discovery that A1R mediate mitogenic effects of adenosine in porcine coronary artery smooth muscle cells, while having minimal effects in aortic smooth muscle cells [65, 69, 70]. Further, A2BR mediated antimitogenic effects in aortic, but not coronary, smooth muscle cells and the A2AR had no effect on mitogenesis in coronary and aortic cells [65-68]. Thus, there is high specificity of AR functions that is dependent on AR subtype, vascular bed, species, etc. Since the vasodilatory effect of adenosine involves

A2R activation [140-143], we propose that A2R and A1R may contribute to impaired adenosine-induced coronary flow in longer duration dyslipidemia after stenting.

We tested two major hypotheses in the present study: 1) A1R antagonism potentiates coronary vasodilation in healthy Ossabaw swine, and 2) coronary stent deployment in dyslipidemic Ossabaw swine elicits impaired vasodilation to adenosine, which is associated with increased A1R/A2AR expression in the microvessels downstream from stented conduit arteries.

3.3. Methods

3.3.1. Animal care and coronary stenting

All protocols involving animals were approved by an Institutional Animal Care and Use Committee and complied fully with standards [105, 106]. Ten control male Ossabaw swine (age 14±4 months) were fed a diet consisting of mini pig chow with 22% kcal from protein, 70% kcal from carbohydrates, and 8% kcal from fat. The data in Figure 3.1, Figure 3.2, and Figure 3.3 were all obtained from those pigs. Another ten male Ossabaw swine (age 14 months; n=5/group) were randomized to control or dyslipidemic groups in the stenting study. The data in Figure 3.4 and Figure 3.5 were obtained from the pigs in the stenting study. The atherogenic diet was composed of mini pig chow supplemented with (percent by weight): cholesterol 2.0, coconut oil 17, corn oil 2.5, and sodium cholate 0.7. This mixture yielded a diet of 13% kcal from protein, 40% kcal from carbohydrates and 47% kcal from fat [107]. Control and dyslipidemic groups were calorie-matched

(3200 kcal/day) for 43 weeks until sacrifice. After 40 weeks on the diets, control and dyslipidemic groups in the stenting study received a bare metal stent (2.5-4.0 mm diameter by 8 mm length; Express2, Boston Scientific, Minneapolis, MN) in the circumflex coronary artery at stent/artery ratio of 1.0 with optimal inflation pressure and recovered for 3 weeks before sacrifice as described previously [11, 70, 92, 109]. Swine received 325 mg aspirin as antiplatelet therapy starting the day before the stenting and continuing for 3 weeks after stenting until completion of the study. Cephalexin (1000 mg) was given twice a day for six days following the stent procedure. All pigs were housed and fed in individual pens and provided a 12-hr light/12-hr dark cycle. Water was provided ad libitum.

3.3.2. Coronary blood flow

The pigs were pre-anesthetized using telazol/xylazine and maintained using 2-4% isoflurane with oxygen. Heart rate, blood pressure, respiratory rate, oxygen saturation, and electrocardiographic data were continuously monitored. The right femoral artery was accessed by surgical cut-down and an 8 F vascular introducer sheath was inserted followed by administration of heparin (200 U/kg). A Cordis 8 F Amplatz L (sizes 0.75-2.0) guiding catheter was advanced into the aortic arch and a guiding catheter was engaged with the ostium of the left main artery. A 0.014-inch diameter Doppler flow-wire (JoMed Inc., Rancho Cordova, CA) or combination pressure- and flow-wire (ComboMap, Volcano Therapeutics, Inc., Rancho Cordova, CA) was advanced down the circumflex artery under angiographic guidance and a non-branching section was selected for baseline

and drug-induced flow measurements [92, 107]. Anatomical landmarks were noted in case the wire moves and requires re-positioning. In some of the pigs an intravascular ultrasound (IVUS; 3.2 F 30 MHz, Boston Scientific, Inc.) catheter was then advanced over the flow-wire and positioned in the circumflex to align the IVUS imaging transducer with the flow-wire tip to obtain accurate diameter measurement of the artery at the location where the flow velocity measurements were acquired [107] (Figure 3.1). For constant infusion of drugs the IVUS catheter was placed with only the tip in the most proximal circumflex and drugs were infused through the IVUS catheter. Flow velocity signals were allowed to stabilize for several minutes for determination of coronary blood flow (CBF) velocity responses. For the pigs with stent deployment, coronary blood flow analysis of in vivo microvascular function was done 3 weeks following stenting and in a non-branching section of the circumflex artery proximal to the stent.

Hyperemia was induced with 3 mL bolus doses of the endothelium-independent vasodilator adenosine (0.167, 0.33, and 1 μg/kg) given via the guiding catheter into the coronary artery as we described [107] and is identical to clinical catheterization assessment in humans [139]. Adenosine injection was followed by 10 mL saline flush. Saline artifact was tested in each animal and, if present (usually less than 10% peak APV induced by adenosine), was subtracted from subsequent flow measurements following bolus. Peak average peak velocity (APV), heart rate, and blood pressure were recorded for each adenosine administration. Figure 3.1A shows baseline instantaneous CBF velocity

measures oscillating in systole and diastole during baseline (base; left) measures and at the peak response to adenosine. Each APV value was calculated on-line using the automated data acquisition system as an average of instantaneous CBF velocity over 2 consecutive cardiac cycles shown by the systolic (S) and diastolic (D) interval markers in Figure 3.1A. Subsequent doses of adenosine were administered only after APV, heart rate, and blood pressure had returned to baseline and stabilized, at which time the baseline parameters were again documented followed by the administration of the next adenosine dose. The effect of adenosine typically lasted 15-30 seconds (Figure 3.1A; right).

The adenosine A2R non-selective agonist CV1808 (10^{-6}, 10^{-5}, 10^{-4} M) was administered via bolus injection. The IVUS catheter was placed in the proximal circumflex in lean swine for steady state infusion of selected drugs to observe their effects over a relatively longer period of time (CCPA, 10^{-5} M, A1R-selective agonist, Tocris Science, Ellisville, MO; DPCPX, 10^{-4} M, A1R-selective antagonist, Tocris Science; DMPX, 10^{-4} M, A2R non-selective antagonist, Sigma, St. Louis, MO; ZM 241385, 10^{-7} M, A2AR-selective antagonist, Tocris Science; MRS 1706, 10^{-7} M, A2BR-selective antagonist, Tocris Science; MRS 1220, 10^{-7} M, A3R-selective antagonist, Tocris Science) at a rate of 1 mL/minute and was followed by concurrent bolus injection of adenosine. Vehicle control (1% DMSO) for DMPX was not used in parallel, which should be used for future experiments. The vehicle controls for other reagents were either water or phosphate-buffered saline. Continuous infusion of saline flush was done between each constant

infusion treatment to make sure the flow returns to baseline. The drug infusions were done in random order in each pig.

The analog Doppler signals were continuously digitized both as instantaneous CBF velocity and APV values. All flow data were stored on videotape and personal computer for further off-line analysis. Data are also expressed as percent APV increase, which equals to [peak APV-base APV] / base APV × 100. Volumetric CBF was calculated as: CBF (in mL/min) = (artery cross sectional area in cm^2) × (velocity in cm/s) × 0.5 × 60 s/min [107]. Vessel cross sectional area was calculated off-line from recorded IVUS images using the commercially available Sonos Intravascular Imaging software package. Angiography and IVUS showed no change in conduit artery diameter during any drug exposures, thus coronary flow velocity represented microvascular effects.

3.3.3. Plasma lipid assays

Venous blood samples were obtained following overnight fasting and were analyzed for triglyceride and total cholesterol [fractionated into high density lipoprotein (HDL) and low density lipoprotein (LDL) components] [95].

3.3.4. Real-time reverse transcription-polymerase chain reaction (Real-time RT-PCR)

RNA was extracted from coronary microvessels downstream of left circumflex coronary artery using Trizol (Invitrogen, Carlsbad, CA, USA), then

treated with DNase (DNA free, Ambion, Austin, TX, USA) to remove contaminating genomic DNA, and analyzed by NanoDrop spectrophotometer (ND-1000; ThermoScientific, Wilmington, DE, USA) to assess purity (A260/280) and concentration. RNA (1 µg) was converted to cDNA using the iScript cDNA synthesis kit (Bio-Rad, Hercules, CA, USA) in a standard thermocycler (DNA Engine PTC-200, MJ Research, Waltham, MA, USA). A1R, A2AR, A2BR and A3R gene expression were assessed using quantitative real-time RT-PCR in an ABI 7500 instrument (Applied Biosystems, Foster City, CA, USA). Primers for PCR amplification were as follows:

A1R: forward, 5'-GGCCATGCTGGCAATTG-3';
reverse, 5'-CCTGAGCGGGATCTTGACA-3';

A2AR: forward, 5'-CCCCTTCATCTATGCCTACCG-3';
reverse, 5'-CATTCCCTCACACTCCCTCCAC-3';

A2BR: forward, 5'- TGTGCTGGCTGCCTCTTCAC-3';
reverse, 5'-ACACGATGGGGTTGACGACC-3';

A3R: forward, 5'-GAACCTCACCTTCCTTTCCTGC-3';
reverse, 5'-GAACTCCCGTCCATAAAATGC-3'

(Integrated DNA Technologies, Coralville, IA, USA). Taqman probes were used to detect A1R gene amplification and were as follows: 5'-/6-FAM/TCGACCGCTACCTCC/MGBNFQ/-3' (Applied Biosystems). SYBRGreen Universal PCR Master Mix (Applied Biosystems) was used to detect A2AR, A2BR and A3R gene expression followed by a dissociation curve to rule out non-specific amplifications and primer-dimers. All results were normalized to the

signal of 18s RNA, which was amplified in separate reactions using TaqMan Universal PCR Master Mix and TaqMan 18s Detection Reagents (Applied Biosystems).

3.3.5. Data Analysis

Data were presented as means ± SEM. Statistical analysis was performed using commercially available software (SPSS version 12 and Prism version 4.0). Means of more than 2 groups were compared by one way Analysis of variance (ANOVA) with Least Significant Difference (LSD) post-hoc analyses (by SPSS) or by 2 way ANOVA followed by Bonferroni post-test (which is the only option in Prism). Means of 2 groups were compared by student t-test (unpaired, two-tailed). In all cases, $p < 0.05$ was considered statistically significant.

3.4. Results

3.4.1. Metabolic characteristics of healthy control and dyslipidemic pigs with coronary stent deployment

Atherogenic diet resulted in significantly higher plasma total cholesterol, LDL, HDL, and LDL/HDL vs. healthy control pigs fed standard chow diet (Table 3.1). There were no differences in body weight, plasma triglycerides, fasting insulin, fasting glucose (Table 3.1), or resting blood pressure (Table 3.2). The plasma lipids defined the atherogenic diet fed group as dyslipidemia, but not having metabolic syndrome.

3.4.2. Adenosine A2 receptors contribution to coronary blood flow

Instantaneous blood flow velocity shows classical oscillations with diastolic APV exceeding systolic APV (Figure 3.1A, left). A typical doubling of the APV and return to baseline in ~30 s in response to a bolus dose of adenosine (1.0 µg/kg) is shown in Figure 3.1A (right). The A2R non-selective antagonist DMPX did not change base APV (Figure 3.1B), but abolished peak APV (Figure 3.1C) response to adenosine at 0.33 and 1.0 µg/kg doses. The A2R non-selective agonist CV1808 elevated percent APV increase ([peak APV-base APV] / base APV × 100) in a dose-dependent manner in the absence of exogenous adenosine (Figure 3.1D). The CV1808-induced percent APV increase at 10^{-4} M dose was comparable to adenosine-induced percent APV increase at 1.0 µg/kg dose, which was calculated from the base and peak APV in panel B and C.

3.4.3. Adenosine A2A, A2B, and A3 receptors contribution to coronary blood flow

Figure 3.2 displays data as absolute blood flow in pigs in which conduit diameter was accurately measured with IVUS before flow measures. Bolus injection of adenosine in the presence of vehicle control increased peak CBF vs. base in a dose-dependent manner (Figure 3.2A). Continuous intracoronary infusion of the A2A-selective antagonist ZM241385 abolished the adenosine-induced peak CBF (Figure 3.2E), while having no effect on baseline CBF (Figure 3.2A and B). The A2BR-selective antagonist MRS1706 (Figure 3.2E) and A3R-selective antagonist MRS1220 (Figure 3.2F) had modest effects on the

adenosine-induced peak CBF compared to ZM241385 and no effect on base CBF (Figure 3.2A, C, and D).

3.4.4. Adenosine A1 receptors contribution to coronary blood flow

Constant infusion of the highly A1R-selective antagonist DPCPX increased base APV in the absence of exogenous adenosine and peak APV response to 1.0 μg/kg adenosine (Figure 3.3). The highly A1R-selective agonist CCPA did not alter base APV in the absence of exogenous adenosine nor alter peak APV response to adenosine (Figure 3.3).

3.4.5. Comparison of coronary blood flow in control and dyslipidemic pigs undergoing stenting

There were no significant differences in hemodynamic characteristics across groups (Table 3.2), e.g. heart rate, mean arterial pressure, rate pressure product, and baseline coronary blood flow. The CBF (Figure 3.4) response to 0.167, 0.33, and 1.0 μg/kg adenosine was decreased in dyslipidemic vs. healthy control pigs 3-week after stenting.

3.4.6. Adenosine receptors expression in coronary microvessels in control and dyslipidemic pigs 3-week after the stent deployment

A1R, A2AR, and A2BR mRNA in coronary microvessels downstream from the stented left circumflex coronary artery were upregulated >5-fold in dyslipidemic

compared to control pigs (Figure 3.5A-C). A3R mRNA was not different between groups (Figure 3.5D).

3.5. Discussion

We present several key findings on adenosine regulation of coronary blood flow. First, adenosine-induced vasodilation was mediated almost exclusively by A2A receptors (A2AR) in Ossabaw swine. Second, adenosine A1 receptors (A1R) antagonism augments vasodilatory effects of some vasodilators other than adenosine in porcine coronary microvessels under basal condition in vivo. Third, bare metal stent deployment in conduit coronary arteries and dyslipidemia in Ossabaw swine elicited microvascular dysfunction, which was associated with increased A1R and, paradoxically, increased A2AR and A2BR expression. Collectively, these data emphasize the delicate balance between A1R and A2AR signaling in control of coronary blood flow in the setting of stenting and dyslipidemia.

Interestingly, there is variance in peak APV response to exogenous adenosine among different animals. Peak APV response to adenosine was partially blunted in Figure 3.3 vs. Figure 3.1C, which coincided with some human studies [146]. It was suggested that varied potencies of adenosine-induced dilations among patients resulted in inconsistent potency of dilations between figures [146]. It is possible that among Ossabaw swine there were variable potencies of dilation in response to adenosine due to differences in age, genetic background, relative

health status, etc. Therefore, the inconsistency in dilation potencies to adenosine could lead to variations in response to adenosine between figures (Figure 3.1C and Figure 3.3)

It was reported that adenosine was a vasodilator in porcine coronary microcirculation via activation of A2AR [147-149]. A2BR was suggested to mediate vasodilation of adenosine in human small coronary arteries [150], rat coronary circulation [151] and murine heart [149, 152]. A3R either inhibited or negatively modulated the vasodilatory effect of adenosine in mouse coronary circulation [153]. Studies in pigs [154] and humans [146] demonstrate A1R mRNA and protein expression in coronary arterioles. In our current study, the non-selective A2R antagonist DMPX did not change base APV (Figure 3.1B); therefore, A2R were not tonically activated under normal, baseline conditions. The A2AR-selective antagonist ZM241385 decreased peak CBF induced by exogenous adenosine (Figure 3.2E), while MRS1706 and MRS1220 showed relatively little effect (Figure 3.2E and F), thus providing evidence that mainly A2AR mediates vasodilatory effects of exogenous adenosine in Ossabaw swine. The highly A1R-selective antagonist DPCPX increased base APV in the absence of exogenous adenosine (Figure 3.3), indicating A1R antagonism by DPCPX might potentiate vasodilatory effects of some physiologically active vasodilators other than adenosine. In contrast, the highly A1R-selective agonist CCPA did not change APV whether in the absence or presence of exogenous adenosine. There are several possible reasons for that. First, CCPA effect could be masked by

endogenous adenosine. Since the binding affinity of adenosine for A1R is higher than A2R, and the desensitization of A1R is much slower than A2R ($t_{1/2}$ = 10 hours vs. 20 minutes) [155], it could be that tonically A1R was activated by adenosine while A2R was not. Second, we used 10^{-5} M CCPA for steady state intracoronary infusion (1 mL/min), which was diluted by continuous coronary blood flow (~20 mL/min) and might not be effective enough to regulate coronary flow. Research done in the isolated hearts from A1R knockout and wild type mice showed that at higher (10^{-5} M) instead of lower concentration (10^{-9}-10^{-7} M) CCPA increased coronary blood flow [144]. Intracoronary infusion of CCPA at different concentrations may help to address that.

Our data support the A1R antagonism-mediated porcine coronary vasodilation, consistent with research done by Pelleg etc. [156] in canine heart and Tawfik etc. in A1R knockout mouse heart [144]. However, Hein etc. [147] suggested that A1R are not functionally significant in porcine microvessels, since A1R blockade did not alter arteriolar dilation to adenosine, consistent with other reports that A1 antagonism did not affect adenosine induced vasodilatation in swine heart [141, 154]. There are several possible reasons for the discrepancies regarding the role of A1R in adenosine-induced CBF, e.g. the difference in experimental design, animal species, and developmental state. A major factor is that Hein etc. [147] used healthy, juvenile domestic pigs, while we used sexually mature adult Ossabaw pigs that are predisposed to metabolic syndrome [11, 70, 92, 142, 157]. Another very important factor for explanation of the difference is the

experimental preparation. Our studies and others were done in vivo [144, 156], while other studies used isolated coronary arterioles in vitro [141, 147, 154]. It is clear that in vitro manipulation cannot always be applied directly to in vivo conditions. The local environment changes once arterioles are isolated from the live animals and the drug dose response and time course can be different between in vivo and in vitro studies. Most importantly, the systemic metabolic feedback and sympathetic feedforward network system can be lost by isolation from the integrated system. We feel more confident in our in vivo study compared to those in vitro studies, although in vitro experiments usually can provide us more flexibility and possibility of manipulation.

Based on our current studies, A2R were not tonically activated under normal, basal conditions, which did not support a role of adenosine in maintenance of CBF under basal conditions. This finding was echoed by numerous studies done under basal conditions and in exercise hyperemia in the normal heart of dogs, swine, or humans [136, 138, 158-160]. However, adenosine plays an important role in coronary vasodilation when the myocardium is ischemic or hypoxic and abundant adenosine release arises [136, 138, 146, 160, 161].

Ossabaw swine are predisposed to metabolic syndrome [11, 70] and possible coronary microvascular dysfunction compared to other animal models. Dyslipidemia in the present study was manifested as described previously [11, 92, 142, 157]. Interestingly, A1R, A2AR, and A2BR genes were all upregulated in

coronary microvessels distal to the stent in dyslipidemic swine (Figure 3.5). The A2BR gene upregulation was reported in ischemic mouse heart [162]. We made a novel discovery that A1R was upreguated in microcirculation downstream from the stent in dyslipidemia. Why did adenosine-induced CBF decrease in the presence of A2AR and A2BR gene upregulation? There are several possible explanations. First, receptor mRNA does not correspond directly to receptor protein. Also, receptor protein, i.e., A2AR and A2BR, may not function normally, especially under the influence of stenting and dyslipidemia. Second, the most important reason could be that the affinity of adenosine for A1R is higher than A2R, and the desensitization of A1R is much slower than A2R ($t_{1/2}$ = 10 hours vs. 20 minutes) [155]. The net result is greater coupling of A1R to adenosine, while less coupling of A2R to adenosine, to regulate CBF. Since A1R gene expression increased in coronary microcirculation in stented, dyslipidemic pigs and A1R could have been occupied with high affinity by adenosine, A1R activation possibly overcame the vasodilatory effect of adenosine mediated by A2R in case of possible elevated adenosine in stenting and dyslipidemia. Third, some other factors besides adenosine receptors are responsible for adenosine-induced vasodilation, e.g., K_{ATP} channels, prostaglandins, etc. [138]. It could be that A1R but not A2R are negatively linked to those factors in regulation of adenosine-induced flow, which deserves further study in the Ossabaw swine.

To our knowledge, this is the first study examining the effects of stenting on coronary microcirculation in a porcine model of dyslipidemia. Stenting and

early dyslipidemia are two possible causes for the dysregulation of adenosine-induced CBF in dyslipidemic Ossabaw swine after 3-week stent deployment (Figure 3.4). Despite the findings that adenosine receptor-mediated coronary flow was impaired in dyslipidemic and metabolic syndrome patients [60, 61], as well as in dyslipidemic swine models [145], previous study in our lab [107] showed that diabetic dyslipidemia in Yucatan pigs did not cause microvascular dysfunction ($0.05<p<0.1$). Coronary stenting has been shown to mechanically damage vascular cells in the target conduit artery segment and endothelium in peri-stent segments [55], and induces downstream microvascular dysfunction [56-60]. However, none of those studies were done in a swine model of dyslipidemia prone to metabolic syndrome and the microcirculation dysfunction was either attributable to endothelium [56] or unclarified [57-59]. Further studies are needed to clarify 1) whether dyslipidemia or stenting alone or the combinations of those two are the cause for the impaired adenosine-induced flow in the setting of dyslipidemia and stenting, and 2) which adenosine receptors are responsible for the flow dysregulation.

We conclude that A1R antagonism by DPCPX might promote vasodilation induced by some vasodilators other than adenosine in “healthy”, anesthetized Ossabaw swine. An imbalance of A1R/A2AR upregulation and signaling in coronary microcirculation distal to a stent may be responsible for the dysregulated adenosine-induced CBF in dyslipidemia. The use of novel

adenosine analogs for vasodilation in the diseased condition deserves further pharmacological and mechanistic study.

3.6. Acknowledgments

The authors thank James Byrd and James W. Wenzel for their excellent technical assistance. This work was supported by National Institutes of Health [grants RR013223, HL062552] to M.S.; Boston Scientific, Inc.; Research Animal Angiography Laboratory of Indiana Center for Vascular Biology & Medicine; Purdue-Indiana University Comparative Medicine Program; Fortune-Fry Ultrasound Research Fund; Indiana University School of Medicine Translational Research Fellowship to J.M.E. and Z.P.N.; National Institutes of Health Translational Research Fellowship [grant UL1 RR025761] to Z.P.N.; and an American Heart Association Predoctoral Fellowship to X.L.

3.7. Figure legends

Figure 3.1. Vasodilation effect of adenosine mediated by adenosine A2 receptors (A2R)

A. Left panel, instantaneous coronary blood flow velocity (cm/s) responses to adenosine during diastole and systole. Base and peak are indicated at the bottom. The start of systole (S) and diastole (D) are indicated by the horizontal lines. Right panel, typical average peak coronary blood flow velocity (APV, cm/s) response to 1.0 μg/kg adenosine vs. time; B-baseline APV, S-time for starting the search for adenosine-induced peak APV, P-peak APV in response to 1.0 μg/kg

adenosine. B, C. Effects of continuous intracoronary infusion of A2R non-selective antagonist DMPX on base APV (B) and peak APV (C) during concurrent bolus injection of 0, 0.167, 0.33, or 1.0 μg/kg adenosine (n=5). Flow signal was measured with an intracoronary flow-wire placed under the guidance of coronary angiogram as described in methods section. D. Effects of intracoronary bolus injection of the A2R non-selective agonist CV1808 on percent APV increase (percent APV increase = [peak APV-base APV] / base APV × 100; n=5). Ado only means pure adenosine dose response, Ado+DMPX means adenosine dose response with concurrent continuous infusion of DMPX. *, $p<0.05$; #, $p<0.001$, vs. Ado only at corresponding dose or as indicated by lines.

Figure 3.2. Adenosine A2A receptors (A2AR), not A3R, contributed to adenosine-induced vasodilation

Base and peak coronary blood flow measurement in typical adenosine dose responses was done in control animals (n=5) as described in Figure 3.1, except that conduit diameter measures enabled calculation of volumetric blood flow. Effects of continuous intracoronary infusion of vehicle control (A), A2AR-selective antagonist ZM241385 (B), A2BR-selective antagonist MRS1706 (C), or A3R-selective antagonist MRS1220 (D) on base and peak coronary blood flow during concurrent bolus injection of adenosine at 0.167, 0.33, or 1.0 μg/kg were depicted. Peak CBF was compared between A2A/2BR antagonism (E) or A3R antagonism (F) and vehicle control. * denotes $p<0.05$, # $p<0.001$, peak vs. base

CBF (A-D), or ZM241285 vs. vehicle control (E) at corresponding adenosine doses.

Figure 3.3. Contribution of adenosine A1 receptor (A1R) to coronary blood flow

Highly A1R-selective agonist CCPA, A1R-selective antagonist DPCPX, or vehicle control was constantly infused through an intracoronary catheter. After coronary blood flow was stabilized, base average peak velocity (APV) was measured (n=10). Concurrent bolus injection of adenosine at 0.167, 0.33, or 1.0 μg/kg was done afterwards and flow signal was measured as in Figure 3.1. Effects of CCPA and DPCPX on peak APV upon adenosine bolus injection was depicted vs vehicle control. *, $p<0.05$ vs. vehicle control at corresponding adenosine dose or at baseline.

Figure 3.4. Adenosine induced coronary flow in control and dyslipidemic pigs undergoing stenting

Flow signal was measured in a non-branching section of the left circumflex coronary artery in control and dyslipidemic pigs 3-week after stenting (n=5/group). Bolus injection of adenosine at 0.167, 0.33, or 1.0 μg/kg was done as in Figure 3.2 to elicit peak CBF response. Change of CBF means peak CBF-base CBF. * indicates $p<0.05$ vs. control.

Figure 3.5. Adenosine receptors expression in coronary microvessels in control and dyslipidemic pigs 3-week after the stent deployment

Gene expression levels of A1R, A2AR, A2BR, and A3R in panels A, B, C, and D, respectively, were determined by real-time RT-PCR in mRNA isolated from coronary microvessels distal from stented coronary conduit segments in control and dyslipidemic pigs (n=5/group). *, $p<0.05$ vs. control.

3.8. Figures

Figure 3.1. Vasodilation effect of adenosine mediated by adenosine A2 receptors (A2R)

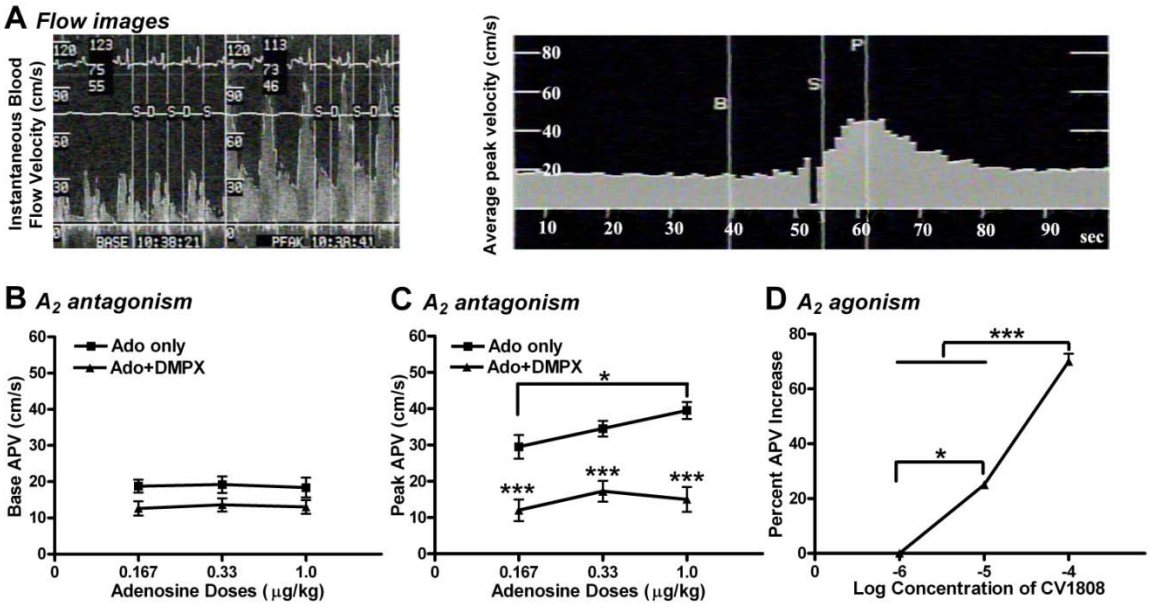

Figure 3.2. Adenosine A2A receptors (A2AR) not A3R contributed to adenosine induced vasodilation

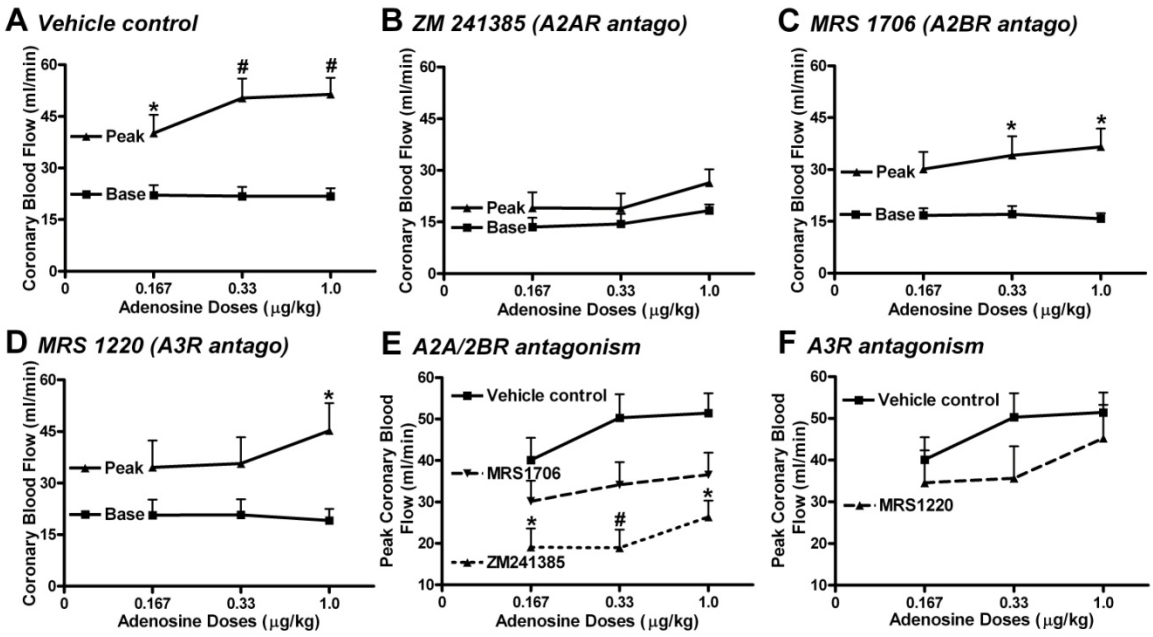

Figure 3.3. Contribution of adenosine A1 receptor (A1R) to coronary blood flow

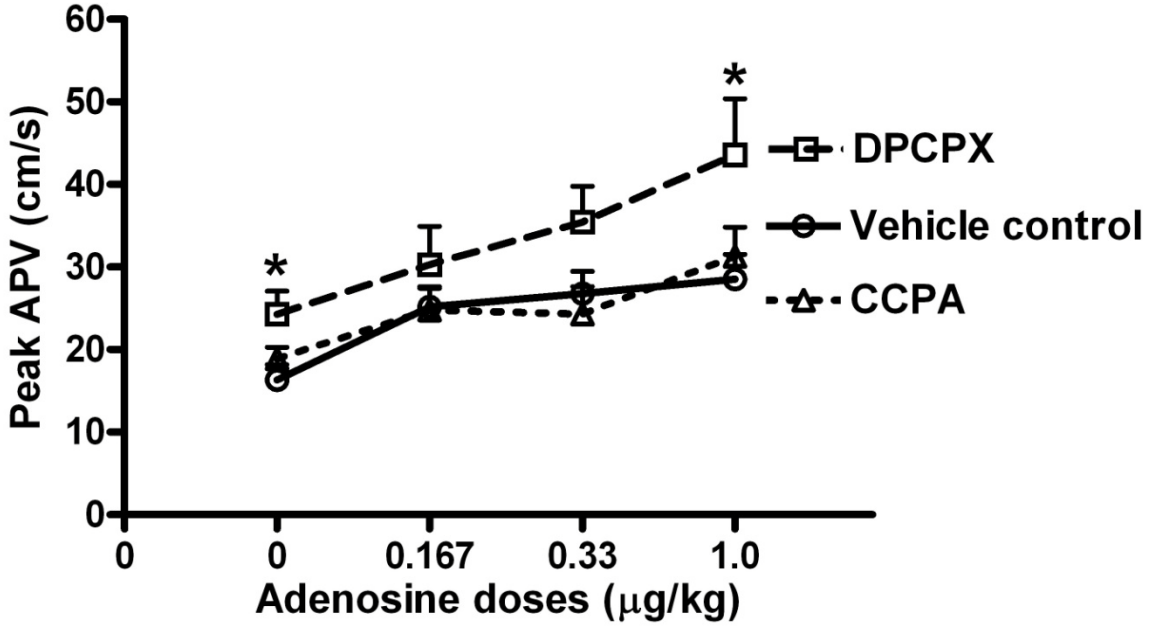

Figure 3.4. Adenosine induced coronary flow in control and dyslipidemic pigs undergoing stenting

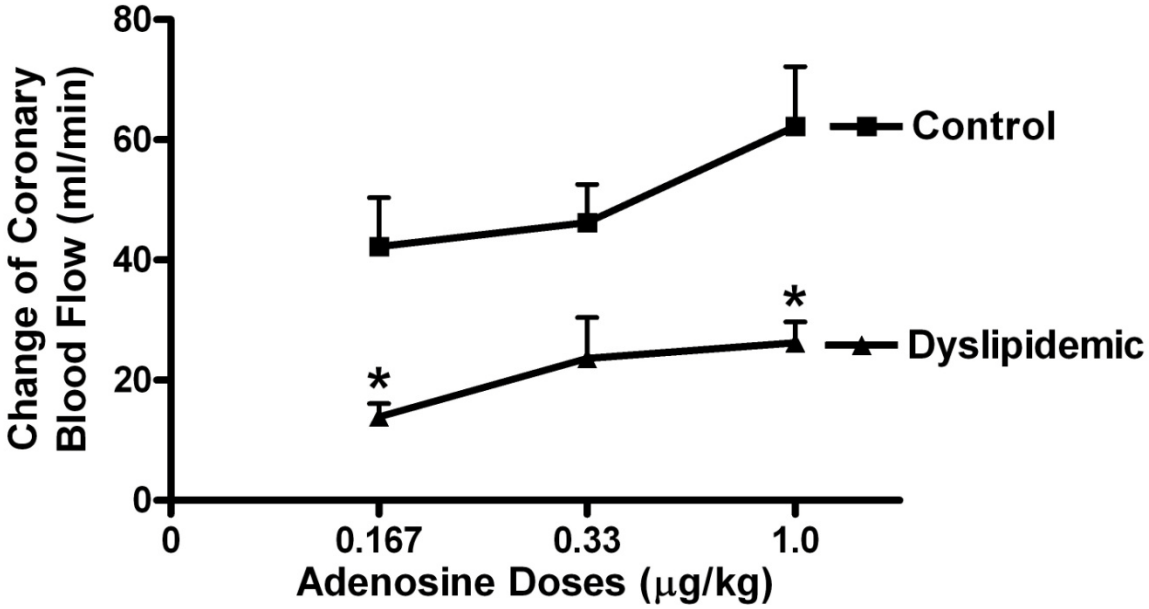

Figure 3.5. Adenosine receptors expression in coronary microvessels in control and dyslipidemic pigs 3-week after the stent deployment

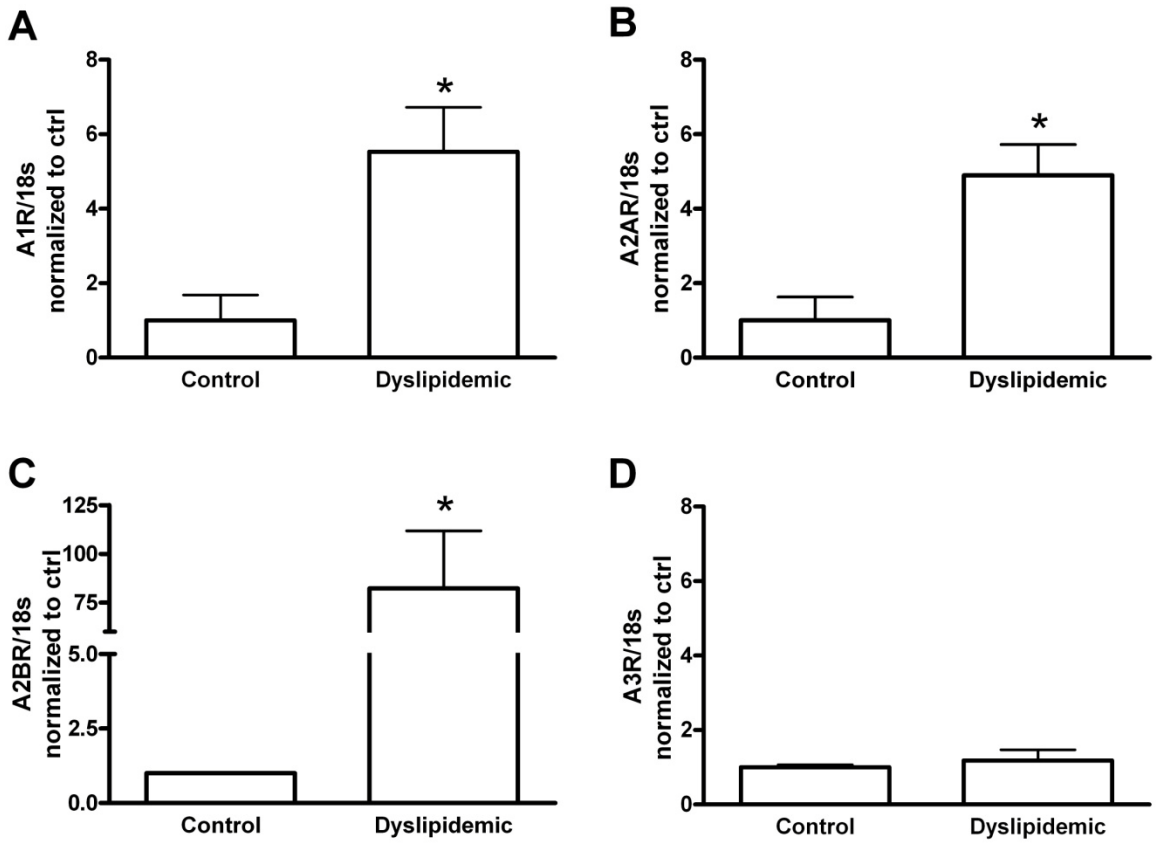

3.9. Tables

Metabolic panel	Control	Dyslipidemic	p value
Body weight (kg)	74 ± 2	76 ± 2	>0.05
Fasting plasma glucose (μU/mL)	74 ± 4	86 ± 5	>0.05
Fasting plasma insulin (mg/dL)	7 ± 1	10 ± 2	>0.05
Total cholesterol (mg/dL)	62 ± 3	299 ± 33	0.0003
LDL (mg/dL)	24 ± 2	216 ± 34	0.001
HDL (mg/dL)	34 ± 1	73 ± 12	0.01
Triglycerides (mg/dL)	19 ± 3	45 ± 12	0.06
LDL/HDL	0.7 ± 0.1	3.6 ± 1.1	0.007

Table 3.1. Metabolic data from control and dyslipidemic pigs with stent deployment.

Hemodynamics	Control	Dyslipidemic	p value
HR (bpm)	101 ± 4	109 ± 4	0.57
SBP (mm Hg)	75 ± 3	76 ± 3	0.78
DBP (mm Hg)	53 ± 3	53 ± 3	0.86
MAP (mm Hg)	60 ± 3	61 ± 3	0.84
RPP (bpm*mm Hg)	7610 ± 820	8340 ± 820	0.54
CBF (mL/min)	46 ± 7	42 ± 6	0.68
CSA (mm^2)	10 ± 1	9 ± 1	0.33

Table 3.2. Hemodynamic characterics comparison during coronary blood flow measures in control and dyslipidemic pigs 3-week after stenting.

HR = heart rate, SBP = systolic blood pressure, DBP = diastolic blood pressure, MAP = mean arterial pressure, RPP = rate pressure product, CBF = coronary blood flow, and CSA = vessel cross sectional area.

CHAPTER 4. ALDOSTERONE REGULATION OF ADENOSINE A1 RECEPTORS IN CORONARY ATHEROSCLEROSIS IN METABOLIC SYNDROME

Xin Long; Raven Elosiebo; Zachary P. Neeb; James P. Byrd;

Mouhamad Alloosh; Michael Sturek

Department of Cellular & Integrative Physiology

Indiana University School of Medicine

Please address correspondence to:

Michael Sturek, Ph.D.

Department of Cellular & Integrative Physiology

Indiana University School of Medicine

635 Barnhill Drive, Room 385

Indianapolis, IN 46202-5120

E-mail: msturek@iupui.edu

Phone: 317-274-7772

Facsimile: 317-274-3318

4.1. Abstract

Background: Coronary artery disease (CAD) is increased several-fold in metabolic syndrome (MetS) and is attenuated by exercise training. We found the adenosine A1 receptor (A1R) paradoxically mediates mitogenic effects of adenosine in cultured coronary smooth muscle cells, suggesting A1R dysregulation could contribute to CAD. Aldosterone is increased in MetS, but the cellular and molecular mechanisms underlying aldosterone actions on the vascular wall are unclear. We utilized the Ossabaw miniature swine model of MetS and CAD and in vitro models of CAD to test the hypothesis that aldosterone regulation of A1R contributes to CAD in MetS and all are attenuated by exercise training. Methods and Results: Lean swine were fed standard chow and sedentary MetS and exercise trained MetS (XMetS) fed excess calorie atherogenic diet for 14 months (n=5/group). Exercise training was 4 d/wk, 30 min/d, at 65-75% maximum heart rate for 7 wk before sacrifice. MetS exhibited all MetS characteristics and none were attenuated in XMetS. MetS had the greatest CAD, aldosterone, and A1R mRNA and protein, which were all attenuated in XMetS. Aldosterone upregulated A1R mRNA and protein expression in subcultured coronary smooth muscle cells. A1R antagonism blocked the increase in medial collagen content in organ culture. Aldosterone further increased medial collagen and aldosterone antagonism partially abolished the effect. Conclusions*:* Aldosterone regulation of A1R in vitro promotes CAD and in vivo in MetS is associated with coronary atherosclerosis and may

contribute to the exercise training-induced attenuation of coronary atherosclerosis.

Key Words*:* adenosine, mineralocorticoid receptor, exercise, Ossabaw miniature swine, spironolactone

4.2. Introduction

Metabolic syndrome (MetS; "pre-diabetes") affects approximately 27% of the U.S. adult population, and is defined as the combination of any three of the following abnormalities: central obesity, dyslipidemia, hypertension, impaired glucose tolerance, and insulin resistance [34]. Coronary artery disease (CAD), the leading cause of death in westernized societies, is increased greatly in patients with MetS [28-33]. Therefore, it is important to delineate cellular and molecular mechanisms underlying coronary atherosclerosis in the setting of MetS.

Phenotypic switching of vascular smooth muscle cells (SMC) from a healthy contractile phenotype to a proliferative (synthetic) phenotype is a pivotal event in CAD [1, 9, 62-64]. SMC contribute to atherosclerotic and fibrotic lesions also through the formation of extracellular matrix, including collagen [1, 9, 14, 62, 63]. Adenosine has been widely shown to elicit coronary vasodilation and attenuate SMC proliferation via adenosine A2A/B receptors, thereby providing cardioprotection [54, 65-68]. Adenosine A1 and A3 receptors are the other 2 adenosine receptor (AR) subtypes cloned and pharmacologically characterized

so far [51]. A pivotal study from our lab demonstrated a trophic effect of adenosine in porcine coronary SMC mediated by the A1R [65, 69]. In addition, A1R expression was upregulated in stented coronary segments compared to non-stented segments in our swine model [70], thus suggesting A1R dysregulation could play a role in CAD.

Renin-angiotensin-aldosterone system (RAAS) blockade exerts potent anti-atherosclerotic effects, not only through antihypertensive actions, but also through anti-inflammatory, anti-proliferative, and antioxidant properties [44, 163]. Aldosterone is synthesized in the adrenal cortex in response to angiotensin II stimulation [164]. Aldosterone antagonism prevented aortic SMC proliferation and vascular inflammation induced by angiotensin II [72, 164-166]. Clinical studies showed aldosterone antagonism reduced morbidity and mortality in patients with heart failure or after myocardial infaction [167, 168], consistent with beneficial effects of angiotensin converting enzyme inhibitors and angiotensin receptor blockers in recent clinical trials [169, 170]. Despite all these exciting findings, the molecular mechanisms underlying aldosterone proatherogenic effects remain elusive to us.

Aldosterone, a steroid hormone, binds to the mineralocorticoid receptor (MR), a ligand-activated transcription factor [164]. The MR belongs to the steroid receptor family that includes the glucocorticoid receptor [46]. Glucocorticoid receptor activation stimulated A1R gene expression in Chinese hamster ovary cells [74], DDT1 MF-2 SMC [75], and rat brain [76]. Both aldosterone and A1R regulate

vascular SMC proliferation via activation of mitogen activated protein kinase in vitro [65, 69, 72, 73]. MR and glucocorticoid receptors share extensive sequence and structural organization similarities [77], therefore MR activation by aldosterone could potentially regulate A1R expression, thereby contributing to coronary atherosclerosis. Finally, since elevated plasma aldosterone is a hallmark of "obesity hypertension" [71], the systemic milieu in MetS seems to be an ideal stimulus for atherosclerosis.

Our group has developed Ossabaw miniature swine as an excellent large humanoid animal model of MetS. When fed excess calorie atherogenic diet, Ossabaw swine develop MetS [11, 92, 95, 96] and, like humans (but different from many other laboratory animal models) develop CAD [11, 92, 95, 97]. Organ culture is a useful in vitro model of coronary atherosclerosis which manifests increased neointimal thickness, collagen content and cellular proliferation [65, 171-175], which are common features of atherosclerosis [1, 9, 14, 62, 63].

Exercise training of patients with CAD elicits beneficial effects, including improvement in exercise tolerance, left ventricular function, etc. [18]. Fleenor and Bowles [27] showed that long-term exercise training of pigs with normal plasma cholesterol attenuated conduit artery neointimal proliferation and collagen expression elicited by overexpansion injury from balloon angioplasty and we showed that exercise training decreased collagen in stented coronary arteries [11]. However, the beneficial effects of exercise on systemic aldosterone, coronary

A1R expression, and native atherosclerosis in MetS have never been explored to our knowledge.

The purpose of this study was first to test the hypothesis that plasma aldosterone and A1R are increased in CAD in MetS and whether exercise training reverses this effect. A second hypothesis is that aldosterone regulates A1R expression, thereby contributing to CAD via A1R upregulation in the in vitro organ culture model of coronary atherosclerosis. Using our novel in vivo MetS swine and in vitro organ culture models, we clearly show for the first time a strong association and causal role, respectively, of aldosterone regulated A1R in the development of CAD in vivo and in vitro. Exercise attenuation of plasma aldosterone elevation, A1R upregulation in atheroma, and CAD strongly supports exercise and antagonism of MR and A1R as treatments for CAD in MetS.

4.3. Methods

4.3.1. Animal care

All protocols involving animals were approved by an Institutional Animal Care and Use Committee and complied fully with recommendations in the Guide for the Care and Use of Laboratory Animals [105] and the American Veterinary Medical Association Panel on Euthanasia [106]. Male Ossabaw swine (age 20±2 months at sacrifice) were assigned to 3 different diet groups for 14 months, 5 in each group and were a subset of another study [11]. Lean control swine were fed were fed standard chow containing 22% kcal from protein, 70% kcal from

carbohydrates, and 8% kcal from fat (5L80; Purina TesDiet, Richmond, IN). Sedentary MetS and exercise trained (XMetS) groups were fed a high fat / 2% cholesterol atherogenic diet composed of lean chow supplemented with (percent by weight): cholesterol 2.0, hydrogenated soybean oil 16.7 (56% trans fatty acids), corn oil 2.5, and sodium cholate 0.7. This mixture yielded a composition of 11% kcal from protein, 43% kcal from carbohydrates and 46% kcal from fat. Pigs in the lean group ate 2500 kcal/day. Atherogenic diet groups ate 6000 kcal/day until sacrifice. All animals were housed in individual pens and provided a 12-hr light / 12-hr dark cycle. Water was provided ad libitum.

4.3.2. Exercise training

Animals randomized to the exercise group began treadmill training 7 weeks before sacrifice as described [11]. During the first week of training, the exercise pigs ran on the treadmill at 4 mph (endurance) with 0% grade for 20-30 minutes and at 5.6 mph (sprint) for 15 minutes. After acclimation a typical daily 45 minute training session continued over the course of the following 6 weeks. The training consisted of the following stages: 1) 5 minute warm-up at 2.2 mph, 2) 5 minute sprint at speeds of 6.1 mph, 3) 30 minute endurance run at 7.7 mph, and 4) 5 minute cool down at 3.5 mph. Exercise protocols were compliant with guidelines from the American Physiological Society [108].

4.3.3. Submaximal stress test

At weeks 1, 4, and 7 of exercise training the endurance trained animals underwent a submaximal stress test consisting of running on a treadmill at 3.1 MPH, 0% grade for 15 minutes at which point heart rate data were collected.

4.3.4. Intravenous glucose tolerance test (IVGTT)

Swine were acclimatized to restraint in a specialized sling for 5-7 days before the IVGTT was conducted. Following percutaneous catheterization of the right jugular vein under isoflurane anesthesia [11, 92, 95], swine were allowed to recover for 3 hours before the IVGTT to avoid any effect of isoflurane on insulin signaling [176]. Conscious swine were restrained in the sling and baseline blood samples were obtained. Dextrose (1 g/kg body weight) was administered intravenously and timed blood samples were collected [176].

4.3.5. Cardiac catheterization procedures

Cardiac catheterization, angiography, and intravascular ultrasound (IVUS) were performed as previously described at sacrifice (detailed description in the online supplemental materials) [11, 70, 92].

4.3.6. Intravascular ultrasound analysis

Native atheroma was quantified as percent circumferential lumen wall coverage. Each cross-sectional IVUS image was divided into 16 equal radial segments, and percent circumferential wall coverage was calculated as (# radial

segments containing atheroma ÷ 16) x 100 %. Images were captured every 1 mm along the whole pullback length of IVUS and 8 images quantified and averaged for each coronary segment [11, 70, 92].

4.3.7. Histological analysis

Masson's trichrome stains were performed on phosphate buffered formalin-fixed and paraffin-embedded sections of organ cultured arteries. Images were captured at × 10 magnification with a Nikon CoolPix 990 (3.34 MegaPixel) digital camera attached to a Nikon Diaphot inverted microscope with a CoolPix MDC optical adapter (Nikon, Melville, NY, USA). Masson's trichrome stain was used to assess collagen content in the media, determined by colorimetric analysis using Image Pro Plus v.4.1 software (Media Cybernetics, Silver Springs, MD, USA) and calculated as (collagen staining area / total area) × 100% [10, 11].

4.3.8. Cell culture

Porcine coronary artery SMC enzymatically dispersed from right coronary arteries of Ossabaw pigs were cultured as previously described in our laboratory [65, 69, 177]. SMC lineage was confirmed by smooth muscle α actin immunocytochemistry. Stock coronary artery SMC cultures were maintained in a subconfluent state and used between passage 4 and 10 [177]. Cells were serum starved for 24 hours before treatment with vehicle control, aldosterone or spironolactone. Vehicle control, aldosterone, and spironolactone were replenished every 24 hours.

4.3.9. Real-time reverse transcription-polymerase chain reaction (Real-time RT-PCR)

Primers for PCR amplification of A1R were designed from the pig A1R sequence (GenBank accession number AY772411) using Primer Express software (Applied Biosystems, Foster City, CA, USA) (detailed description in the online supplemental materials).

4.3.10. Western blotting for A1R, proliferating cell nuclear antigen (PCNA), and p-ERK1/2

Coronary artery segments were pretreated with 10^{-6} M CCPA at 37° C for 5 minutes, then lysed and western blotted for A1R (rabbit polyclonal antibody; 1:1000 dilutions; Abcam, Cambridge, MA, USA), PCNA (mouse monoclonal antibody; 1:1000 dilutions; Cell Signaling, Danvers, MA, USA) and p-ERK1/2 (mouse monoclonal antibody; 1:1000 dilutions; Cell Signaling). Membranes were stripped and re-probed with anti-GAPDH (1:1000; Fitzgerald, Concord, MA, USA; for A1R and PCNA) or anti-total ERK1/2 (1:1000 dilutions; Cell Signaling). For coronary SMC lysis, the same protocol was used as in tissues, except there was no CCPA treatment for cells (detailed description in the online supplemental materials).

4.3.11. In vitro organ culture model of atherosclerosis

Freshly isolated right coronary arteries from lean Ossabaw swine were cut into 2-4 mm segments and cultured for 36 hours, 2 or 4 days in a humidified 5%

CO_2 incubator at 37° C in RPMI Medium 1640 (Invitrogen, Carlsbad, CA, USA) [65, 70, 171-173]. Medium was supplemented with 10^{-6} M 2-Chloro-N6-cyclopentyladenosine (CCPA, TOCRIS, Ellisville, MO, USA), 10^{-5} M 8-Cyclopentyl-1, 3-dipropylxanthine (DPCPX, TOCRIS), 10^{-7} M aldosterone (Sigma, St. Louis, MO, USA), or 10^{-7} M spironolactone (Sigma) as needed.

4.3.12. Blood analysis

Venous blood samples were obtained following overnight fasting. Blood glucose was measured using YSI 2300 STAT Plus Glucose analyzer. Plasma insulin assays were performed by Linco Research Laboratories (St. Charles, MO, USA) [95]. Plasma lipid assays were done using Infinity lipid kit (ThermoFisher Scientific, VA, USA) and a manganese precipitate method validated for swine plasma [95]. Aldosterone was determined in heparinized plasma by radioimmunoassay by Dr. J. Howard Pratt's laboratory at Indiana University School of Medicine [178].

4.3.13. Statistics

Data were presented as mean ± SEM. Statistical analysis was performed using commercially available software (SPSS version 12, Prism version 4.0). Means of 2 groups were compared using Student t test (unpaired, two tailed). Means of more than 2 groups were compared using Kruskal–Wallis one-way analysis of variance (ANOVA) followed by post-hoc testing using Least-

Significant-Difference test. Correlation and linear regression analysis were done between different parameters. $P<0.05$ was considered statistically different.

4.4. Results

4.4.1. Phenotypic comparison between Lean, MetS, and XMetS pigs

Following 14 months of feeding body weight, fasting plasma insulin, fasting plasma glucose, total cholesterol, LDL, HDL, LDL/HDL, triglycerides, mean blood pressure, and plasma aldosterone were all significantly elevated in MetS and Pre-X XMetS (XMetS before the initiation of 7-week exercise training) vs. Lean. Among those factors, only LDL/HDL and plasma aldosterone were significantly reduced by 7-week exercise training in Post-7Wk-X XMetS (XMetS after 7-week exercise training) vs. MetS and Lean (Table 4.1). 7-week exercise training reduced resting heart rate as well as the heart rate response to submaximal stress test (data not shown).

4.4.2. Comparison of native coronary atherosclerosis, A1R, and PCNA expression in Lean, MetS, and XMetS pigs

IVUS analysis done in vivo in left circumflex coronary in Lean, MetS, and XMetS at sacrifice revealed profound native coronary atheroma in MetS vs. Lean and attenuation in XMetS to Lean levels (Figure 4.1A, B). Intact coronary atherosclerotic segments harvested at sacrifice showed A1R mRNA (Figure 4.1C), A1R (Figure 4.1D, E), and PCNA (Figure 4.1D, F) proteins were all elevated in the native coronary atherosclerotic lesions of MetS vs. Lean. A1R

expression decreased in XMetS 7-week post-exercise based on real-time RT-PCR (Figure 4.1C) and quantitative analysis of immunoblots (Figure 4.1E).

4.4.3. Correlation among plasma aldosterone, A1R, and PCNA

To explore possible interactions among different systemic, local factors, and coronary atheroma in lean, MetS and XMetS, different combinations were used for correlation analysis (Figure 4.2). Plasma aldosterone significantly correlated to A1R in native coronary atherosclerotic segments (Figure 4.2A). And A1R correlated to PCNA in coronary segments with atheroma (Figure 4.2B).

4.4.4. Aldosterone upregulation of A1R expression

Subcultured coronary artery SMC isolated from healthy lean Ossabaw right coronary arteries were treated with aldosterone, aldosterone + spironolactone (mineralocorticoid receptor antagonist), or vehicle control for 12, 24, and 36 hours. Both A1R mRNA (Figure 4.3A) and protein (Figure 4.3B) were upregulated by aldosterone treatment at the 36-hour treatment. Interestingly, at 36-hour time point A1R mRNA upregulation was partially attenuated by spironolactone (Figure 4.3A), but A1R protein (Figure 4.3B) was not altered by spironolactone although there seemed a trend toward decrease of A1R protein by spironolactone.

4.4.5. A1R expression, collagen, and A1R-ERK1/2 activity in the in vitro organ culture model of early coronary atherosclerosis

To carry out more manipulations of the factors and proteins, an in vitro organ culture model of early coronary atherosclerosis was utilized to mimic in vivo coronary atherosclerosis. A1R gene, protein expression and exogenous ERK1/2 activation (CCPA-induced ERK1/2 activation; highly A1R-selective agonist CCPA) were assessed in organ cultured coronary artery segments over time vs. freshly harvested coronary segments. Masson's trichrome stain for collagen revealed increased medial collagen content at 4-day organ culture (Figure 4.4A). A1R mRNA was upregulated transiently in 2-day organ culture and returned to the level of fresh arteries by 4-day based on real-time RT-PCR analysis (Figure 4.4B). A1R protein (Figure 4.4C) and exogenous A1R-mediated ERK1/2 activation (Figure 4.4D) were elevated at 4-day organ culture.

4.4.6. A1R antagonism and aldosterone treatment in the in vitro organ culture model of early coronary atherosclerosis

To define the role of A1R in early coronary atherosclerosis in vitro, the highly A1R-selective agonist CCPA and antagonist DPCPX were used in the 4-day organ culture model and followed by histological analysis to assess their direct effects. Organ cultured coronary segments with vehicle control or CCPA treatment showed increased medial collagen content vs. fresh coronary segments and no difference between vehicle control and CCPA treatment. Segments supplemented with DPCPX or CCPA and DPCPX concurrently

showed comparable medial collagen content vs. fresh (Figure 4.5A). To test whether aldosterone affects the atheroma development via regulation of A1R in vitro, 4-day organ culture model was employed (Figure 4.5B). Organ cultured coronary segments with vehicle control had increased medial collagen content vs. fresh and segments supplemented with aldosterone had further increased collagen content vs. vehicle control. Aldosterone plus spironolactone or aldosterone plus DPCPX showed less medial collagen content vs. aldosterone alone, similar content vs. vehicle control, and greater content vs. fresh (Figure 4.5B). There was no difference between aldosterone plus spironolactone and aldosterone plus DPCPX (Figure 4.5B).

4.5. Discussion

We have made the novel findings that plasma aldosterone, and A1R and PCNA expression in atherosclerotic lesions all increased in MetS pigs and those factors correlated with each other. Endurance exercise training attenuated the MetS effects. Using a novel in vitro organ culture model of CAD, we demonstrated for the first time: 1) aldosterone upregulates A1R expression in coronary SMC and intact coronary segments, 2) A1R upregulation and A1R activation contribute to CAD in in vitro organ culture, and 3) aldosterone contribution to CAD in in vitro organ culture was partially mediated by upregulation of A1R.

In the present study, we found A1R elevated in MetS and reduced in XMetS, while A2AR mRNA was not changed in MetS and A2AR, A2BR and A3R mRNA remained high in XMetS (see online supplemental data Figure 4.6). Those data showed that the AR changes in MetS and exercise are A1R subtype specific, not a global change of all adenosine receptors. This suggests that the A1R holds different functions than other adenosine receptors in contribution to coronary atherosclerosis.

This is the first report of A1R upregulation in coronary atherosclerotic lesions in MetS, which is consistent with findings that A1R is elevated in diabetes [179], hypertension [180], and oxidative stress [181] and clearly indicates A1R involvement in different metabolic disorders. Our finding of exercise-induced regression of coronary atherosclerosis in MetS further reinforces the benefit of exercise therapy for human patients with CAD and MetS. Of course, lipid lowering agents show beneficial effects on the vascular wall in humans [182] and swine models [183]. High levels of plasma aldosterone were observed in obese human subjects [184], therefore elevated plasma aldosterone in MetS pigs was an outstanding validation of this porcine model. The effect of MR blockade on diabetes, metabolic syndrome and coronary atherosclerosis has not been evaluated in human subjects yet [47]. The literature above and our novel finding of aldosterone upregulation of A1R provide several new targets (A1R or MR antagonist alone or in combination) for CAD treatment in MetS.

Organ culture is an excellent in vitro model of coronary atherosclerosis [65, 171-175]. Interestingly, upregulation of A1R mRNA was at 2-day organ culture whereas the increase of A1R protein occurred at 4-day organ culture. It is likely that some post-transcriptonal regulation mechanisms are responsible for the lag between mRNA and protein expression. Elevated media collagen content indicates higher synthetic (proliferative) activity of media smooth muscle cells [1, 9, 62, 63], which indirectly supports A1R contribution to coronary atherosclerosis by stimulation of coronary SMC proliferation. A1R antagonism decreased medial collagen content to a level comparable to freshly harvested arteries, regardless of the presence or absence of A1R-selective agonist CCPA, which suggests: 1) there is endogenous adenosine production by the organ cultured coronary segments in the organ culture condition and 2) A1R was the main player in the pure organ culture model to induce medial collagen content.

MR-responsive genes in vascular SMC are poorly characterized, but type I and type III collagen are among them [185]. Type I and type III collagen have been implicated in aldosterone-induced cardiac and conduit fibrosis, which is consistent with our in vitro organ culture findings that aldosterone treatment increased medial collagen content vs. vehicle control [186]. Interestingly, A1R antagonism or MR antagonism in the presence of aldosterone reduced collagen content to vehicle control level, instead of freshly harvested artery level. These data suggest that: 1) the A1R-induced collagen increase mediates only part of the aldosterone-induced collagen synthesis, possibly via A1R actions on SMC

and/or 2) aldosterone acts on the vascular wall in a MR-independent pathway to increase collagen content, i.e. contribute to CAD. It was reported that aldosterone exerts pro-inflammatory effects via MR-dependent and -independent pathways. Treatment with spironolactone or inhibitors of transcription or protein synthesis prevent the late effect of aldosterone, suggesting that this effect occurs through an MR-dependent, genomic pathway. In contrast, spironolactone does not block rapid phosphorylation of ERK1/2 by aldosterone, which is a MR-independent pathway. Besides, aldosterone was shown to affect hepatic gluconeogenesis through the glucocorticoid receptor in cultured mouse hepatocytes [187], which suggests aldosterone could act on glucocorticoid receptors as well as mineralocorticoid receptors in promoting collagen synthesis. Therefore, lack of full blockade by spironolactone could include an MR-independent mechanism [188].

In addition to the possible mitogenic effect mediated by aldosterone regulation of A1R in coronary SMC, MR also function in human vascular endothelial cells, regulating intercellular adhesion molecule-1 (ICAM-1) expression and promoting leukocyte adhesion [189], which may contribute to the beneficial effects of MR antagonism in patients with heart disease. It was reported that MR blockade reversed adipocyte dysfunction and insulin resistance in obese mice [47]. MR activation was reported to promote proliferation, inflammation and fibrosis, which argues for MR antagonism in treatment of CAD to combat multiple facets of CAD [47, 190]. Steroid receptors bind to specific

hormone response elements in the promoters of hormone responsive genes, recruiting cofactors in a ligand-dependent manner, thereby modulating gene expressions [46]. Understanding of the molecular mechanism by which aldosterone regulates A1R and further delineation of other MR-responsive genes relevant to CAD may make our understanding of aldosterone contribution to CAD more complete and potentially identify more therapeutic targets for CAD.

In summary, our in vivo data showing the association of A1R upregulation in coronary atherosclerosis and elevated plasma aldosterone in MetS and exercise attenuation of coronary atheroma, A1R upregulation and aldosterone elevation, provide strong evidence that aldosterone and A1R upregulation might play important roles in coronary atherosclerosis in vivo in MetS. Our in vitro cell studies discovered a novel MR-responsive gene - the A1R in coronary SMC. Aldosterone partially contributed to the development of CAD in the in vitro organ culture model via upregulation of A1R. Collectively, aldosterone regulation of A1R could potentially contribute to the development of coronary atherosclerosis in MetS. Further study defining the role of aldosterone in regulation of A1R in vivo will aid in improving therapeutics for coronary atherosclerosis, especially in the setting of MetS.

4.6. Acknowledgments

The authors would like to thank Dr. Pamela Lloyd, Dr. Eric A. Mokelke, Dr. Jason M. Edwards, Dr. J. Howard Pratt, Mary Anne Wagner and James W.

Wenzel for their excellent technical assistance. This work was supported by NIH grants RR013223, HL062552, T35 HL007802, the Purdue-Indiana University Comparative Medicine Program, and the Fortune-Fry Ultrasound Research Fund of the Department of Cellular & Integrative Physiology at Indiana University School of Medicine (M.S.), an American Heart Association Predoctoral Fellowship (X.L.), and NIH Translational Research Fellowship UL1 RR025761 (Z.P.N.).

4.7. Figure legends

Figure 4.1. A1R expression in native coronary atherosclerotic lesions in lean, metabolic syndrome (MetS), and metabolic syndrome aerobically exercised (XMetS) Ossabaw swine

A. Representative intravascular ultrasound (IVUS) image showing 54 percent of the arterial wall lined with atheroma as marked by the double arrows and arcs (195 / 360 × 100 % = 54 %). The distance between the 2 neighboring dots is 1 mm. B. Native coronary atherosclerosis was quantified as the percent degree of circumferential arterial wall covered with atherosclerotic lesions in the distal left circumflex coronary artery (CFX) in vivo using IVUS right before sacrifice (n=5/group). C. Real-time RT-PCR for detection of A1R mRNA in those three groups (n=5/group). D-F. Immunoblots for detection of A1R and proliferation cell nuclear antigen (PCNA) proteins were performed in intact coronary segments with native atherosclerosis in lean (n=4), MetS (n=3), and XMetS (n=5) right after sacrifice. Representative immunoblots of A1R, PCNA, and GAPDH (loading

control) in lean, MetS, and XMetS were shown in D. Quantitative analysis of the results of A1R/GAPDH (E) and PCNA/GAPDH (F) was depicted as shown. *, $p<0.05$; #, $p<0.001$ as indicated by lines.

Figure 4.2. Correlation study among plasma aldosterone, A1R and PCNA protein expression in native coronary atherosclerosis

Different combinations of those parameters in Lean, MetS and XMetS were used for correlation study. All parameters were determined in Figure 4.1. P values and Pearson r were indicated in each panel.

Figure 4.3. Aldosterone upregulation of A1R expression in vitro

A-B Subcultured coronary artery smooth muscle cells isolated from lean Ossabaw right coronary arteries were treated with vehicle control, aldosterone (10^{-7} M), aldosterone (10^{-7} M) + spironolactone (10^{-7} M, mineralocorticoid receptor antagonist) for either 12, 24, or 36 hours. Real-time RT-PCR in detection of A1R mRNA was done in the treated cells from five independent experiments performed in duplicates (A). Immunoblots of A1R and GAPDH (loading control) were done in the cells treated for 36-hour from five independent experiments performed in duplicates (B). Aldo mean aldosterone treated. * denotes $p<0.05$ vs the other conditions.

Figure 4.4. A1R expression and A1R-ERK1/2 activity in the in vitro organ culture model of early coronary atherosclerosis

A Histology analysis of Masson's trichrome stains was performed in coronary segments (Fresh, 2- and 4-day organ culture) from five different lean pigs. Representative image in each treatment was shown on the right side of the bar graph. Blue indicates collagen staining, and red indicates cellular materials. Internal elastic lamina (IEL) and external elastic lamina (EEL) differentiates intima (I, within IEL) and media (M, between IEL and EEL) from adventitia (A, beyond EEL); lumen (L) is center of each artery. Representative histology images are shown above the group data averages. B-D Real-time RT-PCR for detection of A1R mRNA (B) and immunoblots for detection of A1R protein (C) and A1R-ERK1/2 activity (D) were performed in the coronary segments (Fresh, 2-, and 4-day organ cultured, n=5/group). Representative blots of A1R, GAPDH (C) and phosphorylated-ERK1/2, total-ERK1/2 (D) are shown above the group data averages. Fresh served as control. * shows $p<0.05$ vs. Fresh.

Figure 4.5. Effect of A1R antagonism and aldosterone treatment in the in vitro organ culture model of early coronary atherosclerosis

A Coronary segments from lean pigs were organ cultured for 4 days, either in vehicle control media, or media supplemented with DPCPX (10^{-5} M), highly A1R-selective antagonist, or CCPA (10^{-6} M), highly A1R-selective agonist, or both (n=5/group). B Similarly, coronary segments from lean pigs were organ cultured for 4 days, either in vehicle control media, or media supplemented with

aldosterone (10^{-7} M) alone, or aldosterone (10^{-7} M) and spironolactone (10^{-7} M)-mineralocorticoid receptor antagonist, or both aldosterone (10^{-7} M) and DPCPX (10^{-5} M). Fresh coronary served as control (n=5/group). They were then followed by histology analysis of Masson's trichrome stains. Percent media collagen content was quantitatively analyzed and depicted as shown. Fresh coronary segments are referred to as Fresh; 4-day organ cultured + vehicle treated segments as Vehicle; 4-day organ cultured + DPCPX, or CCPA, or both CCPA and DPCPX, or aldosterone alone, or aldosterone plus spironolactone, or aldosterone plus DPCPX treated segments as DPCPX, CCPA, CCPA + DPCPX, Aldosterone, Aldosterone + Spirono (short for spironolactone) or Aldosterone + DPCPX. * means $p<0.05$ vs non-star labeled groups (A) or vs Fresh (B); #, $p<0.002$ vs Aldo; **, $p<0.0001$ vs Fresh.

4.8. Figures

Figure 4.1. A1R expression in native coronary atherosclerotic lesions in lean, metabolic syndrome (MetS), and metabolic syndrome aerobically exercise trained (XMetS) Ossabaw swine

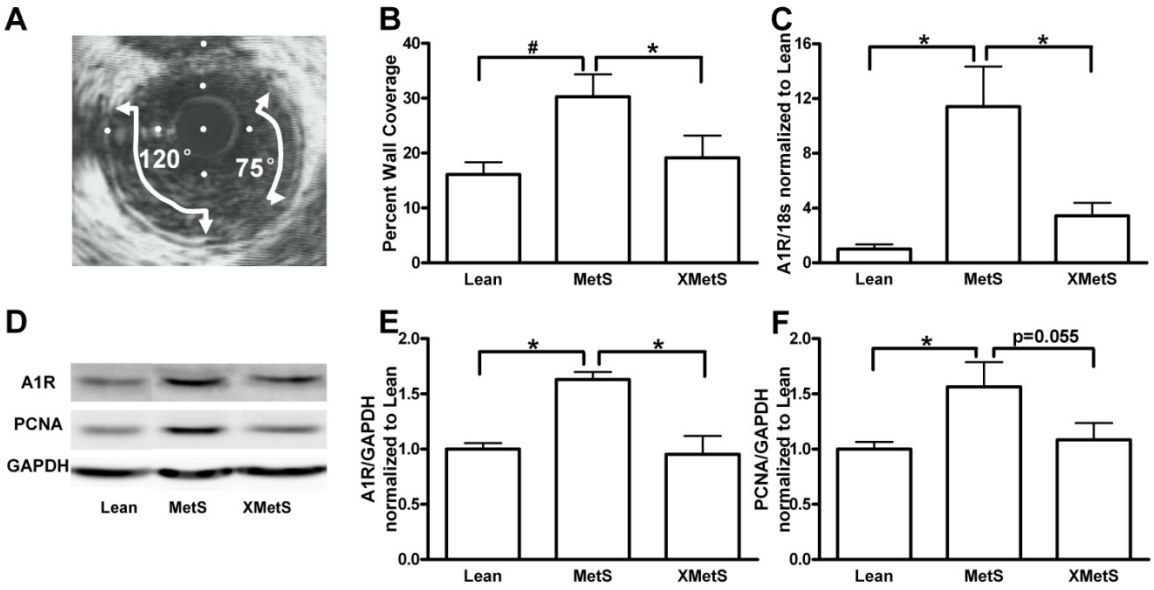

Figure 4.2. Correlation study among plasma aldosterone, A1R and PCNA protein expression in native coronary atherosclerosis

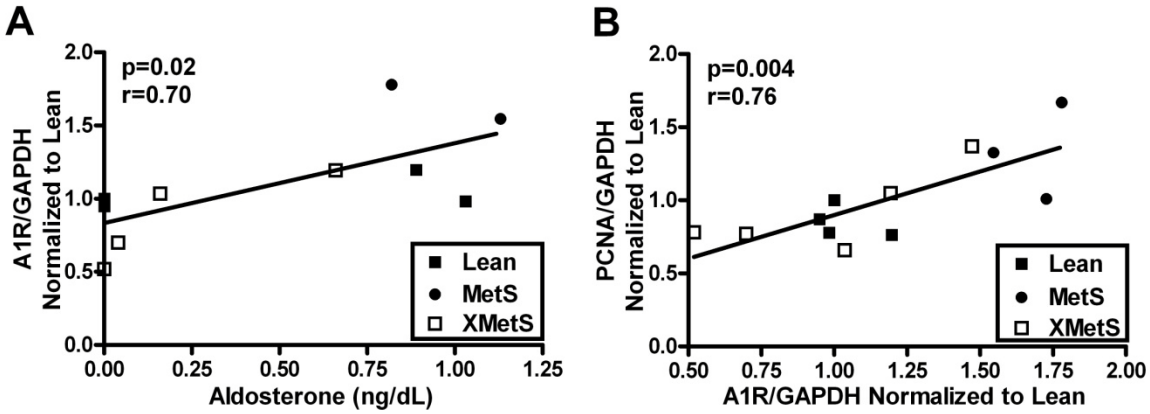

Figure 4.3. Aldosterone upregulation of A1R expression in vitro

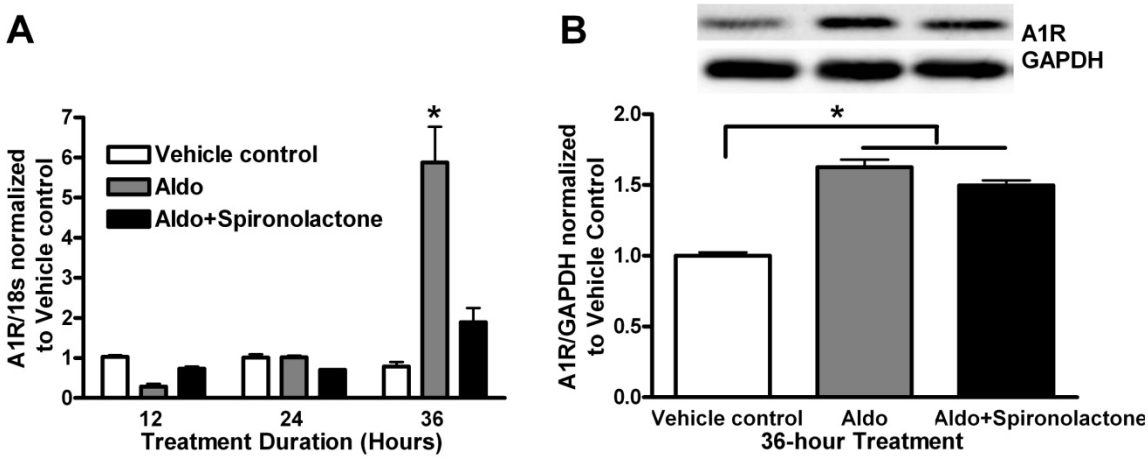

Figure 4.4. A1R expression and A1R-ERK1/2 activity in the in vitro organ culture model of early coronary atherosclerosis

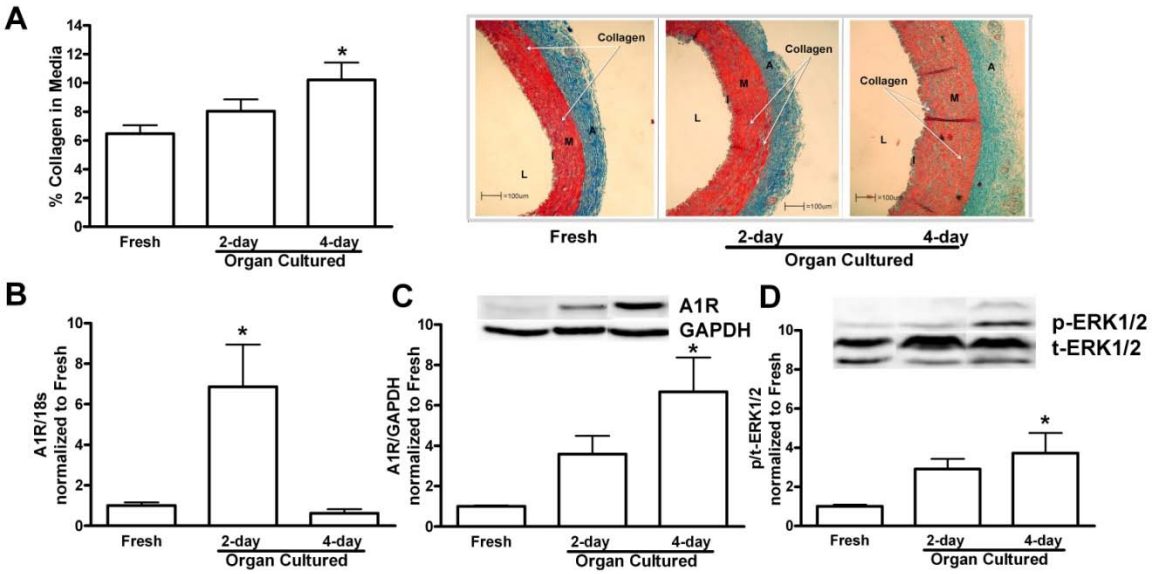

Figure 4.5. Effect of A1R antagonism and aldosterone treatment in the in vitro organ culture model of early coronary atherosclerosis

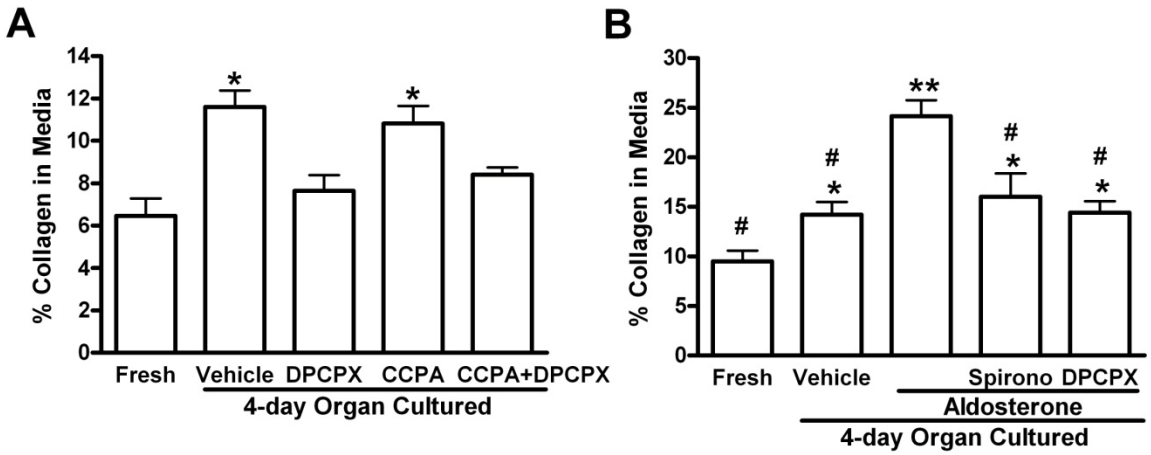

4.9. Table

Metabolic Index	Lean	MetS	Pre-X XMetS	Post-7Wk-X XMetS	Significance ($p<0.05$)
Weight (kg)	71±2	108±10	102±12	105±13	Pre-X XMetS, MetS > Lean
Fasting Plasma Insulin (µU/mL)	10±1	23±1	17±3	26±8	Pre-X XMetS, MetS > Lean
Fasting Plasma Glucose (mg/dL)	62±4	87±3	86±3	88±2	Pre-X XMetS, MetS > Lean
Total Cholesterol (mg/dL)	48±2	243±36	223±40	232±45	Pre-X XMetS, MetS > Lean
LDL (mg/dL)	23±2	183±33	169±38	142±26	Pre-X XMetS, MetS > Lean
HDL (mg/dL)	21±2	56±13	48±4	85±21	Pre-X XMetS, MetS > Lean
LDL/HDL	1.2± 0.2	3.7±0.9	3.5±0.7	1.7±0.2	Pre-X XMetS, MetS > Lean, Post-7Wk-X XMetS
Triglycerides (mg/dL)	17±2	22±3	29±5	29±4	Pre-X XMetS > Lean
Mean Blood Pressure (mm Hg)	84±2	119±4	91±26	108±5	Pre-X XMetS, MetS > Lean
Aldosterone (ng/dL)	0.30± 0.16	2.06± 1.0	2.32± 0.63	0.10± 0.04	Pre-X XMetS, MetS > Lean, Post-7Wk-X XMetS

Table 4.1. Metabolic data and aldosterone of Lean, MetS and XMetS Ossabaw pigs near the end of the 14-month study.

Statistical differences between Lean, MetS, PreX XMetS, and Post-7Wk-X XMetS groups (n=5/group) are indicated in the right column. Pre-X XMetS means XMetS before the initiation of 7-week exercise training, Post-7Wk-X XMetS

means XMetS after 7-week of exercise training. LDL = low-density lipoprotein, HDL = high-density lipoprotein.

4.10. Supplementary methods

4.10.1. Cardiac catheterization procedures

Following an overnight fast, swine received (in mg/kg; i.m.) 0.05 atropine, 2.2 xylazine, and 5.5 telazol. Swine were intubated and anesthesia was maintained with isoflurane (2-4%, with supplemental O_2). The isoflurane level was adjusted to maintain anesthesia with stable hemodynamics. Heart rate, aortic blood pressure, respiratory rate, and electrocardiographic data were continuously monitored throughout the procedure. Under sterile conditions, the right femoral artery was exposed with a surgical cut-down technique and a 7F or 8F vascular introducer sheath was inserted into the femoral artery followed by administration of heparin (200 U/kg). A 7F Amplatz L (sizes 0.75-2.0) guiding catheter (Guidant, Indianapolis, IN, USA) was inserted through the sheath and advanced to engage the left main coronary ostium under angiographic guidance. An Ultracross 3.2, 30 MHz intravascular ultrasound (IVUS) catheter (Boston Scientific, Sunnyvale, CA, USA) was advanced over a guide wire and positioned first in the left anterior descending (LAD) coronary arteries. IVUS images were recorded on videotapes using a Sonos Intravascular Imaging System (Hewlett Packard, Andover, MA, USA) for off-line analysis. Automated IVUS pullbacks were performed at 0.5 mm/sec. The IVUS catheter, guide catheter, and

introducer sheath were removed and the right femoral artery ligated. The incision was closed and the animal was sacrificed then.

4.10.2. Real-time reverse transcription-polymerase chain reaction (Real-time RT-PCR)

RNA was extracted from arterial samples using Trizol (Invitrogen, Carlsbad, CA, USA), then treated with DNase (DNA free, Ambion, Austin, TX, USA) to remove contaminating genomic DNA, and analyzed by NanoDrop spectrophotometer (ND-1000; ThermoScientific, Wilmington, DE, USA) to assess purity (A260/280) and concentration. 1 µg of RNA was converted to cDNA using the iScript cDNA synthesis kit (Bio-Rad, Hercules, CA, USA) in a standard thermocycler (DNA Engine PTC-200, MJ Research, Waltham, MA, USA). A1R, A2AR, A2BR and A3R gene expression was assessed using quantitative real-time RT-PCR in an ABI 7500 instrument (Applied Biosystems, Foster City, CA, USA). Primers for PCR amplification were as follows:

A1R: forward, 5'-GGCCATGCTGGCAATTG-3';
reverse, 5'-CCTGAGCGGGATCTTGACA-3';

A2AR: forward, 5'-CCCCTTCATCTATGCCTACCG-3';
reverse, 5'-CATTCCCTCACACTCCCTCCAC-3';

A2BR: forward, 5'- TGTGCTGGCTGCCTCTTCAC-3';
reverse, 5'-ACACGATGGGGTTGACGACC-3';

A3R: forward, 5'-GAACCTCACCTTCCTTTCCTGC-3';
reverse, 5'-GAACTCCCGTCCATAAAATGC-3'

(Integrated DNA Technologies, Coralville, IA, USA). Taqman probes were used to detect A1R gene amplification and were as follows: 5'-/6-FAM/TCGACCGCTACCTCC/MGBNFQ/-3' (Applied Biosystems). SYBRGreen Universal PCR Master Mix (Applied Biosystems) was used to detect A2AR, A2BR and A3R gene expression followed by a dissociation curve to rule out non-specific amplifications and primer-dimers. All results were normalized to the signal of 18s RNA, which was amplified in separate reactions using TaqMan Universal PCR Master Mix and TaqMan 18s Detection Reagents (Applied Biosystems).

4.10.3. Western Blotting for A1R, PCNA, and p-ERK1/2

For the western blots of A1R, PCNA, and p-ERK1/2, coronary artery segments were pretreated with 10^{-6} M CCPA at 37°C for 5 minutes before lysed with 1% SDS lysis buffer with addition of protease inhibitor cocktail and phosphatase inhibitor cocktail (Sigma, St. Louis, MO, USA). Lysates were sonicated to disrupt DNA before BSA assay (Pierce, Rockford, IL, USA) for protein concentration determination, solubilized in Laemmli sample buffer with 200 M dithiothreitol, and boiled for 2 minutes and proteins were separated on SDS-PAGE gels. The proteins were then electrophoretically transferred to nitrocellulose membrane in 25 M Tris, 192 M glycine, and 20% methanol. The nitrocellulose was blocked with 5% nonfat dry milk in 10 M Tris (pH 7.4), 150 M NaCl, and 0.01% Tween 20. The membranes were probed with the individual primary antibody (anti-adenosine A1 receptor; 1:1000 dilutions; Abcam,

Cambridge, MA, USA; anti-p-ERK1/2; 1:1000 dilutions; Cell Signaling, Danvers, MA, USA) overnight in 10 M Tris (pH 7.4), 150 M NaCl, 5% nonfat dry milk, and 0.01% Tween 20. The blots were washed in 10 M Tris (pH 7.4), 150 M NaCl, and 0.01% Tween 20, and bound antibody was detected by a horseradish peroxidase-conjugated anti-rabbit or anti-mouse IgG and enhanced chemiluminescence (Pierce). Equal protein loading was verified by stripping off the original antibody, and reprobing with the primary antibody anti-GAPDH (1:1000; Fitzgerald, Concord, MA, USA) or anti total-ERK1/2 (1:1000 dilutions; Cell Signaling).

4.11. Supplementary figure legend

Figure 4.6. Adenosine subtypes expression in coronary native atherosclerotic lesions in Lean, MetS and XMetS

Real-time RT-PCR for detection of A1R (A), A2AR (B), A2BR (C), and A3R mRNA (D) was performed in intact coronary segments with native atherosclerosis in lean, MetS, and XMetS (n=5/group) right after sacrifice. Quantitative analysis of the results was depicted as shown. *, $p<0.05$ as indicated by lines.

4.12. Supplementary figure

Figure 4.6. Adenosine subtypes expression in coronary native atherosclerotic lesions in Lean, MetS and XMetS

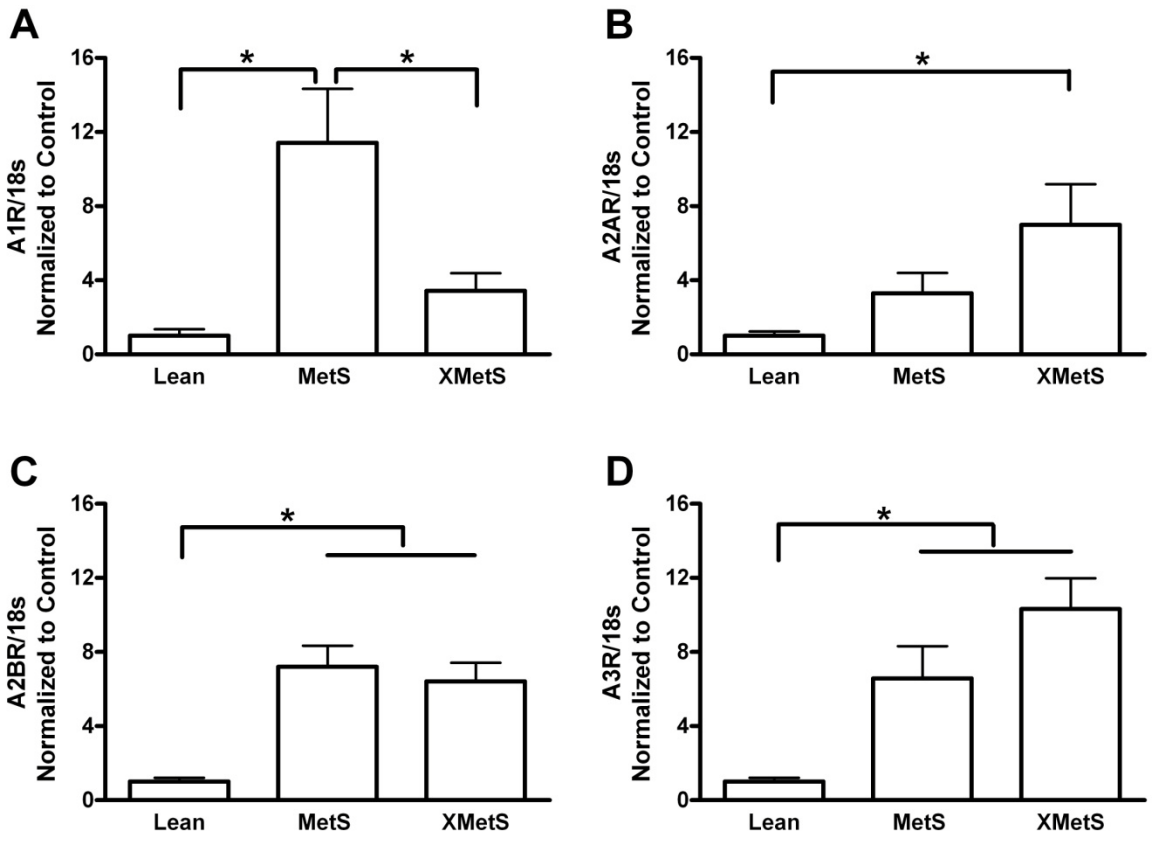

CHAPTER 5. ADENOSINE A1 RECEPTOR ANTAGONISM ATTENUATES CORONARY IN-STENT STENOSIS IN METABOLIC SYNDROME

Xin Long[1]; Mouhamad Alloosh[1]; Jutarat Kitsongsermthon[2]; Yuanzu He[2]; Kinam Park[2]; Michael Sturek[1]

[1]Department of Cellular & Integrative Physiology

Indiana University School of Medicine

[2]Weldon School of Biomedical Engineering, Purdue University

Please address correspondence to:

Michael Sturek, Ph.D.

Department of Cellular & Integrative Physiology

Indiana University School of Medicine

635 Barnhill Drive, Room 385

Indianapolis, IN 46202-5120

E-mail: msturek@iupui.edu

Phone: 317-274-7772

Facsimile: 317-274-3318

5.1. Abstract

Background: Adenosine is widely known to elicit coronary vasodilation and attenuate smooth muscle proliferation, thereby providing cardioprotection. We cloned the porcine adenosine A1 receptor (A1R) subtype and found that it paradoxically stimulated proliferation of cultured coronary smooth muscle cells by the extracellular signal-regulated protein kinases 1 and 2 (ERK1/2) signaling pathways, thus suggesting A1R dysregulation could modulate coronary in-stent restenosis. We utilized the Ossabaw swine model of metabolic syndrome (MetS) and coronary disease to test the hypothesis that A1R upregulation and A1R signaling contribute to coronary in-stent stenosis in MetS. Methods and Results: Swine were fed standard chow or excess calorie atherogenic diet for up to 7 months, which elicited MetS characteristics. Intracoronary stent deployment followed by different durations of recovery from stenting showed A1R upregulation occurred before maximal in-stent stenosis. In MetS selective A1R antagonism with DPCPX-eluting stents decreased coronary ERK1/2 activation and in-stent stenosis ~50%, which rivaled effectiveness of Taxus® (paclitaxel-eluting) stents. Conclusions: A1R upregulation and A1R activation contribute to coronary in-stent stenosis in vivo in the setting of MetS and offer promising targets for drug-eluting stents.

5.2. Introduction

Metabolic syndrome (MetS; “pre-diabetes”) afflicts approximately 27% of the US adult population, drastically increasing in prevalence, and indicates

increased risk of atherosclerotic cardiovascular disease and/or type 2 diabetes mellitus [28-33]. MetS is defined as the combination of any three of the following abnormalities: central obesity, dyslipidemia, hypertension, impaired glucose tolerance, and insulin resistance [34]. First line therapy for flow-limiting coronary atherosclerotic lesions involves stent placement [17]. However, hyperinsulinemic MetS patients have increased restenosis after percutaneous coronary interventions [38-41]. These are compelling reasons for determining cellular and molecular signals for coronary restenosis in the setting of MetS.

The abnormal growth and migration of vascular smooth muscle cells (SMC) play major roles in restenosis after stenting [9, 62-64]. Adenosine has been widely shown to elicit coronary vasodilation and attenuate SMC proliferation, thereby providing cardioprotection [54]. Four adenosine receptor (AR) subtypes have been cloned: A1R, A2AR, A2BR, A3R [51]. The vasodilator effect of adenosine was mediated via the A2AR and/or A2BR, which are expressed by endothelial cells (EC) and SMC [52-54]. In aortic SMC, adenosine was found antimitogenic via the A2BR [65-68]. The exact physiological function of the A3R, which is expressed in some vascular SMC, has not been conclusively characterized [52]. We challenged this dogma with the finding that A1R mediated mitogenic effects of adenosine on porcine coronary artery SMC through activation of ERK1/2 - members of the mitogen-activated protein kinase (MAPK) superfamily, c-Jun-N-terminal kinase (JNK), and PI3K-AKT signaling pathways [65, 69]. We also reported A1R upregulation in in-stent coronary segments 4 weeks

after stent-induced vascular injury [70]. Despite those exciting findings, it remains unknown whether A1R activation plays a causal role in the pathogenesis of coronary in-stent stenosis.

Although drug-eluting stents have substantially decreased restenosis [78], further study is needed because of possible increased risk of platelet aggregation and late stent thrombosis caused by non-selective cytotoxins employed [80-85]. Our goal is to find a novel target for clinical application in reducing coronary in-stent stenosis, while avoiding possible late stent thrombosis in MetS and type 2 diabetes [80]. Several animal models recapitulate MetS [86-91]; however, none are able to fully reproduce symptoms of MetS and CAD. Further, transgenic mouse models are simply not adequate for coronary vascular interventions using stents identical to those used in humans [70, 92, 109, 191-195], which is essential for translation to the clinic. Our group has developed Ossabaw miniature swine as an excellent large humanoid animal model of MetS. Swine coronary arteries are similar to humans in size, anatomical structure, and flow dynamics [92]. When fed excess calorie atherogenic diet, Ossabaw swine develop MetS [11, 92, 95, 96], and like humans (but different from many other laboratory animal models) develop CAD [11, 92, 95, 97]. Because in-stent neointimal hyperplasia is greater in Ossabaws than in other lean swine breeds (e.g. Yucatan) [92], Ossabaw swine provide a unique and nearly ideal model for study of coronary in-stent stenosis, especially in the setting of MetS.

The overall hypothesis is that A1R activation contributes to the development of coronary in-stent stenosis in MetS. Using our novel swine model, we clearly show for the first time the causal role of A1R activation in coronary in-stent neointimal hyperplasia, especially in MetS.

5.3. Results

5.3.1. Relation of A1R upregulation to in-stent stenosis

To determine if A1R upregulation ocurrs before the development of coronary in-stent stenosis for either normal expanded or over-expanded stents, different stenting recovery durations were given to lean pigs with varying degrees of stent-induced injury. Taxus as well as bare metal stents were used to determine if the anti-proliferative property of Taxus relates to A1R regulation or not. After 4-week recovery, all in-stent coronary segments (Figure 5.1A-C) showed maximal in-stent stenosis. A1R protein, determined by immunoblots, was upregulated after 1-, 2- and 4-week stenting recovery in all 3 corresponding in-stent coronary segments: 1.0 (normal expansion) bare metal, 1.3 (over-expansion) bare metal, and 1.0 Taxus (Figure 5.1D, E, and F, respectively). Importantly, A1R protein upregulation preceded the maximal coronary in-stent stenosis for normal-expanded and over-expanded bare metal stents (1.0 and 1.3 bare metal), and drug-eluting stents (1.0 Taxus).

5.3.2. A1R-ERK1/2 signaling in in-stent segments

The highly A1R-selective agonist CCPA-induced ERK1/2 activation (phosphorylated to total ERK1/2 ratio) was measured in right coronary artery segments from healthy lean pigs with CCPA treatment for different durations. CCPA-induced ERK1/2 activation was biphasic, with peaks at 5 and 60 minutes (Figure 5.2A), thus all subsequent measures of CCPA-induced ERK1/2 activation were done after 5-minute CCPA stimulation. To assess A1R downstream mitogenic signaling strength, CCPA-induced ERK1/2 activation was compared in the in-stent (1.0 and 1.3 bare metal and 1.0 Taxus) and non-instrumented coronary segments (non-ST) in the same animals from the above mentioned study. CCPA-induced ERK1/2 activation was significantly reduced in all 3 stented vs. non-stented coronary segments at 1-week stenting recovery (Figure 5.2B). At 2-week recovery from stenting, CCPA-induced ERK1/2 activation was still repressed in 1.0 Taxus stented segments (Figure 5.2C). At 4-week stenting recovery, CCPA-induced ERK1/2 activation remained low in 1.0 Taxus stented vs. non-stented and bare metal stented coronary segments (Figure 5.2D). Collectively, the data in Figure 5.1 and Figure 5.2 show that functional A1R-ERK1/2 signaling lags behind the A1R protein upregulation in the development of in-stent stenosis.

5.3.3. Effects of two different drug-eluting (paclitaxel- and DPCPX-eluting) stents on coronary in-stent stenosis in MetS

To determine the effects of commercially available Taxus (paclitaxel-eluting) stents on in-stent stenosis in the setting of MetS, bare metal and Taxus stents were deployed at both 1.0 and 1.3 stent / artery ratios in coronary arteries of lean and MetS pigs. Following 6 months of feeding body weight, fasting plasma glucose and insulin, total cholesterol, LDL, HDL, LDL/HDL, triglycerides, systolic and diastolic blood pressure were all significantly elevated in MetS vs. Lean (data not shown). At 4-week stenting recovery, Taxus significantly reduced in-stent stenosis compared to bare metal stents in the lean and MetS pigs at both stent / artery ratios (Figure 5.3A and B), more evident at 1.3 stent / artery ratio (Figure 5.3B).

Direct involvement of A1R in coronary in-stent stenosis was assessed 4-week after the deployment of PLGA-coated (Polymer) and DPCPX (highly A1R-selective antagonist)-eluting stents (DPCPX) in coronary arteries of lean and MetS pigs at 1.1 stent / artery ratio. Following 6 months of feeding body weight, peak plasma glucose during IVGTT, total cholesterol, LDL, HDL, LDL/HDL, triglycerides, systolic and diastolic blood pressure were all significantly elevated in MetS vs. Lean (Table 5.1). Intravascular ultrasound (IVUS) quantification revealed that DPCPX significantly reduced coronary in-stent stenosis ~50% compared to Polymer in lean and MetS pigs (Figure 5.3C), which was echoed by representative in vivo angiogram (Figure 5.3D), IVUS images (Figure 5.3E), and

in vitro stereoscope images (Figure 5.3F). These results provide definitive evidence for A1R contribution to coronary in-stent stenosis in healthy swine and in the setting of MetS.

5.3.4. A1R expression and ERK1/2 signaling in DPCPX in-stent segments

For the same groups of pigs as in Figure 5.3C-F, we examined A1R protein expression and CCPA-induced ERK1/2 activation in the in-stent and non-stented coronary segments. A1R was upregulated in both Polymer and DPCPX vs. non-stented segments (Non-ST) in Lean (Figure 5.4A) and MetS (Figure 5.4B) pigs. CCPA-induced ERK1/2 activation significantly decreased in DPCPX vs. Polymer and non-stented segments in Lean (Figure 5.4C) and MetS (Figure 5.4D) pigs. In MetS pigs, CCPA-induced ERK1/2 activation was reduced in Polymer vs. non-stented (Figure 5.4D). For non-stented coronary segments, A1R protein were significantly upregulated in MetS compared to Lean pigs, and CCPA-induced ERK1/2 activation was not different between Lean and MetS pigs (not shown).

5.4. Discussion

We made the novel discovery that the A1R upregulation occurred before the maximal coronary in-stent stenosis in Ossabaw swine, consistent with a causal role of A1R in neointimal proliferation. CCPA-induced ERK1/2 activation paralleled the development of in-stent stenosis for bare metal stent, supporting the involvement of A1R-ERK1/2 signaling in neointimal hyperplasia. Using novel

DPCPX-eluting stents we demonstrated for the first time 1) A1R upregulation and A1R activation contributes to coronary in-stent stenosis and 2) selective A1R antagonism rivals the effectiveness of the clinically used Taxus stents in reducing coronary in-stent stenosis in the Ossabaw swine model of MetS. This work has progressed from a fundamental and paradoxical finding in subcultured vascular cells in vitro to demonstration of a novel, efficacious drug-eluting stent in a MetS and CAD swine model in vivo that mimics complex human disease - collectively significant steps in translational medicine.

The Ossabaw pig is an excellent model for study of in-stent stenosis because it develops MetS and CAD and simulates the response to stent deployment in humans better than juvenile domestic swine [11, 92, 95, 97]. Our clinically used angiography and IVUS methods provide compelling data that are highly relevant to clinical medicine [196] and mirror histopathology measures [11].

A possible uncoupling of post-receptor signaling from A1R was supported by the fact that CCPA-induced A1R-ERK1/2 activation was low in all in-stent vs. non-stent 1-week after stenting (Figure 5.2B). A1R-ERK1/2 activation returned to normal at 2-week after stenting for bare metal stents (Figure 5.2C). This transient uncoupling might exist for the sake of self protection. It was showned that during a brief period of preconditioning ischemia, adenosine release protects the heart by uncoupling of A1R from signal transduction mechanisms that lead to injury [197].

Porcine studies suggested that 1-3 days after coronary stenting there is platelet/fibrin deposition surrounding the stent struts [198]. Potentially, huge amounts of adenosine arises from ATP released by platelets and other cell types, largely occupies and activates A1R in coronary SMC or other cell types, and via negative feedback or some unknown mechanisms uncouples A1R from ERK1/2 signal transduction to protect coronary artery from A1R activation-induced possible smooth muscle cell proliferation.

Besides ERK1/2, JNK1/2 and PI3K/AKT are also downstream of A1R activation [69], which may be involved in the A1R contribution to in-stent stenosis, but those other two signaling pathways (JNK1/2 and PI3K/AKT) were not measured in the present study due to the technical difficulties. Jonas etc. reported that in insulin resistant and diabetic rats, ERK1/2 and AKT signaling changed in different directions in stented vascular segments [199]. Therefore, A1R-JNK1/2 and/or A1R-PI3K/AKT signaling could be upregulated in stented segments (BMS or Polymer) vs. non-stent, although A1R-ERK1/2 signaling was not. Another possible explanation for the similar A1R-ERK1/2 activation in in-stent (BMS) vs. non-stent in Lean (Figure 5.2D and Figure 5.4C), or decreased A1R-ERK1/2 activation in Polymer vs. non-stent in MetS (Figure 5.4D) at 4-week post-stent is that the in-stent coronary segments were much thicker than non-stent due to the in-stent stenosis. Fully exposure to CCPA could be partially blunted by layers of proliferative extracellular matrix, e.g. collagen and elastin, in

the arterial wall of the in-stent segments. Therefore, there might be less CCPA-induced ERK1/2 activation detected in the in-stent segments than it actually would be if there were no layers of barriers preventing CCPA from contacting coronary smooth muscle cells. As for why A1R-ERK1/2 activation decreased in Polymer vs. non-stent in MetS (Figure 5.4D) while not in Lean (Figure 5.4C), it might be due to the self-protection mechasim that the in-stent segments compensate for the high elevation of A1R protein by downregulating A1R-ERK1/2 signaling. It may be the case that A1R-JNK1/2 and/or A1R-PI3K/AKT signaling are in opposite direction to A1R-ERK1/2 signaling in the stent as well.

Interestingly, along the whole time course of recovery from stenting, exogenously A1R-ERK1/2 activity in Taxus stented coronary segments was always lower than non-stented segments. Paclitaxel was reported to cause inactivation of ERK1/2 in human KB-3 carcinoma cells [200]. Also, rapamycin, another major drug-eluting stent compound, was reported to inhibit JNK and p38 MAPK in cultured human coronary smooth muscle cells and in rat carotid artery 14 days following injury [201]. It is possible that Taxus acts partially by inhibition of ERK1/2 signaling to prevent cell proliferation in Ossabaw swine. Although A1R protein expression was similar between bare metal and Taxus stents at 1-, 2-, and 4-week post-stenting, in-stent stenosis was significantly reduced in Taxus vs. bare metal stents only at 4-week post-stenting. Endogenous ERK1/2 activity (not requiring stimulation with CCPA; Figure 5.4) after 4 weeks recovery from stenting

was partially blocked by A1R antagonism by DPCPX. This is consistent with the action of Taxus to attenuate ERK1/2 activity and decrease in-stent stenosis. Collectively, these data suggest that both A1R upregulation and A1R-ERK1/2 are important for development of coronary in-stent stenosis.

Both neointima and media layers of in-stent segments showed parallel A1R expression and exogenous ERK1/2 activity at 4-week post-stenting (data not shown), which suggests that neointima and media layers probably came from the same cell type or different cell types acting in parallel with each other in A1R expression and exogenous ERK1/2 activity. Christen etc. reported that SMCs are the main components of coronary artery neointima after stent deployment [202], which supports the first interpretation. A1R was upregulated in endothelium intact coronary in-stent segments, therefore the increase of A1R can occur in coronary SMC, endothelial cells, or even surrounding macrophages, leucocytes, etc. in the in-stent segments. A1R are expressed in neutrophils, macrophages, and T-cells in human asthma patients [203] and peaked in mouse macrophages during leukocyte recruitment [204]. However, we are not aware of reports of A1R upregulation selectively in those cell types in coronary artery disease or in-stent restenosis, thus indicating that further study is needed.

There are still many discrepancies regarding whether EC express A1R or not. A1R was reported not expressed in human umbilical vein EC and skin microvascular EC [205, 206]. In contrast, A1R was reported to lower basal permeability in human umbilical vein EC in response to oxidant injury [207], or regulate mouse embryonic endothelial progenitor cells adhesion to cardiac microvascular EC [208], or decrease nitric oxide production by human iliac arterial EC and porcine carotid arterial EC [209]. Our study showed that A1R protein is present in subcultured EC isolated from right coronary artery of Ossabaw swine (see Figure 5.5B available in the online data supplement). A1R involvement in proliferation of coronary EC, and other cardioprotective functions mediated by A1R in coronary EC are completely unknown. Since A1R and A2R are coupled with Gi and Gs proteins separately [51, 69] and their functions were reported almost exclusively opposite to each other [65-68], it is highly probably that A1R mediate antimitogenic effect of adenosine in coronary EC. If true, then we further propose that A1R activation has deleterious actions in both coronary SMC and EC. Along this line, the benefit of local administration of the highly selective A1R antagonist DPCPX not only lies in prevention of coronary SMC proliferation, but also in potentiation of coronary EC growth in the in-stent segments, which would help reduce late stent thrombosis risk accompanying clinically used drug eluting stents [80-85]. Since important design criteria for drug eluting stents include more cell-type specificity and promotion of endothelialization and healing [79], DPCPX-eluting stents could be a substantial innovation in drug-eluting stents if the A1R mediates antimitogenic effects of adenosine in coronary EC. Further study is

definitely needed regarding the possible antimitogenic effect of A1R in coronary EC.

Further, A2AR protein was found by immunoblot in subcultured coronary SMC isolated from Ossabaw swine, while A2BR was not detectable (Figure 5.5A), consistent with our previous findings of low levels of A2BR gene in cultured coronary SMC and endothelium-denuded porcine right coronary [65]. In endothelium-intact porcine right coronary arteries there are A1R, A2AR, A2BR and A3R expression revealed by real-time RT-PCR (Figure 5.5C). Since A2BR was not detected in isolated porcine coronary SMC, A2BR are present exclusively in coronary EC, consistent with our previous study [65]. A2BR and A2AR were reported to mediate the antimitogenic effect of adenosine in porcine coronary artery EC and human umbilical vein EC, respectively [210, 211]. Because A2BR is present in porcine coronary EC and may mediate antimitogenic effects of adenosine in coronary EC, A2BR could be another potential target in drug eluting stents (DES) to help reduce late stent thrombosis associated with DES. And A2AR could be targeted to decrease coronary in-stent stenosis if the A2AR mediates antimitogenic effects of adenosine in coronary artery smooth muscle cells.

In summary, our in vivo data showing the association of A1R expression with coronary in-stent stenosis and the attenuation of both events by selective

A1R antagonism provide strong evidence that A1R upregulation and A1R signaling contributes to coronary in-stent stenosis in MetS. Our novel DPCPX-eluting stents offer a promising, novel therapy for coronary in-stent stenosis in human MetS patients.

5.5. Materials and Methods

5.5.1. Animal care and cardiac catheterization procedures

All protocols involving animals were approved by an Institutional Animal Care and Use Committee and complied fully with recommendations in the Guide for the Care and Use of Laboratory Animals [105] and the American Veterinary Medical Association Panel on Euthanasia [106]. Cardiac catheterization, angiography, stenting (detailed description in the online supplemental materials), and intravascular ultrasound (IVUS) were performed as previously described at the time of stent deployment and several weeks later (detailed in the following paragraphs) at sacrifice [70, 92]. To prevent thrombosis after stent placement, each animal received standard daily antiplatelet therapy (75 mg Plavix and/or 325 mg aspirin) beginning the day before the initial catheterization procedure and continuing until sacrifice in accordance with standard clinical postoperative care.

We studied the time course of A1R, A1R-ERK1/2 signaling and coronary in-stent stenosis in Ossabaw swine by allowing 1, 2, or 4 weeks of recovery after coronary stenting (Figure 5.1 and Figure 5.2). Bare metal and paclitaxel-eluting (Taxus; Boston Scientific, Inc., Minneapolis, MN, USA) stents were placed in

either left circumflex or left anterior descending coronary by random assignment in 15 male Ossabaw swine (n=5/group; age 8 ± 0.5 months at sacrifice) that were fed standard chow diet (5L80; Purina TestDiet, Richmond, IN, USA). Right coronary artery served as non-stented control. Stent to artery ratio (determined by intravascular ultrasound) was 1.0 or 1.3 for bare metal and 1.0 for Taxus stents. Due to the limited artery length and dimension, stent / artery ratio of 1.3 was omitted for Taxus. A total of 3 stents was placed in each pig.

The effects, of bare metal and Taxus stents deployed at 1.0 and 1.3 stent / artery ratio on in-stent stenosis were also studied in the setting of MetS in another 10 male Ossabaw swine (n=5/group; age 20 ± 2 months at sacrifice). Pigs were assigned to 2 different diet groups for 6 months. The Lean group was fed standard chow consisting of (% kcal): 18.5 protein, 71 carbohydrate, and 8 fat. The MetS group was fed hypercaloric, atherogenic diet consisting of (% kcal): 8 protein, 18 fructose, 31 complex carbohydrates, and 43 fat. A total of 4 stents (1.0 / 1.3 bare metal and Taxus) were placed in coronary arteries (similar strategy as the above protocol) and 4 weeks of recovery was given before sacrifice.

The effects of the A1R-selective antagonist 8-cyclopentyl-1, 3-dipropylxanthine (DPCPX) on A1R and A1R-ERK1/2 signaling and coronary in-stent stenosis were studied with DPCPX-eluting stents. Ossabaw swine (n=5 pigs/group; age 17 ± 2 months at sacrifice) were assigned to Lean and MetS diet

groups described above for 7 months. The Lean group was again fed standard chow and MetS group fed atherogenic diet very similar to the previous MetS diet, but included mixed fat sources (5B4L; Purina TestDiet). Polymer-coated stents and DPCPX-eluting stents were placed in either circumflex or left anterior descending coronary by random assignment. Stent to artery ratio was 1.1 for both stents and 4 weeks of recovery was allowed before sacrifice.

5.5.2. Polymer/drug loading

The biodegradable polymer used on the drug-eluting stent system was poly(glycolic acid-co-lactic acid) (PLGA), an aliphatic polyester copolymerized from glycolic acid and lactic acid. PLGA is hydrophobic and undergoes bulk erosion as water diffuses into the polymer bulk where hydrolytic degradation occurs. Stents were coated by a solution of PLGA (50: 50) and DPCPX in tetrahydrofuran (final concentration of 30% DPCPX; DPCPX, Tocris Bioscience, Ellisville, MO, USA). The PLGA or PLGA/DPCPX mixture was sprayed onto the stents and dried to constant mass. DPCPX content of the stent was determined by gravimetric analysis and verified by dissolving the coating off the stents and measuring the DPCPX content by high-performance liquid chromatography (HPLC). In vitro elution kinetics were determined on non-expanded stents immersed in 3 ml aliquots of agitated PBS with 0.05% Tween 20 at 37ºC for 28 days [212]. Buffer was changed periodically and the DPCPX content determined by HPLC. The DPCPX-eluting stents contained a 7: 3 polymer-to-DPCPX ratio for a total dose density of 18.75 µg/mm of stent length.

5.5.3. Intravascular ultrasound (IVUS) analysis

IVUS methods identical to human clinical use were used in vivo to determine coronary in-stent stenosis in Lean and MetS swine and off-line analysis was performed by a blinded operator, as described previously [11, 70, 92, 95]. In-stent stenosis was quantified as percent area stenosis and calculated as (plaque area ÷ [original lumen area + plaque area]) × 100%. Images were captured every 1 mm along the whole pullback length of IVUS and 8 images quantified and averaged for each in-stent coronary segment.

5.5.4. Intravenous glucose tolerance test (IVGTT)

Swine were acclimatized to restraint in a specialized sling for 5-7 days before the IVGTT was conducted. Following percutaneous catheterization of the right jugular vein under isoflurane anesthesia [11, 92, 95], swine were allowed to recover for 3 hours before the IVGTT to avoid any effect of isoflurane on insulin signaling [176]. Conscious swine were restrained in the sling and baseline blood samples were obtained. Dextrose (1 g/kg body weight) was administered intravenously and timed blood samples were collected [176]. Blood glucose was measured using YSI 2300 STAT Plus Glucose analyzer. Plasma insulin assays were performed by MILLIPORE Research Laboratories (St. Charles, MO, USA).

5.5.5. Immunoblots for A1R and p-ERK1/2

Coronary artery segments were pretreated with 10^{-6} M of highly A1R-selective agonist 2-chloro-*N*-6-cyclopentyladenosine (CCPA; Tocris Bioscience)

at 37° C for 5 minutes for detection of exogenous A1R activation induced-ERK1/2 activition. Detailed immunoblot methods are included in the online supplemental materials. The membranes were immunoblotted for A1R (rabbit polyclonal antibody; 1:1000 dilutions; Abcam, Cambridge, MA, USA) and p-ERK1/2 (mouse monoclonal antibody; 1:1000 dilutions; Cell Signaling, Danvers, MA, USA). Membranes were stripped and reprobed with anti-GAPDH (1:1000; Fitzgerald, Concord, MA, USA) or anti-total ERK1/2 (1:1000 dilutions; Cell Signaling).

5.5.6. Lipid analysis

Venous blood samples were obtained following overnight fasting and analyzed for triglyceride and total cholesterol [fractionated into high density lipoprotein (HDL) and low density lipoprotein (LDL) components]. Plasma lipid assays were done using Infinity lipid kit (ThermoFisher Scientific, VA, USA). Apolipoprotein-B-containing lipoproteins were precipitated with heparin-$MnCl_2$ and the supernatant was assayed to determine cholesterol in lipoprotein fractions [95]. LDL was calculated from the Friedewald equation: LDL = total cholesterol - HDL - (triglyceride ÷ 5).

5.5.7. Statistics

Data were presented as mean ± SEM. Statistical analysis was performed using commercially available software (SPSS version 12, Prism version 4.0 and SAS). Means of 2 groups were compared using Student t test (unpaired, two

tailed). Means of more than 2 groups (except data from Figure 5.3) were compared using Kruskal-Wallis one-way analysis of variance (ANOVA), followed by post-hoc testing using Least-Significant-Difference test. For data from Figure 5.3A-B, group comparison was done using two-way ANOVA, followed by post-hoc testing using Bonferroni test. For data from Figure 5.3C, general linear model was used for multivariate analysis of variance between groups. The $p<0.05$ level was considered significant.

5.6. Acknowledgments

The authors thank James P. Byrd, James W. Wenzel, Zachary P. Neeb, Hong Fang and Dr. Ian Bratz for their excellent technical assistance and Dr. Eric Mokelke (Boston Scientific, Inc.) for his generous help and support for the study.

Xin Long made essential contributions to experimental design, data acquisition, data analysis and interpretation for all the figures. She drafted the whole article and revised till the current version. Dr. Mouhamad Alloosh took part in all the metabolic data acquisition, analysis and revising critical methods part. Dr. Kinam Park, Jutarat Kitsongsermthon, and Yuanzu He made substantial contributions to the coating design of drug eluting stents, and analysis of data and revising critical part. Dr. Michael Sturek made the biggest contribution to experimental conception and design, analysis and interpretation of data. He made a major contribution to revision of the article as well. All authors finally approved the version to be published.

This work was supported by NIH grants RR013223, HL062552, a gift from Boston Scientific, Inc. to M.S., and an American Heart Association Predoctoral Fellowship to X.L.

5.7. Figure legends

Figure 5.1. Coronary in-stent stenosis and A1R expression in pigs with different amounts of stent expansion and durations of recovery from stenting

Stent/artery expansion ratio were 1.0 (normal artery diameter) and 1.3 (30% over-expansion in artery diameter). Stenting recovery durations were 1, 2 or 4 weeks. A-C: In-stent stenosis of 1.0 bare metal (A), 1.3 bare metal (B) and 1.0 Taxus (C) was quantified in vivo using intravascular ultrasound (IVUS) as percent area stenosis along the whole length of in-stent segments. Percent area in-stent stenosis = (Area of Neointima) / (Area of Original Lumen indicated by stent struts) x 100. Inset in A shows a representative IVUS image of in-stent stenosis with the stent struts (dotted line), artery lumen (dashed line), and neointima (area between stent struts and lumen) marked for clarity. D-F: Immunoblots for detection of A1R protein were performed in in-stent coronary segments with varying stent/artery ratio (D-1.0 bare metal, E-1.3 bare metal, F-1.0 Taxus) harvested from lean pigs after 1, 2 or 4-week stenting recovery (n=5/group with different stenting recovery). Non-stented (Non-ST) coronary segments served as control. Representative blots of A1R (upper lanes) and GAPDH (lower lanes) are shown above group data averages. *, $p<0.05$ vs indicated groups; #, $p<0.01$ vs marked groups; **, $p<0.001$ vs indicated groups.

Figure 5.2. A1R-ERK1/2 signaling in non-stented and in-stent coronary segments with different stent types and different stenting recovery durations (same as described in Figure 5.1)

A: Right coronary segments freshly harvested from lean pigs were treated with the highly A1R-selective agonist CCPA at 10^{-6} M for different durations (5, 10, 15, 30, or 60 minutes). Immunoblots of phosphorylated ERK1/2 (p-ERK1/2) and total ERK1/2 (t-ERK1/2) were done in the CCPA-treated and non-treated coronary segments. The p-ERK1/2 to t-ERK1/2 ratio (p/t-ERK1/2) with CCPA treatment, as determined by immunoblot quantification, was used to evaluate exogenous A1R activation (CCPA-induced ERK1/2 activation). B-D: P-ERK1/2 and t-ERK1/2 levels were determined by immunoblot in non-stented and in-stent coronary segments (1.0 bare metal, 1.3 bare metal, and 1.0 Taxus, as in Figure 5.1) harvested from pigs either 1- (B), 2- (C), or 4-week (D) after stenting (n=5/group with different stenting recovery). All segments were treated with CCPA for 5 minutes before immunoblot analysis to determine exogenous A1R-ERK1/2 activity. Non-stented (Non-ST) served as control. Representative blots of p-ERK1/2 and t-ERK1/2 are shown above the group data averages. *, $p<0.05$ vs. samples at 0, 10, 15, 30-minute treatment (A); #, $p<0.01$ vs. samples at 0, 10, 15, 30-minute treatment (A) or marked groups (B-D).

Figure 5.3. In-stent stenosis in pigs treated with bare metal stents and Taxus or DPCPX (highly A1R-selective antagonist)-eluting stents

Bare metal stents and Taxus stents were deployed in coronary arteries in lean and metabolic syndrome (MetS) Ossabaw pigs (n=5/group) with stent / artery ratios of 1.0 (A) and 1.3 (B). Polymer-coated (Polymer) and DPCPX-eluting stents (DPCPX) were deployed concurrently in coronary arteries with stent / artery ratio of 1.1 in lean and MetS pigs (n=5/group). Polymer served as control (C). A-C: Intravascular ultrasound (IVUS) was done 4 weeks after stenting in vivo to evaluate in-stent stenosis for different conditions. Percent area stenosis along the whole length of in-stent segments was quantified by IVUS, as defined in Figure 5.1. D-F: Representative images of two in-stent coronary segments (Polymer, DPCPX) from the same MetS pig under in vivo angiography (D), IVUS (E) and stereomicroscope (F). D: Left anterior oblique 30 degree view of LAD: White arrows indicate DPCPX; black arrows indicate polymer. E: Stent struts (dotted line), artery lumen (dashed line), and neointima (area between stent struts and lumen) were depicted for clarification. The distance between each neighboring dot horizontally or vertically is 1 mm. F: In-stent coronary segments were cut open after harvesting at sacrifice. Adventitia was outside stainless steel struts and neointima was inside the stent struts. *, $p<0.01$ as indicated by lines.

Figure 5.4. A1R and ERK1/2 activation in non-stented and in-stent coronary segments

As in Figure 5.3C, polymer-coated (Polymer) and DPCPX-eluting stents (DPCPX) were deployed concurrently in coronary arteries with stent / artery ratio of 1.1 in lean and MetS Ossabaw pigs (n=5/group). Coronary segments were harvested freshly for analysis 4-week after stenting. Immunoblots of A1R, GAPDH (A-B), phosphorylated-, and total-ERK1/2 (p-ERK1/2, t-ERK1/2, C-D) were done in non-stented (Non-ST), and in-stent coronary segments (Polymer, DPCPX) in the Lean (A, C) and MetS (B, D) pigs. Representative blots of A1R and GAPDH, p-ERK1/2 and t-ERK1/2 are shown above group data averages. GAPDH served as loading control. P-ERK1/2 to t-ERK1/2 ratio (p/t-ERK1/2) was used to evaluate CCPA-induced ERK1/2 activation. *, $p<0.05$; #, $p<0.01$ as indicated by lines.

5.8. Figures

Figure 5.1. Coronary in-stent stenosis and A1R expression in pigs with different amounts of stent expansion and durations of recovery from stenting

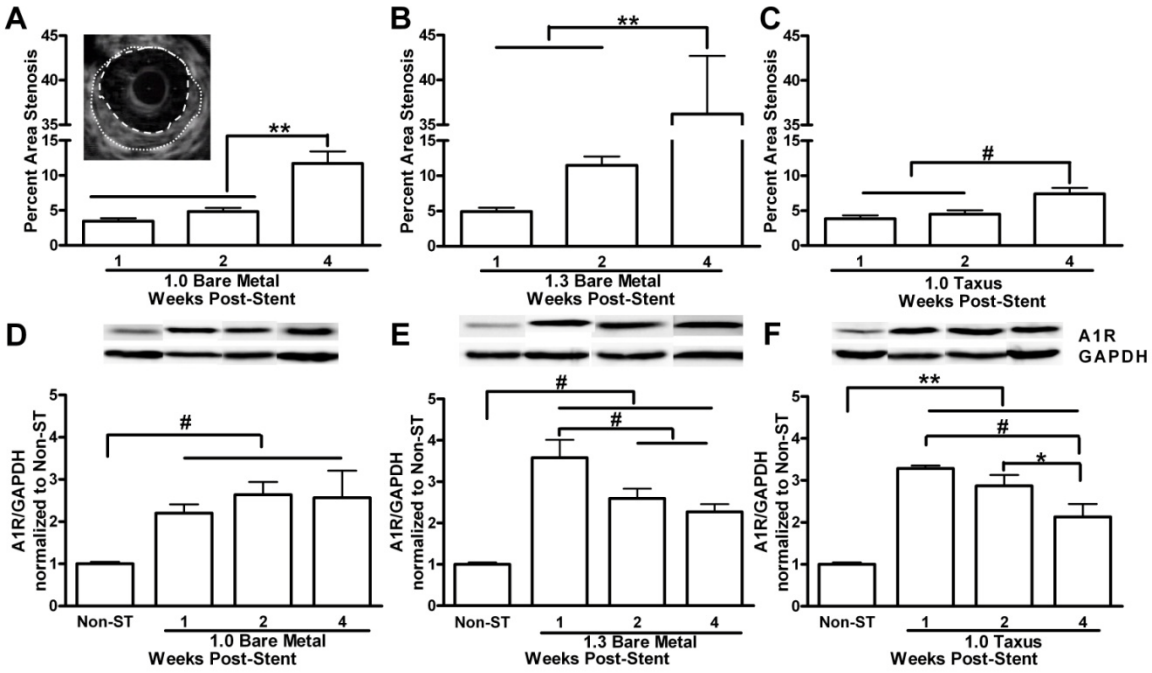

Figure 5.2. A1R-ERK1/2 signaling in non-stented and in-stent coronary segments with different stent types and different stenting recovery durations

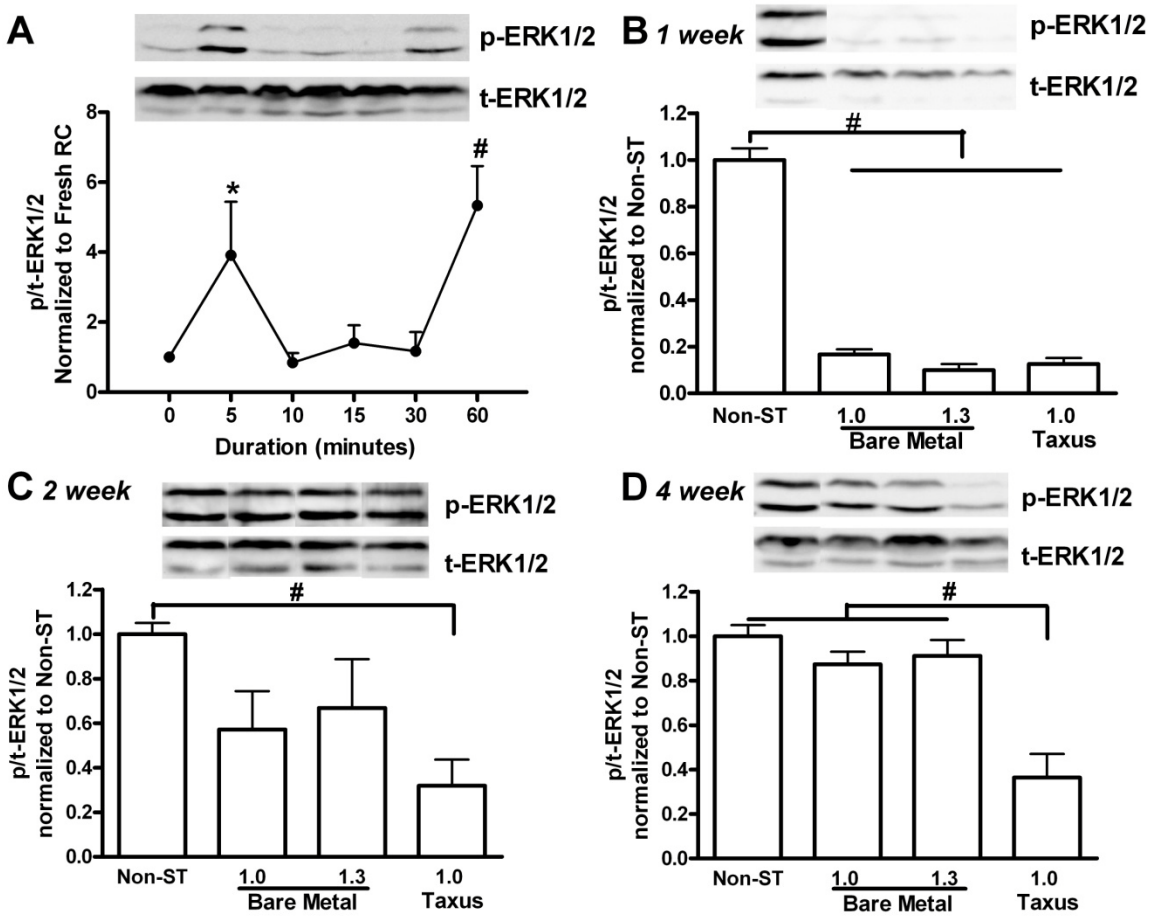

Figure 5.3. In-stent stenosis in pigs treated with bare metal stents and Taxus or DPCPX (highly A1R-selective antagonist)-eluting stents

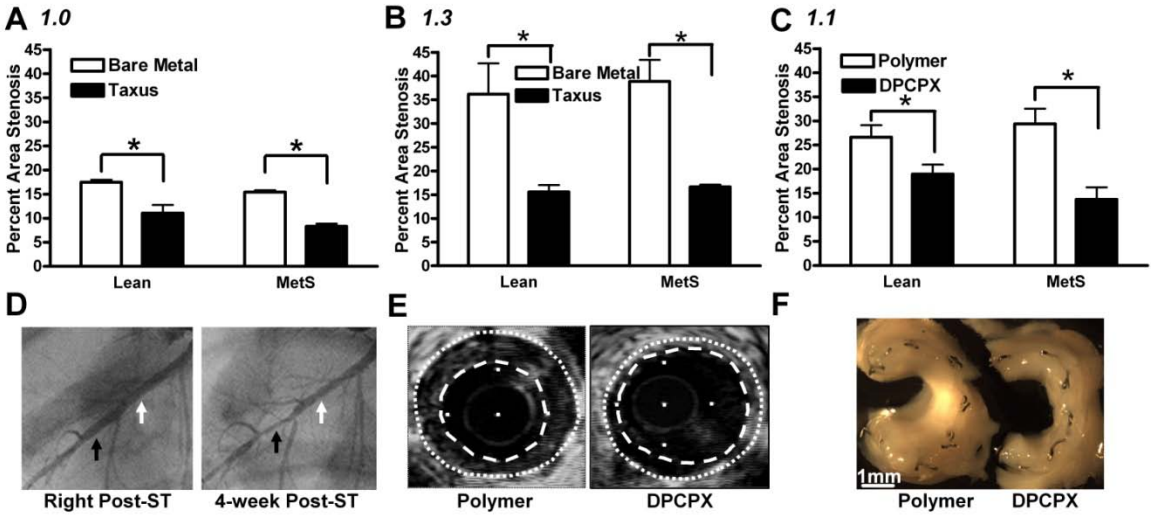

Figure 5.4. A1R and ERK1/2 activation in non-stented and in-stent coronary segments

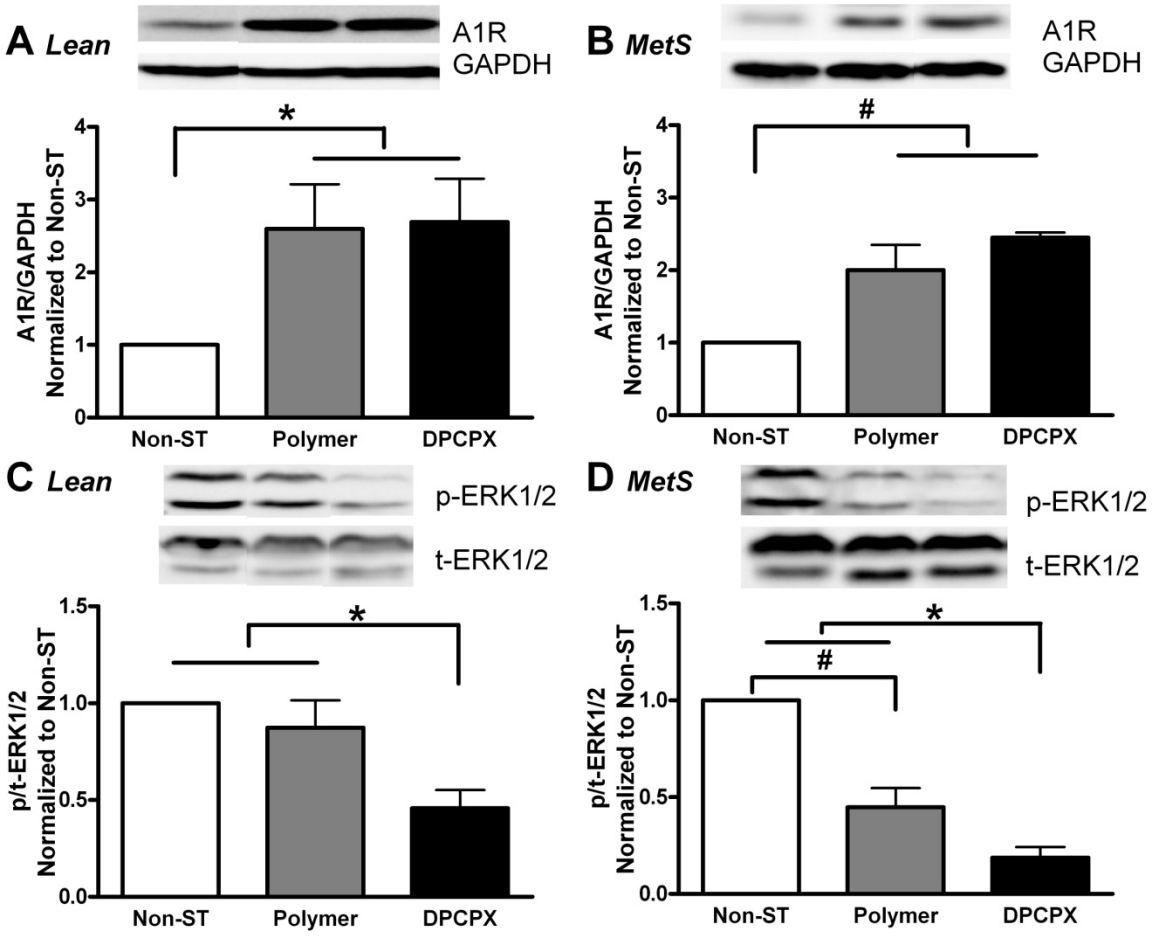

5.9. Table

Metabolic Index	Lean	MetS	p value
Body Weight (kg)	110.5 ± 1.8	140.4 ± 2.1	0.0001
Peak Plasma Insulin (μU/mL)	72.0 ± 7.4	123.0 ± 28.6	0.11
Peak Plasma Glucose (mg/dL)	595.2 ± 25.6	710.6 ± 44.8	0.0499
Total Cholesterol (mg/dL)	58.6 ± 2.7	457.3 ± 51.8	0.00005
LDL (mg/dL)	27.3 ± 1.7	340.7± 37.9	0.0008
HDL (mg/dL)	26.7 ± 1.7	103.9 ± 18.5	0.0004
LDL/HDL	1.0 ± 0.1	4.3 ± 0.8	0.001
Triglycerides (mg/dL)	23.0 ± 1.5	63.1 ± 13.8	0.0118
Systolic Blood Pressure(mm Hg)	110.0 ± 1.8	140.4± 2.1	0.00003
Diastolic Blood Pressure(mm Hg)	68.0± 2.2	92.9 ± 1.6	0.000063

Table 5.1 Metabolic data of the Lean and MetS Ossabaw pigs in Figure 5.3C-F and Figure 5.4.

Statistical difference between the Lean and MetS groups are indicated in the right column. LDL = low-density lipoprotein, HDL = high-density lipoprotein.

5.10. Supplementary methods

5.10.1. Western Blotting for A1R and p-ERK1/2

For the western blots of p-ERK1/2 and A1R, coronary artery segments were pretreated with 10^{-6} M CCPA at 37° C for 5 minutes before lysed with 1% SDS lysis buffer with addition of protease inhibitor cocktail and phosphatase inhibitor cocktail (Sigma, St. Louis, MO, USA). Lysates were sonicated to disrupt DNA before BSA assay (Pierce, Rockford, IL, USA) for protein concentration determination, solubilized in Laemmli sample buffer with 200 M dithiothreitol, and boiled for 2 minutes and proteins were separated on SDS-PAGE gels. The proteins were then electrophoretically transferred to nitrocellulose membrane in 25 M Tris, 192 M glycine, and 20% methanol. The nitrocellulose was blocked with 5% nonfat dry milk in 10 M Tris (pH 7.4), 150 M NaCl, and 0.01% Tween 20. The membranes were probed with the individual primary antibody (anti-adenosine A1 receptor; 1:1000 dilutions; Abcam, Cambridge, MA, USA; anti-p-ERK1/2; 1:1000 dilutions; Cell Signaling, Danvers, MA, USA) overnight in 10 M Tris (pH 7.4), 150 M NaCl, 5% nonfat dry milk, and 0.01% Tween 20. The blots were washed in 10 M Tris (pH 7.4), 150 M NaCl, and 0.01% Tween 20, and bound antibody was detected by a horseradish peroxidase-conjugated anti-rabbit or anti-mouse IgG and enhanced chemiluminescence (Pierce). Equal protein loading was verified by stripping off the original antibody, and reprobing with the primary antibody anti-GAPDH (1:1000; Fitzgerald, Concord, MA, USA) or anti total-ERK1/2 (1:1000 dilutions; Cell Signaling).

5.11. Supplementary figure legends

Figure 5.5. AR expression in porcine coronary SMC, EC, and endothelium-intact right coronary artery

A. Immunoblots of A1R, A2AR, A2BR were done in subcultured coronary SMC isolated from Ossabaw right coronary artery. GAPDH served as control. B. Immunoblots of A1R were done in subcultured coronary EC isolated from Ossabaw right coronary. Vinculin served as loading control. C. RT-PCR for detection of the A1R, A2AR, A2BR, and A3R mRNA expression levels was performed with endothelium-intact right coronary artery freshly isolated from Ossabaw swine. RT-PCR done without reverse transcriptase or without template is indicated as -RT or NTC, respectively.

Figure 5.6. Other adenosine receptor subtype expression in 1.0 bare metal stent during time course following stenting recovery

Real-time RT-PCR for detection of A2AR (A) and A2BR (B) mRNA expression levels was performed in 1.0 bare metal stent (as denoted in Figure 5.1) in pigs 1-, 2-, and 4-week post stenting (n=5/group).

5.12. Supplementary figures

Figure 5.5. AR expression in porcine coronary SMC, EC, and endothelium-intact right coronary artery

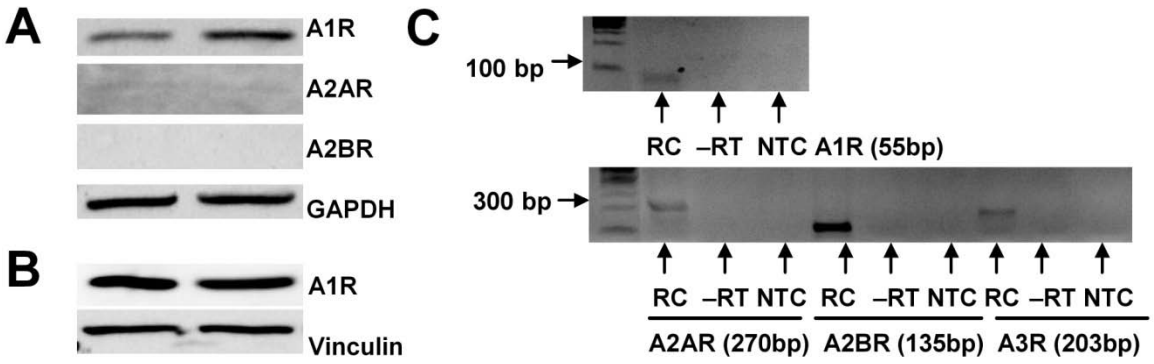

Figure 5.6. Other adenosine receptor subtype expression in 1.0 bare metal stent 1-, 2-, or 4-week following stenting

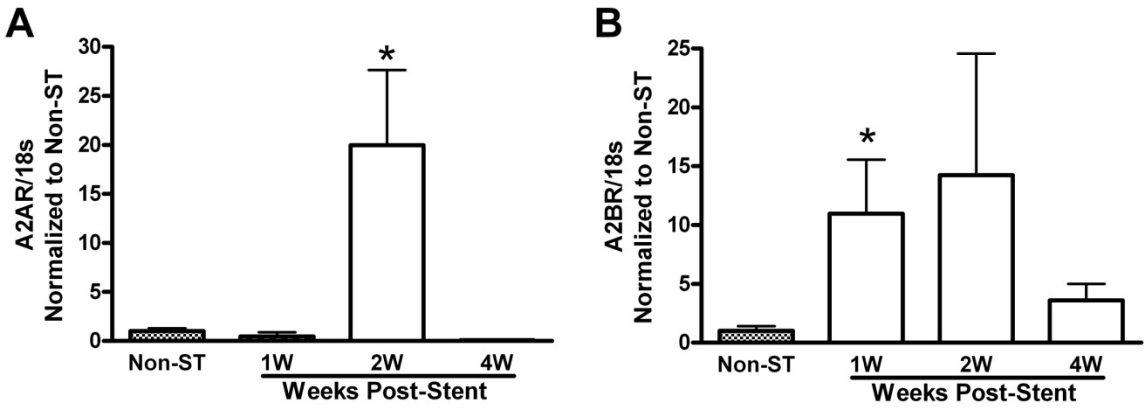

CHAPTER 6. COMPREHENSIVE DISCUSSION

6.1. General overview

Adenosine was widely thought to mediate vasodilation and also attenuate SMC proliferation, thus providing cardioprotection [54]. A1R became really interesting to us in that SMC proliferation plays an important role in CAD and restenosis [9, 62-64] and our lab made a novel discovery that A1R mediated mitogenic effect of adenosine in coronary SMCs. The work in this thesis focused on the role of A1R in native coronary atheroma, in-stent stenosis and coronary blood flow regulation (Chapter 4, 5 and 3 respectively). In general, the effects of exercise were usually opposite to those elicited by MetS and CAD. Exercise training in this thesis consisted of 7-week treadmill running and was used to evaluate the beneficial effects of exercise in circumstances of microvessel dysfunction (Chapter 2) and macrovascular atherosclerosis with or without stenting (Chapter 2 and 4 respectively). Most of the studies presented in this dissertation utilized the Ossabaw swine model of MetS and CAD (Chapter 4 and 5) or dyslipidemia (Chapter 3). Yucatan swine was used in addition to that (Chapter 2). The major findings from these studies include 1) A1R promotes CAD in vitro and may contribute to coronary atherosclerosis in vivo in the setting of MetS (Chapter 4); 2) A1R upregulation and A1R signaling contribute to coronary in-stent stenosis in MetS (Chapter 5); 3) A1R antagonism by DPCPX might promote vasodilation induced by some vasodilators other than adenosine in “healthy” Ossabaw swine and an imbalance of A1R/A2AR upregulation and signaling in coronary microcirculation distal to a stent may contribute to the

impaired adenosine-induced flow in dyslipidemia (Chapter 3); 4) Short-term exercise training near the time of stenting prevented stent-induced microvascular dysfunction and attenuated native atheroma in the genetically lean Yucatan swine (Chapter 2) as well as Ossabaw swine (Chapter 4).

6.2. A1R contribution to native coronary atherosclerosis and in-stent stenosis

SMC proliferation is a key step in the development of occlusive vascular diseases, like atherosclerosis and restenosis after stenting [9, 62-64]. The novel findings of the A1R-mediated trophic effect of adenosine via ERK1/2 activation in coronary SMCs led to the hypothesis that A1R upregulation and A1R signaling contribute to both native coronary atherosclerosis and in-stent stenosis in MetS (Chapter 4 and 5 respectively). Selective A1R antagonism strongly supported the causal role of A1R activation in in-stent stenosis in vivo and atherosclerosis in vitro (Chapter 5 and 4 separately). To our knowledge this is the first discovery that A1R contributes to coronary atherosclerosis in vitro and in-stent stenosis in vivo in the setting of MetS.

A1R activation produced myocardial preconditioning in the canine heart by opening K_{ATP} channels [213, 214] and reduced ischemia-induced ventricular arrhythmias and fibrillation in the porcine heart [215], thus providing cardioprotection. Adenosine A2A receptor (A2AR) activation inhibited foam cell formation by stimulation of the reverse cholesterol transport protein expression, thereby preventing atherosclerosis [216]. The functions of A1R and A2R were

reported almost exclusively opposite to each other [65-68], so A1R could potentially promote atherosclerosis, contradictory to its traditional role. The in vitro studies done in the thesis verified proatherogenic actions of the A1R (Chapter 4 and 5).

Aldosterone is often elevated in MetS and contributes to CAD by altered insulin/IGF-1 signaling pathways, reactive oxygen species formation, etc. [44]. Dexamethasone was reported to regulate A1R expression [74-76], but aldosterone regulation of A1R has never been reported. We discovered for the first time that aldosterone upregulated A1R mRNA and protein expression in subcultured coronary SMCs (Chapter 4, Figure 4.3). Aldosterone contribution to CAD in the in vitro organ culture model was found partially mediated through A1R activation, which is a novel discovery (Chapter 4, Figure 4.5). Interestingly, aldosterone was reported to increase neointimal formation after balloon injury [48], suggesting possible contribution of aldosterone regulation of A1R in coronary in-stent stenosis as well, which deserves further study.

A1R upregulation was observed in both types of occlusive coronary diseases, native atherosclerosis and in-stent stenosis in MetS (Chapter 4 and 5 respectively). We propose that aldosterone contributes to A1R upregulation in native atheroma (Chapter 4, Figure 4.5); however, other factors could contribute to the A1R upregulation in the occlusive coronary disease as well. Angiotensin II in relation to A1R expression was studied, but the connection was not observed (data not shown). Lipids, reactive oxygen species, inflammatory factors, and

cytokines are all possible driving forces for A1R upregulation in atherosclerosis and in-stent stenosis, which may need further clarification.

As a summary for the role of A1R contribution to CAD and in-stent stenosis, I have refined the model originally proposed by Shen etc. [65, 69] (Chapter 6, Figure 6.1). Large amounts of platelets adhere to coronary stents, resulting in ATP release from platelets and coronary endothelial cells. ATP breaks down into adenosine, which leads to A1R and downstream signaling activation in coronary SMCs, and promotes coronary in-stent stenosis. In MetS, aldosterone elevates and activates mineralocorticoid receptor (MR) or other factors, which potentially serves as a transcriptional factor and upregulates A1R in coronary SMCs, thus contributing to coronary atherosclerosis.

6.3. Adenosine and adenosine receptors in regulation of coronary blood flow

Adenosine is a nucleoside with a half life < 20 seconds in human blood [139], and regulates coronary blood flow especially during stress and ischemia [136-139]. Adenosine is largely an endothelium independent vasodilator, especially in the porcine coronary microcirculation, with little influence on the macrocirculation [138, 139]. There are 4 different subtypes of adenosine receptors (AR)-A1R, A2AR, A2BR and A3R [51]. Adenosine binds to adenosine A2 receptor (A2R), increases cytosolic cyclic adenosine monophosphate (cAMP) as the second messenger, and results in vasorelaxation [139], which is consistent with our finding that A2R

mainly A2AR mediates vasodilation effects in porcine coronary microcirculation (Chapter 3, Figure 3.2).

We found adenosine A1 receptor (A1R) antagonism potentiates vasodilatory effects of some vasodilators other than adenosine in the porcine coronary microvessels under basal conditions (Chapter 3, Figure 3.3), consistent with research done by Pelleg etc. in canine heart [156], while in sharp contrast to the findings that A1R does not contribute to adenosine-induced flow in swine [141, 147, 154]. Experimental design might count for the differences, but experimental condition might be a more important cause. Our study and Pelleg study [156] were done in vivo, and in vitro manipulations were done by the other groups [141, 147, 154]. As the in vivo experiments are more integrative and systemic, our in vivo study is more physiologically relevant vs. in vitro studies.

We found that bare metal stent deployment in conduit coronary arteries elicited impaired adenosine-induced flow in dyslipidemic Ossabaw swine (Chapter 3, Figure 3.4) and hypercholesterolemic Yucatan miniature swine (Chapter 2, Figure 2.2), which was associated with increased A1R and A2AR expression (Chapter 3, Figure 3.5). The altered balance between A1R and A2AR signaling might contribute to that. However, AR specific agonists or antagonists were not used in either control or dyslipidemic swine, which would be a further step in the future.

6.4. Beneficial effects of exercise in macrovascular and microvascular circulation

Exercise training of patients with CAD induces multi-benefits, including improvement in exercise tolerance and increased coronary conduit and microvessel dilation [18-23]. We found that short-term exercise training partially restored the impaired braydkinin and/or adenosine-induced flow in hypercholesterolemic swine after stenting (Chapter 2, Figure 2.2) and decreased coronary conduit atheroma burden in MetS (Chapter 4, Figure 4.1) and hypercholesterolemia (Chapter 2, Figure 2.3). Noticeably, the beneficial effects of exercise were independent of changes in plasma lipids in MetS and hypercholesterolemia (Chapter 4, Table 4.1, and Chapter 2, Table 2.1, respectively). Interestingly, plasma aldosterone and A1R protein expression in native atheroma were altered by exercise in MetS (Chapter 4, Figure 4.1), suggesting aldosterone and A1R could contribute to decreased atheroma by exercise.

The findings of impaired responses to adenosine (largely endothelium-independent vasodilator) suggest that the microvascular dysfunction was not limited to endothelium, but smooth muscle function could be adversely affected as well. We also found that hypercholesterolemia decreased microvessel density and exercise training prevented that (Chapter 2, Figure 2.4), suggesting that microvessel rarefaction might be the underlying mechanism for microvascular dysfunction in hypercholesterolemia.

6.5. Future directions

The A1R contribution to coronary atherosclerosis was verified in the in vitro organ culture model of coronary atherosclerosis. However, the causal role of the A1R in coronary atherosclerosis in vivo was not verified yet. We may be able to test the causal role of A1R in atherosclerosis in vivo via chronic systemic infusion of A1R-selective antagonist DPCPX. If DPCPX decreases the coronary atherosclerosis vs. vehicle infusion in MetS, it suggests that A1R plays a causal role in the development of CAD in vivo.

A1R was upregulated by aldosterone in coronary SMCs, however, the umderlying mechanisms were not explored yet. Upon ligand binding, steroid receptors interact with specific hormone response elements in the promoters of hormone responsive genes, recruiting cofactors in a ligand-dependent manner, thereby regulating gene expressions [46]. Aldosterone is a steroid hormone [164], upon binding to MR (a ligand-activated transcription factor) [164], enters the nucleus and possibly binds to the corresponding DNA sequence or other factors to regulate A1R gene expression. We could perform luciferase and ß-galactosidase assays with plasmid construction in coronary SMCs to test if aldosterone-MR complex directly binds to A1R promoter and thus increases A1R transcriptional activity or not. Promoter A and B controls A1R gene expression [74]. Promoter A is more active but only observed in selected tissues and promoter B is constitutively expressed but at much reduced levels. It was reported that A1R expression was enhanced when only promoter B was present [74]. It could be

aldosterone upregulation of A1R was mediated through interaction with promoter B, and we can determine if promoter B is involved in the gene regulation process or not in the above mentioned experiments.

Aldosterone possibly contributes to coronary atherosclerosis, which shares similar pathophysiological process with in-stent stenosis, thus aldosterone could potentially regulate A1R expression in in-stent stenosis as well. To test the hypothesis, we could first determine if aldosterone increases in the stented pigs or not. If that is the case, we could go further with systemic infusion of aldosterone-specific antagonist-spironolactone in the pigs with stent deployment. If spironolactone infusion decreases A1R expression and the in-stent stenosis vs. vehicle infusion, aldosteone regulation of A1R plays a causal role in the development of in-stent stenosis. The finding will be of great therapeutic potential in alleviating in-stent stenosis.

Besides aldosterone, other mechanisms could upregulate A1R expression in native coronary atherosclerosis and in-stent stenosis. Possible contributors include: lipids, reactive oxygen species, and inflammatory factors, all of which deserves our research attention. We could explore their possible roles in regulation of A1R expression by combination of in vitro cell or tissue culture and in vivo animal study as we did with aldosterone regulation of A1R gene.

The research presented in this thesis dissertation unveiled the important roles of A1R in native coronary atherosclerosis, in-stent stenosis, and coronary blood flow regulation especially in MetS. The beneficial effects of exercise in alleviation of coronary conduit atheroma and microvessel dysfunction in dyslipidemia were also discovered. These novel findings provide new targets for possible clinical application in reducing coronary in-stent stenosis, which potentially will benefit many patients with severe coronary atherosclerosis.

6.6. Figure legend

Figure 6.1. Proposed model of A1R contribution to coronary atherosclerosis and in-stent stenosis

Stent placement in coronary arteries leads to platelets adherence to the stent and adenosine release from platelets as well as endothelial cells. Adenosine activates A1R and downstream mitogenic signaling pathways (ERK, JNK, PI3K-AKT) in coronary SMCs, thus promoting in-stent stenosis. In metabolic syndrome, elevated aldosterone binds to mineralocorticoid receptor (MR) or acts via some unknown mechanisms, potentially upregulates A1R in coronary SMCs, and contributes to the development of coronary atherosclerosis in vivo. ERK, JNK are both mitogen-activated protein kinase family members. ERK, the extracellular signal-regulated kinases; JNK, the c-Jun-N-terminal kinases.

6.7. Figure

Figure 6.1. Proposed model of A1R contribution to coronary atherosclerosis and in-stent stenosis

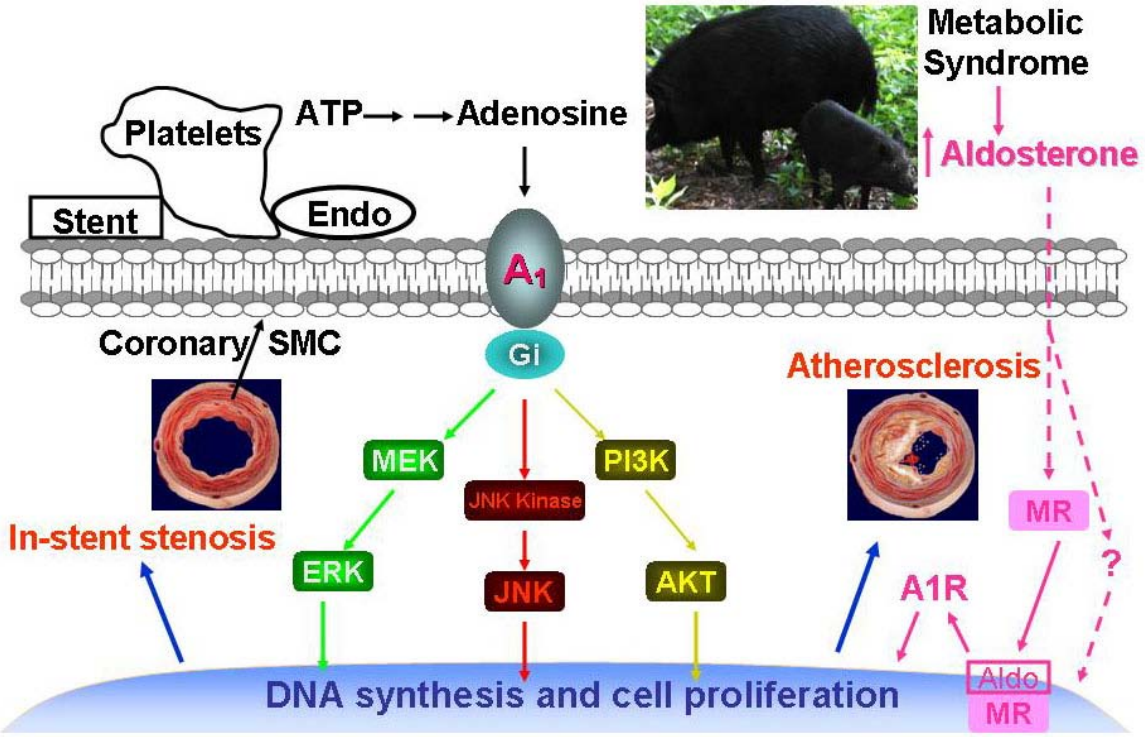

LIST OF APPENDICES

A. Monolayer Culture of Vascular Smooth Muscle Cells

Xin Long, Michael Sturek, PhD

A.1. Primary culture of vascular smooth muscle cells

A.1.1. Artery harvest

Get arteries immediately after sacrifice and rinse them in 70% ethanol for 2 seconds. This method was different than done previously in the laboratory for the past more than 20 years.

Rinse the arteries fiercely with phosphate-buffered saline (PBS, GIBCO, catalog number 10010-072) or sterile saline twice to get rid of the ethanol and put the arteries in DMEM culture media (GIBCO, catalog number 11885-092, 0% serum) to keep the cell viable. Always keep arteries on ice to reduce cell

degradation.

[Animal: # _____, Age ___, Time dead ____, Misc. _____]

[Portion of artery: Proximal _, Middle _, Distal

Artery: LAD_ RC _ CFX _ Peripheral___]

[Date __-__-__, Time ___]

A.1.2. Clean artery

In a Class II laminar airflow culture cabinet, dissect free the extravascular tissue (e.g. fiber, lipid) in PBS in a 100 mm Petri dish. Arteries need to be on ice as always.

At this point, the artery can be stored in the refrigerator in storage media for up to 5 days, if necessary.

[Storage media = _____ + _____+ _____% penicillin-streptomycin (P/S, GIBCO, catalog number 15140-122)]

[In refrigerator: Date __-__-__ Time ___, Misc._____]

A.1.3. Pin down the arteries for dispersion

Cut arteries open, lumen facing up, pin the arterial wall down in 30 mL jars with Sylgard in the bottom containing ~2 mL Low Ca. Expose the intima as much as possible to increase its contact area with digestion enzyme and thus increase digestion efficiency.

A.1.4.

Remove Low Ca and add 1.5-2.0 mL collagenase solution to each jar. Put jars in shaking water bath (55-65 strokes/min) at 37° C for 40-60 minutes. The jars should be placed correctly so that the direction of the shaking is parallel with blood flow direction in the vessel.

Be careful to set the lids of jars higher than the water surface level in water bath to prevent contamination of arteries. The jars can be wrapped in cellophane to ensure separation from water, if needed.

[Collagenase batch: Date __-__-__, Lot # _____]

[Dispersion: Date __-__-__, Time started _____, Time ended _____]

[Misc.: _____]

Misc. is for notes regarding uniqueness of dispersion, etc.

A.1.5.

In culture hood aspirate supernatant in jars and pipette over arterial lumen several times forcefully to remove endothelial cells stuck in lumen. Transfer supernatant to 1.7 mL Eppendorf tubes.

Centrifuge for 3 minutes at 900 RPM only if the artery is very small, thus few cells would be expected. Remove supernatant, leave 100-150 µL enzyme solution to resuspend the pellet (if centrifuged). For the arteries in jars, add 2 mL more collagenase solution and start shaking again as in step 4.

A.1.6.

Place drop of supernatant from step A.1.5 or resuspended pellet in 35 mm petri dish and observe under microscope. Dispersion may vary from day to day. At this point, mostly debris of connective tissue, endothelial cells, etc. are seen, but few SMC. The endothelial cells (EC) are round and clump together in bunches.

Note appropriately: A) If few SMCs, you can discard (unless EC fraction will be retained for fresh use or culture). B) If many SMCs, keep for cell culture. C) If no SMCs, discard it and that means you need more time to digest the intima and media. Label as $CORE_D$ 1.00 Month - Day - Year Species Vessel (e.g., 5-8-06 Porcine CFX included in blanks as date, species, and vessel, respectively. The subscript "D" refers to enzymatic dispersion and "CORE" denotes coronary EC. AORE could denote aortic EC. CORSMC could denote coronary smooth muscle cell.

$CORE_D$ 1.00 __-__-_____ _____ _____

Ignore this section if discarded _____

[EC _____; SMC _____]

A.1.7.

For conditions in step A.1.6: A), you can shake the jars for another 30-50 minutes before you collect the supernatants again as in step A.1.5. For condition B), you can shake the jars for another 30-40 minutes. For condition C), you can

shake the jars for another 20-40 minutes till you can see SMCs under microscope.

A.1.8.

Repeat step A.1.4 to A.1.7 until the arteries seem mostly digested.

[Dispersion: Time started _____, Time ended _____]

_____D __.00 __-__-_____ _____ _____

[EC _____; SMC _____]

A.1.9.

For the cell suspension need to culture, add 1 mL DMEM + 10-20% fetal bovine serum (FBS, GIBCO, catalog number 16000-044) + 1% P/S and pipette up and down to make cells evenly distributed.

[Growth media = _____ + _____ + _____ P/S]

A.1.10.

Obtain cell count by loading 10 µL of cell suspension onto the hemacytometer, counting the cells (using a hand counter) in the 25 squares, and multiplying the resulting count by 1×10^2. This will give the cell density (cells/mL). To determine total number of cells, multiply cell density by total volume of medium cells that are suspended in. If the cell density is great (determined by visualization), one can count 5 squares (usually the 4 corner and the middle squares) and multiply resulting cell count by 5×10^2.

Inoculate at 10,000 cells per cm^2 in culture dishes or flasks for rapid growth (e.g. primary cell culture), or at 6,000 cells per cm^2 for regular subculturing. Following inoculation, swirl the medium in the culture vessel to distribute the cells. CSMC attach to culture surfaces quickly. If the medium is not distributed immediately following inoculation, the cells may grow in uneven patterns.

Put culture dishes or flasks in 37° C, 5% CO_2 / 95% air, humidified cell culture incubator O/N. For best results, do not disturb the culture for at least 24 hours after the culture has been initiated.

A.2. Maintenance of cultured VSM cells

Cells may be maintained as a viable culture by feeding and splitting as necessary, depending on how rapidly you wish the cells to proliferate. Change the culture medium to freshly supplemented medium 24 to 36 hours after establishing the primary cultured cells. For subsequent subcultures, change the medium 48 hours after establishing the subculture. Change the medium every other day thereafter, until the culture is approximately 80% confluent. Once the culture reaches 80% confluence, change the medium every day. To achieve the highest cell densities, the culture medium should be changed every day as the cultures approach confluence.

To feed the cells, remove the old medium by aspiration. Gently pipet the appropriate volume of fresh culture medium into the dish or flask - 1mL for 96-well plate, 2 mL for 35 mm dish or 6-well tissue culture plate (Falcon, catalog number 353046), 5 mL for 60 mm dish, 10 mL for 100 mm dish, 15 mL for 150mm dish, 5 mL for 25 cm^2 flask, 15-20 mL for 75 cm^2 flask.

Label culture vessel and be sure to include the correct passage # and date. For coronary SMC, we can label as $CORSMC_D$ 1.00 Month - Day - Year - Species – Vessel. Here the decimal values indicated the passage number. In this case, since the cells are still primary, they are 1.00. After you subculture once (in steps below), the cells would be 1.01; a second subculture (thus second trypsinization) would be 1.02, etc. We retained the whole number value to denote the fraction from which we harvested the SMC. This might be important, since fraction 1.00 would be closer to the intima, thus perhaps different properties than fraction 2.00 or 3.00, which would be farther into the media and perhaps closer to the adventitia.

Incubate cultures in a 37° C, 5% CO_2 / 95% air, humidified cell culture incubator.

A.3. Subculture of VSM cells

For rapidly proliferating subcultures, cells should be subcultured before the culture becomes confluent.

Once the culture reaches 90% confluence, remove all of the culture medium from the flask by aspiration. Wash the flask with PBS and remove the solution by aspiration. Pipette certain volume of Trypsin/EDTA solution (GIBCO, catalog number 25200-056) to the culture vessel - 100 µL for 96-well plate, 400 µL for 35 mm dish or 6-well plate, 1 mL for 60 mm dish or 25 cm^2 flask, 2 mL for 100 mm dish, 3 mL for 150 mm dish or 75 cm^2 flask. Rock the culture vessel gently to ensure that the entire surface is covered. Put the culture vessel back into the cell incubator.

Take flask out of cell incubator in 2-3 minutes and view the culture under a microscope. If cells are detached, they mostly will become round. By gently tapping the bottom of the flask some cells can dislodge from the surface of the flask. When most of cells become detached from the culture vessel, add Trypsin Neutralizer solution (DMEM growth medium, 3 to 4 times volume of Trypsin/EDTA solution) to the culture vessel.

[Trypsin neutralizer media = _____ + _____ + _____ P/S]

Transfer the detached cells to a sterile 15 mL conical tube. Observe culture vessel under microscope, if there are more than 20% cells attaching at the culture vessel surface, repeat trysinization and neutralization steps. Add the solution to the 15 mL conical tube too. Centrifuge the cells at 180 × g for 7 min. Observe the cell pellet. Discard supernatant, being careful not to dislodge the cell

pellet. Resuspend the cell pellet in 2 mL DMEM growth medium. Pipette the cells up and down with 10 mL pipette to ensure a homogeneous cell suspension.

[Growth media = _____ + _____ + _____ P/S]

Determine the concentration of cells in the suspension (as described above). Dilute the cells in prewarmed, pregassed growth medium and seed new culture flask with 6,000 cells / cm^2. Instead of counting cell density, you can simply transfer the cell suspension (in equal volume) to new culture vessel containing appropriate volume of prewarmed, pregassed growth medium (3 dishes for 1:3 split, 5 dishes for 1:5 split, etc.). Incubate cultures in a 37° C, 5% CO_2 / 95% air, humidified cell culture incubator.

A.4. Cryopreservation of cultured VSM cells

If you wish to preserve the cells for long-term storage, later use, etc., it is recommended that the cells be frozen in liquid nitrogen (-196° C). Again, the cells are harvested off the culture vessel by trypsinization (see above), diluted with 5-10 mL medium, placed into a 15 mL tube, and centrifuged for 10 minutes at the minimum setting.

Discard the supernatant then add 1 mL freezing medium (DMEM + 20% FBS + 1% P/S + 10% DMSO). Transfer cell suspension into appropriately labeled Nunc tubes.

[Freezing media = _____ + _____ + _____% P/S + _____% DMSO]

Place Nunc tubes in freezing tray in liquid nitrogen refrigerator. After 2-4 hr, place tube(s) in a cane of liquid nitrogen tank. Take a record of the relative position of labelled Nunc tubes in liquid nitrogen tank.

A.5. Initiating cultures from cryopreserved cells

To bring cells up from liquid nitrogen, place cryovial in a 50 mL tube in 37° C water bath (to prevent too-rapid thawing and also ensure sterility). After contents of the vial thaw, wipe the outside of vial with 70% ethanol and move to a Class II laminar flow culture hood. Transfer vial contents in a 15 mL tube, add 5-10 mL growth medium.

[Growth media = _____ + _____ + _____ P/S]

Centrifuge 10 min at the minimum setting to remove DMSO. Discard supernatant, add 1 mL growth medium. Pipette the suspension up and down with 1 mL pipette to disperse the cells. Remove 10-20 µL from the vial, using a hemacytometer, determine the number of viable cells per mL. Dilute the contents of the vial so that cells can be seeded at 6,000 cells / cm^2 (XL noted on 3/26/09 that primary cultured CASM cells can be seeded at 10, 000 cells / well for 6-well plate) in culture dish or flask. Add 5 mL of cell suspension to each 25 cm^2 culture flask or 15 mL of cell suspension to each 75 cm^2 culture flask.

[Growth media = _____ + _____ + _____ P/S]

Incubate cultures in a 37° C, 5% CO_2 / 95% air, humidified cell culture incubator. From here, the cells can be maintained in culture (as described above) or used for experiments, etc. NOTE IMPORTANTLY: To keep the hood from possible contamination, please clean the suction tubing right after your usage with 10% bleach or 70% ethanol followed by distilled water and dispose of the remaining bleach or ethanol in the cylinder. The waste container inside the hood needs to be cleaned either when the liquid reaches 700 mL or when the hood is inactive for a couple of weeks.

A.6. Collagenase solution

Collagenase Recipe (in Low Ca)

Components	Final Concentration	20 mL total	10 mL total
BSA, Fraction V	0.2% (wt/vol)	40 mg	20 mg
Soybean Trypsin Inhibitor, Type I-S	0.1%	20 mg	10 mg
DNase I, Type IV		4 mg	2 mg
Collagenase, CLS II		20 mg	10 mg

[Collagenase batch: Date __-__-__, Lot # _____]

Note: Adjust pH of Low Ca to 7.55, and then add collagenase and pH will be exactly 7.40. Then filter with 0.2 µm syringe driven filter unit (Millipore, catalog number SLGV013SL). Make in 10-20 mL quantities. Each step of isolation above mentioned requires at least 4-6 mL collagenase. Remaining collagenase solution may be frozen at -20° C for at least 10 days.

B. Immunoblots

B.1. Preparation of cell lysates

Prepare mixture of 100 µL lysis buffer + 1 µL protease inhibitor cocktail (Sigma, catalog number P8340). If phosphorylated proteins are detected later, add 1 µL phosphatase inhibitor cocktail 1 (Sigma, catalog number P2850) + 1 µL phosphatase inhibitor cocktail 2 (Sigma, catalog number P5726) in addition to the 100 µL lysis buffer mix. Remove the culture media or other buffer and wash cells with PBS twice. Lyse the cells with 100 µL 1% SDS lysis buffer mix for each well of 6-well plate at room temperature for 1 minute. Scrape cell lysates off the plate. For cells in a 75 cm^2 flask, add 120 µL lysis buffer mixture, resulting in higher protein concentration.

Sonicate cell lysis to break genomic DNA, or use 25G / 1.5 needle 10 times up and down. Spin at 14,000 rpm (16,000 × g) in an Eppendorf microfuge for 10 minutes at 4° C. Transfer the supernatant to a new tube and discard the pellet. Determine the protein concentration by Bradford BCA assay (Pierce, catalog number 23225). Mix 1000 µL of Reagent A + 20 µL Reagent B (1:50 dilution) for each sample. 5 µL sample + 45 µL ddH_2O (1:10 dilution) or 50 µL BSA standards + 950 µL Reagent mix, incubate for 30 minutes at 60° C, then do protein concentration assay.

Take X µL (= Y µg protein) and mix with X µL of 2 × Laemmli sample buffer (Bio-rad, catalog number 161-0737) with 200 mM dithiothreitol (Sigma,

catalog number D9163). Make the protein loading amount equal for each well. The loading volume doesn't matter. Heat the mix for 3-5 minutes at 95° C. Cool at room temperature for 5 seconds. Flash spin to bring down condensation prior to loading gel. Use immediately to load gel or store at -20° C (reboil before loading gel).

B.2. Gel electrophoresis

Setup gel in electrophoresis apparatus, fill reservoirs with 1 × Running Buffer. Remove comb and rinse wells with 1 × Running Buffer.

Boil samples (15-35 µL for 15-well mini-gel, 20-75 µL for 10-well mini-gel) for 5 minutes, flash spinning the samples, then load samples and 5 µL standards (Precision plus protein dual color standard, Bio-Rad, catalog number 161-0374) to the gel. Run until bromophenol blue (BPB)-dye reaches bottom of gel (about 1.5-hr for mini-gel at 25 mA per gel, about 2-2.5 hrs for mini-gel at 100V).

B.3. Gel to Filter Blotting

Remove gel from plate-sandwich (note left to right orientation), cut away stacking gel, and rinse running gel briefly in 1 × Transfer Buffer. Cut two Whatmman filter papers and one nitrocellulose filter membrane (Bio-rad, catalog number 162-0112) to the size of the gel, make mark in the nitrocellulose membrane and then wet all filters with 1 × Transfer Buffer.

a) Lay 2-gel plastic manifold in Electro-blotter.
b) Lay 1 wetted filter paper for each gel onto platform of Blotter.
c) Place nitrocellulose membrane onto filters (need to mark or cut notch on desired corner of filter to maintain gel-lane orientations).
d) Place gel in known orientation onto the nitrocellulose filter membrane (Stacking gel heading up, the nitrocellulose membrane should be closer to + anode (white plastic manifold) than the gel is).
e) Lay 1 wetted filter paper on top of the gel. Remove bubbles by rolling pipets.
f) Install top of Electro-blotter (Membrane facing white stack and anode) and run at 80 mA overnight.

Remove nitrocellulose membrane, transfer the membrane to small dish and add 10 mL Ponceau S solution (Sigma, catalog number P7170) to confirm the transfer of proteins to the membrane. (Usually, you will be able to see protein ladders in all the samples and standards.) After you are done, put Ponceau S back to the container for reuse. Can begin western probing immediately or store filter, either

a) rinse in 1 × TBST for 3-time, place in seal-bag and store at 4° C, or
b) place in Blocking Solution in seal-bag and store at -20° C.

B.4. Probing the Filter

Rinse filter in 1 × TBST for 3 × 5-10 minutes, then place in seal-bag or small blotting box with 10-20 mL Blocking Solution for at least one hour at room temperature. For A1R, incubate for 3-5 hours at room temerature to reduce non-specific binding. Blocking Solution: 5% nonfat dry milk in 1 × TBST buffer (10 mM Tris, pH 7.4, 150 mM NaCl, and 0.1% Tween 20) or StartingBlock (TBS) blocking buffer (Pierce, catalog number 37542) with 0.1% Tween-20 (TBST blocking buffer). If for p-ERK detection, the TBST buffer is different from for A1R, so please refer to B.5. After blocking the membranes will be probed with a rabbit polyclonal antibody specific for the A1R (1:1000 dilutions, Abcam, catalog number AB3460-100) in Blocking Solution or TBST blocking buffer at 4° C overnight. Five-six mL is enough for each membrane. Put the membrane on a rocker from this step on. To reuse the primary antibody, add 10-12 mL of 10% sodium azide to the primary antibody. The antibody is good for 1 week if in 5% nonfat dry milk or 3 weeks if in TBST blocking buffer.

The next day, wash the membrane 3 × 5-10 minutes with 1 × TBST. Add 10-20 mL Blocking Solution and Secondary Antibody to the dilution of 1:5000 (a horseradish peroxidase-conjugated anti-rabbit IgG). Incubate at room temperature for 1 hour. Wash filters with two quick rinses, then 3 × 5-10 minutes with TBST. The longer wash it takes, the less background signal there is. To develop the membrane with electrogenerated chemiluminescent (ECL) Kit (Pierce, catalog number 34080) or supersignal ECL kit (Supersignal West Dura

Extended Duration Substrate, Pierce, catalog number 34075): mix equal part of ECL solutions A and B (~2 ml per filter for regular ECL kit; ~1 ml per filter for supersignal ECL kit)

a) Spread ECL Solution Mix onto protein side of filter and incubate for 3-5 minutes.
b) Drain filter and wrap in plastic wrap, and expose to ECL developing machine. Exposure times range from 30 seconds to 10 min.

If the next target protein on the same membrane has similar molecular weight to A1R, or will be detected with a rabbit primary antibody as well, the membrane may need to be stripped, reblocked and reprobed. Procedure of stripping blot:

a) Rinse blot off with 1 × TBST.
b) Put blot into small immunoblot box.
c) Add about 10 to 20 ml Stripping buffer (Pierce, catalog number 21059).
d) Immerse into 37° C shaking water bath and incubate for 20-50 minutes.
e) Rinse blot off with 1 × TBST 5-10 minutes for 3 times.
f) Continue and reblock and reprobe as described previously.

B.5. Immunoblot buffers (Based on recipes in lab of Drs. Gallagher and Herring)

1% SDS lysis buffer (in autoclaved ddH_2O)

Component	Stock Concentration	50 mL total
SDS (PH 6.8)	20%	2.5 mL
NaCl	5 M	1 mL
Tris (PH 7.4)	1M	2.5 mL
Water		44 mL

Note: 20% SDS solution (USB, catalog number BP2436-1).

1 × TBST buffer (in autoclaved ddH_2O, for A1R and p-ERK separately)

Component	Stock Concentration	A1R: 1 L total	p-ERK: 1 L total
NaCl	5 M	30 mL	100 mL
Tris (PH 7.4)	1 M	10 mL	20 mL
Tween 20		1 mL	1 mL
Water		959 mL	879 mL

2 × Separating gel buffer (in autoclaved ddH_2O, PH 8.8)

Component	Stock Concentration	500 mL total	Final Concentration
Tris (Base)		45.4 g	0.75 M
SDS	20%	5 mL	0.2%
Water		< 500 mL	

Note: Dissolve above components in ~ 400 mL ddH_2O. Adjust pH to 8.8 with concentrated (30%) HCl. Ajust final volume to 500 mL with ddH_2O. Sterile filter into a clean, sterile glass bottle. Store at room temperature indefinitely.

2 × Stacking gel buffer (in autoclaved ddH_2O, PH 6.8)

Component	Stock Concentration	500 mL total	Final Concentration
Tris (Base)		15.2 g	0.25 M
SDS	20%	5 mL	0.2%
Water		< 500 mL	

Note: Dissolve above components in ~ 400 mL ddH_2O. Adjust pH to 6.8 with concentrated (30%) HCl. Ajust final volume to 500 mL with ddH_2O. Sterile filter into a clean, sterile glass bottle. Store at room temperature indefinitely.

Polyacrylamide gel electrophoresis (10% separating gel for A1R, p-ERK)

Component	Stock Conc.	Separating gel		Stacking gel	
		1-gel	2-gel	1-gel	2-gel
Sterile water		1.25 mL	2.5 mL	1.75 mL	3.5 mL
Separating gel buffer	2 ×	3.75 mL	7.5 mL	N/A	N/A
Acrylamide/Bis solution	30%	2.5 mL	5.0 mL	0.75 mL	1.5 mL
Stacking gel buffer	2 ×	N/A	N/A	2.5 mL	5.0 mL
Ammonian persulfate	10%	38 µL	75 µL	30 µL	60 µL
TEMED		8 µL	15 µL	5 µL	10 µL

Note: Pipet and mix above components well. Use 6-6.5 mL separating gel and 4 mL stacking gel each. 30% Acrylamide/Bis solution (Bio-rad, catalog number 161-0158); Ammonian persulfate (Sigma, catalog number A3678); TEMED (Bio-rad, catalog number 161-0800).

1 × Transfer buffer (in autoclaved ddH_2O)

Component	Stock Concentration	1 L total
Transfer buffer	10 ×	100 mL
Methanol		200 mL
Water		700 mL

Note: 10 × Transfer buffer (Bio-rad, catalog number 161-0771); methanol (Fisher Scientific, catalog number 67-56-1).

1 × Running buffer (in autoclaved ddH_2O)

Component	Stock Concentration	1 L total
Running buffer	10 ×	100 mL
Water		900 mL

Note: 10 × Running buffer (Bio-rad, catalog number 161-0772).

C. Organ Culture

Xin Long, Zachary P. Neeb

C.1. Preparation of sterile arterial segments

C.1.1. Sterile dissection of coronary artery from intact heart

Rough / gross dissection of coronary arteries from heart occurs ensues immediately after mass of heart is obtained and within 60 seconds following removal of heart from chest cavity.

a) Rinse coronary artery area on heart with cold, sterile 2CaNa + 2% P/S.

b) Scissors are run from within 5 mm of coronary ostium into cardiac tissue on either side of each artery. Artery is cut away from heart with some cardiac tissue still attached. The aim of this step is expediency to place in sterile buffer solution.

c) Rinse dissected arteries again thoroughly with ~20-50 mL of 2CaNa + 2% P/S.

d) Quickly plunge arteries into 500 mL ice-cold 2CaNa + 2% P/S. Container should be kept on ice through entire dissection procedure.

e) Immediately take arteries to dissecting microscope in cell culture hood for further dissection.

C.1.2. Other sterile techniques

Each step should be completed with sterile techniques under Class II laminar flow culture hood. Utensils, dissecting dish, and gloves should be sterile. Solutions should be sterile filtered with 0.2 μm filter (Millipore, catalog number SCGPU02RE). Sterilization of tissue is accomplished by quick rinse with 70% ethanol followed by thorough rinse with PBS twice if the segments are for RNA extraction or immunoblots later.

C.1.3. Cleaning of coronary artery

Under magnification, all adventitia and adipose should be carefully removed from artery segment dedicated to organ culture. Do not perforate artery wall. Dissection of adventitia and adipose along the long axis of the artery avoids much perforation. Do not crimp or otherwise disturb the artery wall. Healthy looking artery equals healthy cells. Note that coronary artery should be on ice all the time to reduce possible RNA or protein degradation and keep cell viability. Any coronary artery that needs to be isolated or frozen for later molecular analysis should be attended to first.

C.2. Preparation of organ culture media

RPMI 1640 culture media need to be prepared from powder into sterile solution following the protocols described on the package of the RPMI powder which is located in the upper shelf of the refrigerator in the entry room to the cell culture room. Sterile filter (Pre-sterilized vacuum driven disposable filtration

system, Millipore, catalog number SCGPU02RE) the RPMI 1640 solution under Class II laminar flow culture hood, add 10 mL of P/S in 1 L RPMI 1640 culture media and mix them well.

C.3. Arterial segments in organ culture

Cut arterial segment into smaller segments of ~equal length. Put arterial segments into 6-well plate supplied with sterile RPMI + 1% P/S, 3-5 mL/well to keep arterial segments immersed. Incubate cultures in a 37° C, 5% CO_2 / 95% air, humidified cell culture incubator.

C.4. Maintenace of arterial segments in organ culture

RPMI culture media are replenished with every 2 days to keep the arterial segments supplied with nutrients until ready for different experiments. We have kept arterial segments in organ culture for up to 14 days. Histological analysis is underway at the time of writing this appendix.

D. Total RNA Isolation

Xin Long, Pamela G. Lloyd

This is modified from TRIzol® Reagent (Invitrogen, catalog number 15596-018) manual.

D.1. Homogenization

D.1.1. Tissues

Homogenize tissue samples using a cold tissue pulverizer and pestle before into 1 mL of TRIzol® Reagent per 50-100 mg of tissue, or homogenize tissue samples already in TRIzol® Reagent with power homogenizer. The sample volume should not exceed 10% of the volume of TRIzol® Reagent used for homogenization. Centrifuge at 12,000 × g for 10 minutes at 2-8° C. Transfer supernatant to a fresh heavy gel phase lock tube (Eppendorf, catalog number FP2302830). Discard tubes with pellets in biohazard box.

D.1.2. Cells grown in monolayers

Lyse cells directly in a culture dish by adding 1 mL of TRIzol® Reagent to a 35 mm diameter dish, and passing the cell lysate several times through a pipette. The amount of TRIzol® Reagent added is based on the area of the culture dish (1 mL per 10 cm^2) and not on the number of cells present. An insufficient amount of TRIzol® Reagent may result in contamination of the isolated RNA with DNA.

D.2. Phase separation

Incubate the homogenized samples for 5 minutes at 15 to 30° C to permit the complete dissociation of nucleoprotein complexes. Add 0.2 mL of chloroform per 1 mL of TRIzol® Reagent. Cap sample tubes securely. Shake tubes vigorously by hand for 15 seconds and incubate them at 15 to 30° C for 2 to 3 minutes. Centrifuge the samples at no more than 12,000 × g for 15 minutes at 2 to 8° C. Following centrifugation, the mixture separates into a lower red, phenol-chloroform phase, an interphase, and a colorless upper aqueous phase. RNA remains exclusively in the aqueous phase. The volume of the aqueous phase is about 60% of the volume of TRIzol® Reagent used for homogenization. We use heavy gel phase lock tube for centrifugation, so the red, phenol-chloroform phase and interphase will be locked by the gel from the aqueous RNA-containing phase.

D.3. RNA precipitation

After centrifugation, carefully transfer the aqueous phase to a fresh tube, and save the organic phase if isolation of DNA or protein is desired. Discard tubes containing phenol phase in biohazard box. Precipitate the RNA from the aqueous phase by mixing with isopropyl alcohol (isopropanol). Use 0.5 mL of isopropyl alcohol per 1 mL of TRIzol® Reagent used for the initial homogenization. Incubate samples at 15 to 30° C for 10 minutes and centrifuge at no more than 12,000 × g for 10 minutes at 2 to 8° C. The RNA precipitate, often invisible before centrifugation, forms a gel-like pellet on the side and bottom of the tube.

D.4. RNA wash

Remove the supernatant carefully with the suction system on benchtop designated for RNA extraction. Be careful not to dislodge the RNA pellet (white). Wash the RNA pellet once with 75% ethanol, adding at least 1 mL of 75% ethanol per 1 mL of TRIzol® Reagent used for the initial homogenization. Mix the sample by vortexing and centrifuge at no more than 7,500 × g for 5 minutes at 2 to 8° C.

D.5. RNA resuspension

After centrifugation carefully remove as much ethanol from the tube as possible with the suction system described previously. Air-dry the RNA pellet until it is almost dry (5-10 minutes, or until semi-transparent). Do not dry the RNA by centrifugation under vacuum. It is important not to let the RNA pellet dry completely as this will greatly decrease its solubility. Partially dissolved RNA samples have an A260/280 < 1.6. Dissolve RNA in certain volume of (depending on the original tissue amount and RNA extraction efficiency) RNase-free water or 0.5% SDS solution by passing the solution a few times through a pipette tip, and incubating in heating block for 10 minutes at 55 to 60° C. (Avoid SDS when RNA will be used in subsequent enzymatic reactions.) Put on ice and store at -80° C. RNA can also be redissolved in 100% deionized formamide and stored at -80° C.

D.6. RNA isolation notes

For small quantities of tissue (1 to 10 mg) or cell (10^2 to 10^4) samples, add 750 µL of TRIzol® to the tissue or cells. Following sample lysis, add chloroform and proceed with the phase separation as described in D.2. Prior to precipitating the RNA with isopropyl alcohol, add 5-10 µg RNase-free glycogen (Invitrogen, catalog number 10814) as carrier to the aqueous phase. To reduce viscosity, shear the genomic DNA with 2 passes through a 26 gauge needle prior to chloroform addition. The glycogen remains in the aqueous phase and is co-precipitated with the RNA. It does not inhibit first-strand synthesis at concentrations up to 4 mg/mL and does not inhibit PCR.

After homogenization and before addition of chloroform, samples can be stored at -60 to -70° C for at least one month. The RNA precipitate (D.4, RNA Wash) can be stored in 75% ethanol at 2 to 8° C for at least one week, or at least one year at -5 to -20° C.

Always wear gloves when working with RNA and change them frequently. Keep tissue frozen until it is placed in TRIzol®, or the RNA will degrade. TRIzol® contains phenol-toxic-causes burns-use in hood. Always use RNase-, DNase-free water in every step. Dispose tubes containing phenol in biohazard box.

E. DNase Treatment and Spectrophotometric Analysis of RNA

Xin Long, Pamela G. Lloyd

This protocol is for 50 µL of RNA samples and based on Turbo DNA-free kit (Ambion, catalog number 1907) manual.

E.1. Preparation

Fill a bucket with ice and turn on the heating block. Retrieve RNA samples to be treated from the -80° C freezer. Thaw the samples briefly and place on ice.

E.2. DNase treatment

Add 5 µL 10 × DNase I buffer and 1 µL of DNase I to the RNA sample. For multiple samples, prepare a stock mixture of buffer and enzyme, then add 6 µL to each tube. Mix gently and spin briefly in the nanofuge to bring all liquid to the bottom of the tube. Incubate the tubes at 37° C for 20-30 minutes.

E.3. DNase inactivation

Resuspend the DNase Inactivation Reagent (stored in -20° C refrigerator) by flicking or vortexing the tube. Add 5 µL to the samples. Watch carefully while pipetting to be sure that the aliquot added is mostly white rather than just clear fluid. Incubate for 2 minutes at room temperature. Flick 2-3 times during incubation to resuspend the inactivation reagent. Centrifuge at 10,000 × g for 90 seconds to pellet the Inactivation Reagent. Transfer the supernatant to a clean 0.5 mL tube and place tubes on ice.

E.4. RNA concentration analysis

Analyze RNA by NanoDrop spectrophotometer (ND-1000; locating in MS 354) to assess purity (A260/280) and concentration. Clean the spectrophotometer before usage as indicated on the screen. Choose nucleotides and RNA mode. After blanking with nuclease-free water, load 1.5-2.0 µL of RNA sample to the spectrophotometer and get A260/280 and concentration readings. A260/280 ration should be ~ 2.0. A ratio below 1.7 indicates degration or impurity of the RNA sample.

F. Complementary DNA (cDNA) Synthesis

Xin Long, Pamela G. Lloyd

This is an example of cDNA synthesis, and the volumes may need to change in different conditions. This is based on the iScript cDNA synthesis kit (Bio-rad, catalog number 170-8891) manual.

F.1. Prepare iScript reaction mix

Component	20 µL reaction	Total volume
5 x iScript reaction mix	4 µL	40 µL
iScript reverse transcriptase	1 µL	10 µL
Nuclease-free water	(15-X) µL	
RNA template (100 ng to 1 µg)	X µL	
Number of samples	10	
Tubes needed	10	
Extra for pipetting error	0	
Total tubes	10	

Note: At least 500 ng of RNA is needed for 20 µL reaction from those extracted from 5-10 mm long coronary segments. When using larger amounts of input RNA (>1 µg), the reaction should be scaled up, e.g. 40 µL reaction for 2 µg RNA, 100 µL reaction for 5 µg RNA.

F.2. Transfer mix to PCR tubes

Transfer 5 µL of reaction mix (5 x iScript reaction mix + iScript reverse transcriptase) to each flat-top PCR tube (Fisher Scientific, catalog number 14-230-225).

F.3. Add RNA samples and nuclease-free water

Add 15 µL RNA template and nuclease-free water to each PCR tube.

F.4. Place tubes in thermocycler and perform RT reaction

Use the DNA engine thermocycler in MS 366 for RT reactions. Reaction conditions: 5 minutes at 25° C, 30 minutes at 42° C, 5 minutes at 85° C, hold at 4° C. Program is saved on the thermocycler as iScript RT.

F.5. Store cDNA at -20° C

This cDNA (undiluted) will be used for PCR of target mRNAs (e.g., adenosine A1 receptor, A1R). The maximum amount of the cDNA reaction that is recommended for downstream PCR is one-tenth of the reaction volume, typically 2 µL.

G. Real-time RT-PCR of Adenosine Receptors

Xin Long, Pamela G. Lloyd

This is an example of real-time RT-PCR, and the volumes may need to adjust in different conditions.

G.1. Prepare PCR reaction mix for 18s rRNA (endogenous control)

Component	Stock Concentration	25 µL reaction	Total volume
TaqMan universal PCR master mix	2 ×	12.5 µL	750 µL
18s control reagents	20 ×	1.25 µL	75 µL
DNA sample (variable)		2 µL	
Nuclease-free water		9.25 µL	555 µL

G.2. Prepare PCR reaction mix for adenosine A1 receptor (A1R)

Component	Stock Concentration	25 µL reaction	Total volume
TaqMan universal PCR master mix	2 ×	12.5 µL	750 µL
A1R Forward primer	10 µM	2.25 µL	135 µL
A1R Reverse primer	10 µM	2.25 µL	135 µL
TaqMan A1R probe	6.25 µM	1 µL	60 µL
DNA sample (variable)		2 µL	
Nuclease-free water		5 µL	300 µL

G.3. Prepare PCR reaction mix for adenosine A2A and A2B receptors (A2A/BR)

Component	Stock Concentration	25 µL reaction	Total volume
SYBRGreen PCR master mix	2 ×	12.5 µL	750 µL
A2A/BR Forward primer	10 µM	0.75 µL	45 µL
A2A/BR Reverse primer	10 µM	0.75 µL	45 µL
DNA sample (variable)		2 µL	
Nuclease-free water		9 µL	540 µL

G.4. Prepare PCR reaction mix for adenosine A3 receptor (A3R)

Component	Stock Concentration	25 µL reaction	Total volume
SYBRGreen PCR master mix	2 ×	12.5 µL	750 µL
A2A/BR Forward primer	10 µM	0.75 µL	45 µL
A2A/BR Reverse primer	10 µM	0.75 µL	45 µL
DNA sample (variable)		2 µL	
Nuclease-free water		9 µL	540 µL
Number of samples			27
Wells needed			54
Extra for pipetting error			6
Total wells per target			60

Note: TaqMan universal PCR master mix (Applied Biosystems, catalog number 4304437); SYBRGreen PCR master mix (Applied Biosystems, catalog number 4309155); 18s control reagents (Applied Biosystems, catalog number

4319413E); primer powders from Integrated DNA Technology and dissolved in nuclease-free water at 10 × stock concentration (100 µM).

G.5. Pipet 23 µL of reaction mix into wells according to plate map

Note: 96-well semi-skirt PCR plate (Fisher Scientific, catalog number 14-230-44).

G.6. Add 2 µL of cDNA to wells according to plate map.

Cover the top of PCR plate with an optical adhesive cover (Applied Biosystems, catalog number 4311971), and centrifuge at 1000 × RPM for one minute.

G.7. Perform PCR on ABI 7500 instrument in Room MS 366

H. Genotyping

Xin Long, Kara Standley

H.1. DNA extraction: Hot Sodium Hydroxide and Tris (HotSHOT) method

Cut the sample into small pieces (2 × 2 mm earpunch), place in a 1.5 mL centrifuge tube, add 75 µL lysis buffer (25 mM NaOH, 0.2 mM disodium EDTA, and a PH of 12 is prepared by dissolving the salts in water without adjusting the PH). If the sample piece is relatively large, increase the amount of lysis buffer accordingly.

Heat at 95° C for 30 minutes. Cool to 4° C. Add 75 µL neutralizing buffer (40 mM Tris-HCl not Tris base and a PH of 5 achieved with adding Tris-HCl directly without adjusting the PH) or equal volume to lysis buffer if not 75 µL to each sample and mix. Store at 4° C. 1-5 µL of the final preparation are used per each 10 µL PCR volume.

Note: Tissue sample must be small (2 × 2 mm). Too large a sample can cause the methods to fail.

H.2. PCR reaction

This is an example of PCR reaction for AMPK γ 3, and the volumes may need to adjust in different conditions.

Component	Stock Concentration	20 µL reaction	Total volume
Betaine		6.5 µL	65 µL
AMPK γ 3 Forward primer	10 µM	1 µL	10 µL
AMPK γ 3 Reverse primer	10 µM	1 µL	10 µL
KTLA buffer	10 ×	2 µL	20 µL
Water		4.2 µL	42 µL
dNTP		0.05 µL	0.5 µL
Cresol red		0.1 µL	1 µL
KTLA Taq Polymerase		0.04 µL	0.4 µL
DNA sample (variable)		5 µL	65 µL

Number of samples	9
Number tubes/sample	1
Extra for pipetting error	1
Total number of reactions	10

Note: Betaine (Sigma, catalog number B-0300); cresol red (Sigma, catalog number 114480-56); KTLA Taq Polymerase, dNTP, KTLA buffer (DNA Polymerase Technology, Klentaq.com, catalog number Klentaq-LA).

Mix all the preparation materials except Klentaq and DNA. Then add Klentaq to the mixture and mix. Add 15 µL of final mixture solution into each PCR tube. Add 5 µL DNA preparation into each tube and mix well.

Use the DNA engine thermocycler in MS 366 for PCR reactions. Reaction program: Step 1 - 20 seconds at 95° C, step 2 - 30 seconds at 60° C, step 3 - 45 seconds at 72° C. (Step 2 and 3 repeat 30 cycles.) Step 4 - hold at 4° C. Program is saved on the thermocycler as Xin genotyping.

After the PCR reaction is finished, electrophorese each entire PCR sample through a 2% agarose gel at 120 V for approximately an hour.

H.3. Restriction enzyme digestion

Component	Stock Concentration	40 µL reaction	Total volume
NEBuffer	10 ×	4 µL	40 µL
BSA	100 ×	0.5 µL	5 µL
Water		15 µL	150 µL
PCR products		20 µL	
BsaHI enzymes		0.5 µL	
Number of samples	9		
Extra for pipetting error	1		
Total number of reactions	10		

Note: This is an example of enzyme digestion recipe. NEBuffer, BSA, BsaHI (New England BioLabs, catalog number R0556S). Mix buffer, BSA, and water. Add 19.5 µL of mixture into each 1.5 mL centrifuge tube. Add 0.5 µL BsaHI enzyme into each tube. Then add PCR products individually. Incubate at 37° C for 5 hours or O/N. Then 80° C for 20 minutes for heat inactivation of BsaHI if step H.4 does not occur right away.

H.4. Digestion product running on 2% agarose gel

Mix sample buffer: DNA at 1:3. Load 5 µL ladder and 40 µL DNA sample buffer mix into wells. Run at 80 mA for 40-50 minutes or 160 V for 10 minutes.

H.5. Agarose gel development for 2-10 seconds

Determine the size of enzyme digestion products.

I. Immunocytochemistry

I.1. Cell culture

Seed SMC on round coverslips in a 6-well plate and incubate cultures in a 37° C, 5% CO_2 / 95% air, humidified cell culture incubator. Change culture media (DMEM + 10% FBS + 1% P/S) every 2 days till SMC reach 70% confluence.

Switch culture media to DMEM + 1 / 0.5 / 0.1% FBS + 1% P/S, culture for 2 days to switch SMC to more differentiated phenotype.

I.2. Fixation and incubation

Wash each well with PBS 3 times. Fix cells with 1 mL methanol per well at -20° C for 5 minutes, wash in PBS 3 times.

Preincubate cells in 2 mL PBS + 1% BSA for 20 minutes at room temperature to block nonspecific binding. Gently remove the PBS with suction system. Incubate with pairs of primary antibodies overnight at 4° C and wash in PBS 3 times. Incubate with the appropriate combination of secondary antibodies, wash in PBS 3 times.

I.3. Coverslip preparation

Coverslips are mounted with mounting media. (Note, the surface with cells will face toward coverslips and try to avoid air bubbles.) For long term storage, add organic mounting media around the edge of the coverslips.

LIST OF REFERENCES

(1) Ross R. The pathogenesis of atherosclerosis: a perspective for the 1990s. Nature 1993;362:801-9.

(2) Christensen KL, Mulvany MJ. Location of resistance arteries. J Vasc Res 2001;38:1-12.

(3) Best PJM, McKenna CJ, Hasdai D, Holmes DR, Jr., Lerman A. Chronic endothelin receptor antagonism preserves coronary endothelial function in experimental hypercholesterolemia. Circulation 1999;99:1747-52.

(4) Taner CB, Severson SR, Best PJM, Lerman A, Miller VM. Treatment with endothelin-receptor antagonists increases NOS activity in hypercholesterolemia. J Appl Physiol 2001;90:816-20.

(5) Weisbrod RM, Griswold MC, Du Y, Bolotina VM, Cohen RA. Reduced responsiveness of hypercholesterolemic rabbit aortic smooth muscle cells to nitric oxide. Arterioscler Thromb Vasc Biol 1997;17:394-402.

(6) Madan P, Madan R. Endothelium-Independent Microvascular Dysfunction in Cardiac Syndrome X. Am J Med 2007;120:e23.

(7) Busse R, Fleming I. Endothelial dysfunction in atherosclerosis. J Vasc Res 1996;33:181-94.

(8) Costa F, Biaggioni I. Role of nitric oxide in adenosine-induced vasodilation in humans. Hypertension 1998;31:1061-4.

(9) Lusis AJ. Atherosclerosis. Nature 2000 September 14;407:233-41.

(10) Dixon JL, Shen S, Vuchetich JP, Wysocka E, Sun G, Sturek M. Increased atherosclerosis in diabetic dyslipidemic swine: protection by atorvastatin involves decreased VLDL triglycerides but minimal effects on the lipoprotein profile. J Lipid Res 2002;43:1618-29.

(11) Edwards JM, Neeb ZP, Alloosh MA, Long X, Bratz IN, Peller CR, Byrd JP, Kumar S, Obukhov AG, Sturek M. Exercise training decreases store-operated Ca^{2+} entry associated with metabolic syndrome and coronary atherosclerosis. Cardiovasc Res 2010;85:631-40.

(12) Stary HC. Changes in components and structure of atherosclerotic lesions developing from childhood to middle age in coronary arteries. Basic Res Cardiol 1994;89 Suppl 1:17-32.

(13) Wang H-W, Langohr IM, Sturek M, Cheng J-X. Imaging and quantitative analysis of atherosclerotic lesions by CARS-based multimodal nonlinear optical microscopy. Arterioscler Thromb Vasc Biol 2009;29:1342-8.

(14) Rader DJ, Daugherty A. Translating molecular discoveries into new therapies for atherosclerosis. Nature 2008;451:904-13.

(15) Stary HC. Evolution and progression of atherosclerotic lesions in coronary arteries of children and young adults. Arteriosclerosis 1989;9 Suppl:I19-I32.

(16) Pendyala L, Jabara R, Shinke T, etc. Drug-eluting stents: present and future. Cardiovasc Hematol Agents Med Chem 2008;6:105-15.

(17) Sturek M, Reddy HK. Editorial: New tools for prevention of restenosis could decrease the 'oculostento' reflex. Cardiovasc Res 2002;53:292-3.

(18) Conn E, Williams RS, Wallace AG. Exercise responses before and after physical conditioning in patients with severely depressed left ventricular function. Am J Cardiol 1982;49(2):296-300.

(19) Ehsani AA, Heath GW, Hagberg JM, Sobel BE, Holloszy JO. Effects of 12 months of intense exercise training on ischemic ST-segment depression in patients with coronary artery disease. Circulation 1981;64:1116-24.

(20) Maddahi J, Garcia EV, Berman DS, Waxman A, Swan H, Forrester J. Improved noninvasive assessment of coronary artery diesease by quantitative analysis of regional stress myocardial distribution and washout of thallium-201. Circulation 1981;64:924-35.

(21) Belardinelli R, Georgiou D, Ginzton L, Cianci G, Purcaro A. Effects of moderate exercise training on thallium uptake and contractile response to low-dose dobutamine of dysfunctional myocardium in patients with ischemic cardiomyopathy. Circulation 1998;97:553-61.

(22) Hambrecht R, Walther C, Möbius-Winkler S, Gielen S, Linke A, Conradi K, Erbs S, Kluge R, Kendziorra K, Sabri O, Sick P, Schuler G. Percutaneous coronary angioplasty compared with exercise training in patients with stable coronary artery disease. Circulation 2004;109:1371-8.

(23) Hambrecht R, Wolf A, Gielen S, Linke A, Hofer J, Erbs S, Schoene N, Schuler G. Effect of exercise on coronary endothelial function in patients with coronary artery disease. N Engl J Med 2000;342:454-60.

(24) Hosokawa S, Hiasa Y, Takahashi T, Itoh S. Effect of regular exercise on coronary endothelial function in patients with recent myocardial infarction. Circulation 2003;67:221-4.

(25) Pasquali S, Alexander K, Coombs L, Lytle B, Peterson E. Effect of cardiac rehabilitation on functional outcomes after coronary revascularization. Am Heart J 2003;145:445-51.

(26) Belardinelli R, Paolini I, Cianci G, Piva R, Georgiou D, Purcaro A. Exercise training intervention after coronary angioplasty: the ETICA trial. J Am Coll Cardiol 2001;37:1891-900.

(27) Fleenor BS, Bowles DK. Exercise training decreases the size and alters the composition of the neointima in a porcine model of percutaneous transluminal coronary angioplasty (PTCA). J Appl Physiol 2009;107:937-45.

(28) Wilson PW, D'Agostino RB, Parise H, Sullivan L, Meigs JB. Metabolic syndrome as a precursor of cardiovascular disease and type 2 diabetes mellitus. Circulation 2005;112:3066-72.

(29) Grundy SM, Cleeman JI, Daniels SR, etc. Diagnosis and management of the metabolic syndrome: an American Heart Association/National Heart, Lung, and Blood Institute scientific statement. Circulation 2005;112:2735-52.

(30) Arner P. Resistin: yet another adipokine tells us that men are not mice. Diabetologia 2005;48:2203-5.

(31) Ford ES, Giles WH, Mokdad AH. Increasing prevalence of the metabolic syndrome amoung U.S. adults. Diabetes Care 2004;27:2444-9.

(32) Grundy SM, Brewer HB Jr, Cleeman JI, Smith SC Jr, Lenfant C; American Heart Association; National Heart, Lung, and Blood Institute. Definition of metabolic syndrome. Circulation 2004;109:433-8.

(33) Lorenzo C, Williams K, Hunt KJ, Haffner SM. Trend in the Prevalence of the Metabolic Syndrome and Its Impact on Cardiovascular Disease Incidence: The San Antonio Heart Study. Diabetes Care 2006;29(3):625-30.

(34) Grundy SM, Becker D, Clark LT. Third Report of the National Cholesterol Education Program (NCEP) Expert Panel: Final Report. Circulation 2002;106:3143-421.

(35) Eckel RH, Grundy SM, Zimmet PZ. The metabolic syndrome. Lancet 2005;365:1415-28.

(36) Alexander CM, Landsman PB, Teutsch SM, Haffner SM. NCEP-defined metabolic syndrome, diabetes, and prevalence of coronary heart disease among NHANES III participants age 50 years and older. Diabetes 2003;52:1210-4.

(37) Bonora E, Kiechl S, Willeit J, Oberhollenzer F, Egger G, Bonadonna RC, Muggeo M; Bruneck study. Carotid atherosclerosis and coronary heart disease in the metabolic syndrome: prospective data from the Bruneck study. Diabetes Care 2003;26:1251-7.

(38) Tommasino A, Burzotta F, Trani C, Giammarinaro M, Schiavoni G. Impact of metabolic syndrome on angiographic and clinical outcome after stenting. Am J Cardiol 2008;101:1679.

(39) Pons D, Monraats PS, Zwinderman AH, de Maat MP, Doevendans PA, de Winter RJ, Tio RA, Waltenberger J, Jukema JW. Metabolic background determines the importance of NOS3 polymorphisms in restenosis after percutaneous coronary intervention: A study in patients with and without the metabolic syndrome. Disease Markers 2009;26:75-83.

(40) Takagi T, Yoshida K, Akasaka T, Kaji S, Kawamoto T, Honda Y, Yamamuro A, Hozumi T, Morioka S. Hyperinsulinemia during oral glucose tolerance test is associated with increased neointimal tissue proliferation after coronary stent implantation in nondiabetic patients: A serial intravascular ultrasound study. J Am Coll Cardiol 2000;36(3):731-8.

(41) Piatti P, Di Mario C, Monti LD, Fragasso G, Sgura F, Caumo A, Setola E, Lucotti P, Galluccio E, Ronchi C, Origgi A, Zavaroni I, Margonato A, Colombo A. Association of insulin resistance, hyperleptinemia, and impaired nitric oxide release with in-stent restenosis in patients undergoing coronary stenting. Circulation 2003;108:2074-81.

(42) Steiner G. Dyslipoproteinemias in diabetes. Clin Invest Med 1995;18:282-7.

(43) Byrne CD, Maison P, Halsall D, Martensz N, Hales CN, Wareham NJ. Cross-sectional but not longitudinal associations between non-esterified fatty acid levels and glucose intolerance and other features of the metabolic syndrome. Diabet Med 1999;16:1007-15.

(44) Cooper SA, Whaley-Connell A, Habibi J, Wei Y, Lastra G, Manrique C, Stas S, Sowers JR. Renin-angiotensin-aldosterone system and oxidative stress in cardiovascular insulin resistance. Am J Physiol Heart Circ Physiol 2007;293:H2009-H2023.

(45) Simpson SA, Tait JF, Bush IE. Secretion of a salt-retaining hormone by the mammalian adrenal cortex. The Lancet 1952;260:226-8.

(46) Tsai M, O'Malley BW. Molecular mechanisms of action of steroid/thyroid receptor superfamily members. Ann Rev Biochem 1994;63:451-86.

(47) Hirata A, Maeda N, Hiuge A, Hibuse T, Fujita K, Okada T, Kihara S, Funahashi T, Shimomura I. Blockade of mineralocorticoid receptor reverses adipocyte dysfunction and insulin resistance in obese mice. Cardiov Res 2009;84:164-72.

(48) Van Belle E, Bauters C, Wernert N, Hamon M, McFadden EP, Racadot A, Dupuis B, Lablanche JM, Bertrand ME. Neointimal thickening after balloon denudation is enhanced by aldosterone and inhibited by spironolactone, and aldosterone antagonist. Cardiov Res 1995;29:27-32.

(49) Wakabayashi K, Suzuki H, Sato T, Iso Y, Katagiri T, Takeyama Y. Eplerenone suppresses neointimal formation after coronary stent implantation in swine. Int J Cardiol 2006;107:260-6.

(50) Olsson RA, Pearson JD. Cardiovascular purinoceptors. Physiol Rev 1990;70:761-845.

(51) Fredholm BB, IJzerman AP, Jacobson KA, Klotz KN, Linden J. International Union of Pharmacology. XXV. Nomenclature and Classification of Adenosine Receptors. Pharmacol Rev 2001;53:527-52.

(52) Shen J, DiCorleto PE. Adenosine Prompts the Heart to Recruit Endothelial Progenitors. Circ Res 2008;102:280-2.

(53) Tabrizchi R, Bedi S. Pharmacology of adenosine receptors in the vasculature. Pharmacology & Therapeutics 2001;91:133-47.

(54) Burnstock G. Purinergic signaling and vascular cell proliferation and death. Arterioscler Thromb Vasc Biol 2002;22:364-73.

(55) Kim JW, Seo HS, Park JH, Na JO, Choi CU, Lim HE, Kim EJ, Rha SW, Park CG, Oh DJ. A prospective, randomized, 6-month comparison of the coronary vasomotor response associated with a Zotarolimus- versus a Sirolimus-eluting stent: differential recovery of coronary endothelial dysfunction. J Am Coll Cardiol 2009;53:1653-9.

(56) Monnink S, Tio R, Veeger N, Amoroso G, Van Boven AJ, Van Gilst WH. Exercise-induced ischemia after successful percutaneous coronary intervention is related to distal coronary endothelial dysfunction. Journal of Investigative Medicine 2003;51:221-6.

(57) Van Liebergen RAM, Piek JJ, Koch KT, De Winter RJ, Lie KI. Immediate and long-term effect of balloon angioplasty or stent implantation on the absolute and relative coronary blood flow velocity reserve. Circulation 1998;98:2133-40.

(58) Kern MJ, Puri S, Bach RG, etc. Abnormal coronary flow velocity reserve after coronary artery stenting in patients - role of relative coronary reserve to assess potential mechanisms. Circulation 1999;100:2491-8.

(59) Werner GS, Emig U, Bahrmann P, Ferrari M, Figulla HR. Recovery of impaired microvascular function in collateral dependent myocardium after recanalisation of a chronic total coronary occlusion. Heart 2004;90:1303-9.

(60) Camici PG, Crea F. Coronary Microvascular Dysfunction. N Engl J Med 2007;356:830-40.

(61) Pirat B, Bozbas H, Simsek V, Yildirir A, Sade LE, Gursoy Y, Altin C, Atar I, Muderrisoglu H. Impaired coronary flow reserve in patients with metabolic syndrome. Atherosclerosis 2008;201:112-6.

(62) Dzau VJ, Braun-Dullaeus RC, Sedding DG. Vascular proliferation and atherosclerosis: New perspectives and therapeutic strategies. Nature Med 2002;8:1249-56.

(63) Ross R, Glomset JA. Atherosclerosis and the arterial smooth muscle cell: proliferation of smooth muscle is a key event in the genesis of the lesions of atherosclerosis. Science 1973;180:1332-9.

(64) Owens GK, Kumar MS, Wamhoff BR. Molecular regulation of vascular smooth muscle cell differentiation in development and disease. Physiol Rev 2004;84:767-801.

(65) Shen J, Halenda SP, Sturek M, Wilden PA. Novel mitogenic effect of adenosine on coronary artery smooth muscle cells: role for the A_1 adenosine receptor. Circ Res 2005;96:982-90.

(66) Dubey RK, Gillespie DG, Mi Z, Jackson EK. Adenosine inhibits growth of human aortic smooth muscle cells via A2B receptors. Hypertension 1998;31:516-21.

(67) Dubey RK, Gillespie DG, Osaka K, Suzuki F, Jackson EK. Adenosine inhibits growth of rat aortic smooth muscle cells - Possible role of A_{2b} receptor. Hypertension 1996;27:786-93.

(68) Dubey RK, Gillespie DG, Shue H, Jackson EK. A_{2B} receptors mediate antimitogenesis in vascular smooth muscle cells. Hypertension 2000 January;35:267-72.

(69) Shen J, Halenda SP, Sturek M, Wilden PA. Cell signaling evidence for adenosine stimulation of coronary smooth muscle proliferation via the A_1 adenosine receptor. Circ Res 2005;97:574-82.

(70) Edwards JM, Alloosh MA, Long XL, Dick GM, Lloyd PG, Mokelke EA, Sturek M. Adenosine A_1 receptors in neointimal hyperplasia and in-stent stenosis in Ossabaw miniature swine. Cor Art Dis 2008;19:27-31.

(71) Hall JE. The kidney, hypertension, and obesity. Hypertension 2003;41:625-33.

(72) Xiao F, Puddefoot J, Vinson GP. Aldosterone mediates angiotensin II-stimulated rat vascular smooth muscle cell proliferation. J Endocrinol 2000;165:533-6.

(73) Ishizawa K, Izawa Y, Ito H, Miki C, Miyata K, Fujita Y, Kanematsu Y, Tsuchiya K, Tamaki T, Nishiyama A, Yoshizumi M. Aldosterone stimulates vascular smooth muscle cell proliferation via big mitogen-activated protein kinase 1 activation. Hypertension 2005;46:1046-52.

(74) Ren H, Stiles GL. Dexamethasone stimulates human A1 adenosine receptor (A1AR) gene expression through multiple regulatory sites in promoter B. Mol Pharm 1999;55:309-16.

(75) Gerwins P, Fredholm BB. Glucocorticoid receptor activation leads to up-regulation of adenosine A1 receptors and down-regulation of adenosine A2 responses in DDT1 MF-2 smooth muscle cells. Mol Pharm 1991;40:149-55.

(76) Svenningsson P, Fredholm BB. Glucocorticoids regulate the expression of adenosine A1 but not A2A receptors in rat brain. J Pharmacol Exp Ther 1997;280:1094-101.

(77) Lombès M, Binart N, Oblin ME, Joulin V, Baulieu EE. Characterization of the interaction of the human mineralocorticosteroid receptor with hormone response elements. Biochem J 1993;292:577-83.

(78) Marx SO, Marks AR. Bench to bedside: the development of rapamycin and its application to stent restenosis. Circulation 2001;104:852-5.

(79) Ako J, Bonneau HN, Honda Y, Fitzgerald PJ. Design criteria for the ideal drug-eluting stent. Am J Cardio 2007;100:S3-S9.

(80) Holmes DR Jr, Kereiakes DJ, Laskey WK, Colombo A, Ellis SG, Henry TD, Popma JJ, Serruys PW, Kimura T, Williams DO, Windecker S, Krucoff MW. Thrombosis and drug-eluting stents: an objective appraisal. J Am Coll Cardiol 2007;50:109-18.

(81) Virmani R, Kolodgie FD, Farb A. Drug-eluting stents: are they really safe? Am Heart Hosp J 2004;2:85-8.

(82) McFadden EP, Stabile E, Regar E, Cheneau E, Ong AT, Kinnaird T, Suddath WO, Weissman NJ, Torguson R, Kent KM, Pichard AD, Satler LF, Waksman R, Serruys PW. Late thrombosis in drug-eluting coronary stents after discontinuation of antiplatelet therapy. Lancet 2004;364:1519-21.

(83) Stone GW, Ellis SG, Colombo A, Dawkins KD, Grube E, Cutlip DE, Friedman M, Baim DS, Koglin J. Offsetting impact of thrombosis and restenosis on the occurrence of death and myocardial infarction after paclitaxel-eluting and bare metal stent implantation. Circulation 2007;115:2842-7.

(84) Daemen J, Wenaweser P, Tsuchida K, Abrecht L, Vaina S, Morger C, Kukreja N, Jüni P, Sianos G, Hellige G, van Domburg RT, Hess OM, Boersma E, Meier B, Windecker S, Serruys PW. Early and late coronary stent thrombosis of sirolimus-eluting and paclitaxel-eluting stents in routine clinical practice: data from a large two-institutional cohort study. Lancet 2007;369:667-78.

(85) Pfisterer M, Brunner-La Rocca HP, Buser PT, Rickenbacher P, Hunziker P, Mueller C, Jeger R, Bader F, Osswald S, Kaiser C; BASKET-LATE Investigators. Late clinical events after clopidogrel discontinuation may limit the benefit of drug-eluting stents: an observational study of drug-eluting versus bare-metal stents. J Am Coll Cardiol 2006;48:2584-91.

(86) Phillips RW, Panepinto LM, Spangler R, Westmoreland N. Yucatan miniature swine as a model for the study of human diabetes-mellitus. Diabetes 1982;31:30-6.

(87) Christoffersen BO, Grand N, Golozoubova V, Svendsen O, Raun K. Gender-associated differences in metabolic syndrome-related parameters in Gottingen minipigs. Comp Med 2007;57:493-504.

(88) Masuzaki H, Paterson J, Shinyama H, Morton NM, Mullins JJ, Seckl JR, Flier JS. A transgenic model of visceral obesity and the metabolic syndrome. Science 2001;294:2166-70.

(89) Peterson RG. The Zucker diabetic fatty (ZDF) rat. In: Sima AAF, Shafrir E, editors. Animal models of diabetes: A Primer.Amsterdam: Harwood Academic Publishers; 2001;109-28.

(90) Bellinger DA, Merricks EP, Nichols TC. Swine models of type 2 diabetes mellitus: insulin resistance, glucose tolerance, and cardiovascular complications. ILAR J 2006;47:243-58.

(91) Hsueh W, Abel ED, Breslow JL, Maeda N, Davis RC, Fisher EA, Dansky H, McClain DA, McIndoe R, Wassef MK, Rabadán-Diehl C, Goldberg IJ. Recipes for creating animal models of diabetic cardiovascular disease. Circ Res 2007;100:1415-27.

(92) Sturek M, Alloosh M, Wenzel J, etc. Ossabaw Island miniature swine: cardiometabolic syndrome assessment. In: Swindle MM, editor. Swine in the Laboratory: Surgery, Anesthesia, Imaging, and Experimental Techniques. 2nd Edition. Boca Raton: CRC Press; 2007;397-402.

(93) Crick SJ, Sheppard MN, Ho SY, Gebstein L, Anderson RH. Anatomy of the pig heart: comparisons with normal human cardiac structure. J Anat 1998;193:105-19.

(94) Skold BH, Getty R, Ramsey FK. Spontaneous athersclerosis in the arterial system of aging swine. Am J Vet Res 1966;27:257-273.

(95) Dyson M, Alloosh M, Vuchetich JP, Mokelke EA, Sturek M. Components of metabolic syndrome and coronary artery disease in female Ossabaw swine fed excess atherogenic diet. Comp Med 2006;56:35-45.

(96) Lee L, Alloosh M, Saxena R, Van Alstine W, Watkins BA, Klaunig JE, Sturek M, Chalasani N. Nutritional model of steatohepatitis and metabolic syndrome in the Ossabaw miniature swine. Hepatology 2009;50:56-67.

(97) Bratz IN, Dick GM, Tune JD, Edwards JM, Neeb ZP, Dincer UD, Sturek M. Impaired capsaicin-induced relaxation of coronary arteries in a porcine model of the metabolic syndrome. Am J Physiol: Heart Circ Physiol 2008;294:H2489-H2496.

(98) Hlatky MA, Boothroyd DB, Bravata DM, Boersma E, Booth J, Brooks MM, Carrié D, Clayton TC, Danchin N, Flather M, Hamm CW, Hueb WA, Kähler J, Kelsey SF, King SB, Kosinski AS, Lopes N, McDonald KM, Rodriguez A, Serruys P, Sigwart U, Stables RH, Owens DK, Pocock SJ. Coronary artery bypass surgery compared with percutaneous coronary interventions for multivessel disease: a collaborative analysis of individual patient data from ten randomised trials. The Lancet 2009;373:1190-7.

(99) Feuerstein GZ. Restenosis: basic research and clinical perspective. In: Feuerstein GZ, editor. Restenosis: From Genetics to Therapeutics.NY: Marcel Dekker Inc.; 1997;1-4.

(100) Gregorini L, Marco J, Farah B, Bernies M, Palombo C, Kozàkovà M, Bossi IM, Cassagneau B, Fajadet J, Di Mario C, Albiero R, Cugno M, Grossi A, Heusch G. Effects of selective a_1- and a_2-adrenergic blockade on coronary flow reserve after coronary stenting. Circulation 2002;106:2901-7.

(101) Prati F, Pawlowski T, Gil R, Labellarte A, Gziut A, Caradonna E, Manzoli A, Pappalardo A, Burzotta F, Boccanelli A. Stenting of culprit lesions in unstable angina leads to a marked reduction in plaque burden: A major role of plaque embolization?: a serial intravascular ultrasound study. Circulation 2003;107:2320-5.

(102) Marty B, Leu AJ, Mucciolo A, von Segesser LK. Biologic fixation of polyester- versus polyurethane-covered stents in a porcine model. J Vasc Interv Radiol 2002;13:601-7.

(103) Meier P, Zbinden R, Togni M, Wenaweser P, Windecker S, Meier B, Seiler C. Coronary collateral function long after drug-eluting stent implantation. J Am Coll Cardiol 2007;49:15-20.

(104) Kern MJ. Attenuated coronary collateral function after drug-eluting stent implantation: a new downside of drug-eluting stents? J Am Coll Cardiol 2007;49:21-2.

(105) National Research Council. Guide for the care and use of laboratory animals. Washington, D.C.: National Academy Press; 1996.

(106) Beaver BV, Reed W, Leary S, etc. 2000 Report of the AVMA panel on euthanasia. JAMA 2001;218:669-96.

(107) Mokelke EA, Dietz NJ, Eckman DM, Nelson MT, Sturek M. Diabetic dyslipidemia and exercise affect coronary tone and differential regulation of conduit and microvessel K+ current. Am J Physiol Heart Circ Physiol 2005;288:H1233-H1241.

(108) Committee to Develop a Resource Book for Animal Exercise Protocols, Sturek M. Resource Book for the Design of Animal Exercise Protocols. Bethesda, MD: American Physiological Society; 2006.

(109) Lloyd PG, Sheehy AF, Edwards JM, Mokelke EA, Sturek M. Leukemia inhibitory factor is upregulated in coronary arteries of Ossabaw miniature swine after stent placement. Cor Art Dis 2008;19:217-26.

(110) Demacker PN, Hessels M, Toenhake-Dijkstra H, Baadenhuijsen H. Precipitation methods for HDL-C measurement compared, and final evaluation under routine operating conditions of a method with a low sample-to-reagent ratio. Clin Chem 1997;43:663-8.

(111) Dyson M, Mokelke EA, Vuchetich J, Sturek M. Use of computed tomography to evaluate intra-abdominal fat stores in a swine model of the metabolic syndrome (abstract). FASEB J 2005;19:A191.

(112) Reddy KG, Nair RN, Sheehan HM, Hodgson JM. Evidence that selective endothelial dysfunction may occur in the absence of angiographic or ultrasound atherosclerosis in patients with risk factors for atherosclerosis. J Am Coll Cardiol 1994;23:833-43.

(113) Gilligan DM, Guetta V, Panza JA, García CE, Quyyumi AA, Cannon RO 3rd. Selective loss of microvascular endothelial function in human hypercholesterolemia. Circulation 1994;90:35-41.

(114) Pitkänen OP, Nuutila P, Raitakari OT, Porkka K, Iida H, Nuotio I, Rönnemaa T, Viikari J, Taskinen MR, Ehnholm C, Knuuti J. Coronary flow reserve in young men with familial combined hyperlipidemia. Circulation 1999;99:1678-84.

(115) Pitkänen OP, Raitakari OT, Niinikoski H, Nuutila P, Iida H, Voipio-Pulkki LM, Härkönen R, Wegelius U, Rönnemaa T, Viikari J, Knuuti J. Coronary flow reserve is impaired in young men with familial hypercholesterolemia. J Am Coll Cardiol 1996;28:1705-11.

(116) Hinschen AK, Rose'meyer RB, Headrick JP. Age-related changes in adenosine-mediated relaxation of coronary and aortic smooth muscle. Am J Physiol Heart Circ Physiol 2001;280:H2380-H2389.

(117) Thompson PD. The benefits and risks of exercise training in patients with chronic coronary artery disease. JAMA 1988;259:1537-40.

(118) Hambrecht R, Fiehn E, Weigl C, Gielen S, Hamann C, Kaiser R, Yu J, Adams V, Niebauer J, Schuler G. Regular physical exercise corrects endothelial dysfunction and improves exercise capacity in patients with chronic heart failure. Circulation 1998;98:2709-15.

(119) Linxue L, Nohara R, Makita S, Hosokawa R, Hata T, Okuda K, Hamazaki H, Fujita M, Sasayama S. Effects of long-term exercise training on regional myocardial perfusion changes in patients with coronary artery disease. Jap Circ J 1999;63:73-8.

(120) Kubo H, Yano K, Hirai H, Yabuki S, Machii K. Preventive effect of exercise training on recurrent stenosis after percutaneous transluminal angioplasty (PTCA). Jap Circ J 1992;56:413-21.

(121) Hofman-Bang C, Lisspers J, Nordlander R, Nygren A, Sundin O, Ohman A, Rydén L. Two-year results of a controlled study of residential rehabilitation for patients treated with percutaneous transluminal coronary angioplasty. A randomized study of a multifactorial programme. Eur Heart J 1999;20:1465-74.

(122) Mobius-Winkler S, Hambrecht R. A randomized comparison of coronary stent placement and exercise training in the treatment of stable coronary artery disease. Circulation 2002 (Abstract).

(123) O'Connor GT, Buring JE, Yusuf S, Goldhaber SZ, Olmstead EM, Paffenbarger RS Jr, Hennekens CH. An overview of randomized trials of rehabilitation with exercise after myocardial infarction. Circulation 1989;80:234-44.

(124) Schuler G, Hambrecht R, Schlierf G, Grunze M, Methfessel S, Hauer K, Kübler W. Myocardial perfusion and regression of coronary artery disease in patients on a regimen of intensive physical exercise and low fat diet. J Am Coll Cardiol 1992;19:34-42.

(125) Schuler G, Hambrecht R, Schlierf G, Niebauer J, Hauer K, Neumann J, Hoberg E, Drinkmann A, Bacher F, Grunze M. Regular physical exercise and low-fat diet: Effects on progression of coronary artery disease. Circulation 1992;86:1-11.

(126) Popma JJ, Califf RM, Topol EJ. Clinical trials of restenosis after coronary angioplasty. Circulation 1991;84:1426-36.

(127) Lincoff AM, Califf RM, Topol EJ. Platelet glycoprotein IIb/IIIa receptor blockade in coronary artery disease. J Am Coll Cardiol 2000;35:1103-15.

(128) Schwartz RG, Pearson TA, Kalaria VG, Mackin ML, Williford DJ, Awasthi A, Shah A, Rains A, Guido JJ. Prospective serial evaluation of myocardial perfusion and lipids during first six months of prvastatin therapy: coronary artery disease regression single photon emission computed tomography monitoring trial. J Am Coll Cardiol 2003;42:600-10.

(129) Huggins GS, Pasternak RC, Alpert NM, Fischman AJ, Gewirtz H. Effects of short-term treatment of hyperlipidemia on coronary vasodilator function and myocardial perfusion in regions having substantial impairment of baseline dilator reverse. Circulation 1998;98:1291-6.

(130) Leung W, Lau CP, Wong C-K. Beneficial effect of cholesterol-lowering therapy on coronary endothelium-dependent relaxation in hypercholesterolemic patients. Lancet 1993;341:1496-500.

(131) Egashira K, Hirooka Y, Kai H, Sugimachi M, Suzuki S, Inou T, Takeshita A. Reduction in serum cholesterol with pravastatin improves endothelium dependent coronary vasomotion in patients with hypercolesterolemia. Circulation 1994;89:2519-4.

(132) Treasure CB, Klein JL, Weintraub WS, Talley JD, Stillabower ME, Kosinski AS, Zhang J, Boccuzzi SJ, Cedarholm JC, Alexander RW. Beneficial effects of cholesterol-lowering therapy on the coronary endothelium in patients with coronary artery disease. N Engl J Med 1995;332:481-7.

(133) Levine GN, Keaney Jr. JF, Vita JA. Cholesterol reduction in cardiovascular disease: clinical benefits and possible mechanisms. N Engl J Med 1995;332:512-21.

(134) Lee DL, Wamhoff BR, Katwa LC, Reddy HK, Voelker DJ, Dixon JL, Sturek M. Increased endothelin-induced Ca^{2+} signaling, tyrosine phosphorylation, and coronary artery disease in diabetic dyslipidemic swine are prevented by atorvastatin. J Pharmacol Exp Ther 2003;306:132-40.

(135) Heaps CL, Sturek M, Price EM, Laughlin MH, Parker JL. Sarcoplasmic reticulum Ca^{2+}-ATPase uptake is impaired in coronary smooth muscle distal to chronic occlusion. Am J Physiol: Heart Circ Physiol 2001;281:H223-H231.

(136) Tune JD, Gorman MW, Feigl EO. Matching coronary blood flow to myocardial oxygen consumption. J Appl Physiol 2004;97:404-15.

(137) Liem DA, Verdouw PD, Ploeg H, Kazim S, Duncker DJ. Sites of action of adenosine in interorgan preconditioning of the heart. Am J Physiol Heart Circ Physiol 2002;283:H29-H37.

(138) Duncker DJ, Bache RJ. Regulation of coronary blood flow during exercise. Physiol Rev 2008;88:1009-86.

(139) Kern MJ, Lerman A, Bech JW, De Bruyne B, Eeckhout E, Fearon WF, Higano ST, Lim MJ, Meuwissen M, Piek JJ, Pijls NH, Siebes M, Spaan JA; American Heart Association Committee on Diagnostic and Interventional Cardiac Catheterization, Council on Clinical Cardiology. Physiological assessment of coronary artery disease in the cardiac catheterization laboratory: a scientific statement from the American Heart Association Committee on diagnostic and interventional cardiac catheterization, council on clinical cardiology. Circulation 2006;114:1321-41.

(140) Standen NB, Quayle JM. K^+ channel modulation in arterial smooth muscle. Acta Physiol Scand 1998;164:549-57.

(141) Hein TW, Belardinelli L, Kuo L. Adenosine A2A receptors mediate coronary microvascular dilation to adenosine: role of nitric qxide and ATP-sensitive potassium channels. J Pharmacol Exp Ther 1999;291:655-64.

(142) Bender SB, Tune JD, Borbouse L, Long X, Sturek M, Laughlin MH. Altered mechanism of adenosine-induced coronary arteriolar dilation in early-stage metabolic syndrome. Experimental Biology and Medicine 2009;234:683-92.

(143) Dick GM, Bratz IN, Borbouse L, Payne GA, Dincer UD, Knudson JD, Rogers PA, Tune JD. Voltage-dependent K^+ channels regulate the duration of reactive hyperemia in the canine coronary circulation. Am J Physiol Heart Circ Physiol 2008;294:H2371-H2381.

(144) Tawfik HE, Teng B, Morrison RR, Schnermann J, Mustafa SJ. Role of A1 adenosine receptor in the regulation of coronary flow. Am J Physiol Heart Circ Physiol 2006;291:H467-H472.

(145) Zhu XY, Daghini E, Chade AR, Versari D, Krier JD, Textor KB, Lerman A, Lerman LO. Myocardial microvascular function during acute coronary artery stenosis: effect of hypertension and hypercholesterolaemia. Cardiov Res 2009;83:371-80.

(146) Sato A, Terata K, Miura H, Toyama K, Loberiza FR Jr, Hatoum OA, Saito T, Sakuma I, Gutterman DD. Mechanism of vasodilation to adenosine in coronary arterioles from patients with heart disease. Am J Physiol Heart Circ Physiol 2005;288:H1633-H1640.

(147) Hein TW, Wang W, Zoghi B, Muthuchamy M, Kuo L. Functional and molecular characterization of receptor subtypes mediating coronary microvascular dilation to adenosine. J Mol Cell Cardiol 2001;33:271-82.

(148) Hein TW, Kuo L. cAMP-independent dilation of coronary arterioles to adenosine - role of nitric oxide, G proteins, and K_{ATP} channels. Circ Res 1999;85:634-42.

(149) Talukder MAH, Morrison RR, Ledent C, Mustafa SJ. Endogenous adenosine increases coronary flow by activation of both A2A and A2B receptors in mice. J Cardiovasc Pharmacol 2003;41:562-70.

(150) Kemp BK, Cocks TM. Adenosine mediates relaxation of human small resistance-like coronary arteries via A2B receptors. Br J Pharmacol 1999;126:1796-800.

(151) Hinschen AK, Rose'meyer RB, Headrick JP. Adenosine receptor subtypes mediating coronary vasodilation in rat hearts. J Cardiovasc Pharmacol 2003;41:73-80.

(152) Morrison RR, Talukder MAH, Ledent C, Mustafa SJ. Cardiac effects of adenosine in A2A receptor knockout hearts: uncovering A2B receptors. Am J Physiol Heart Circ Physiol 2002;282:H437-H444.

(153) Talukder MAH, Morrison RR, Jacobson MA, Jacobson KA, Ledent C, Mustafa SJ. Targeted deletion of adenosine A3 receptors augments adenosine-induced coronary flow in isolated mouse hearts. Am J Physiol Heart Circ Physiol 2002;282:H2183-H2189.

(154) Wang J, Whitt SP, Rubin LJ, Huxley VH. Differential coronary microvascular exchange responses to adenosine: roles of receptor and microvessel subtypes. Microcirculation 2005;12:313-26.

(155) Stiles GL. Adenosine receptors. J Biol Chem 1992;267:6451-4.

(156) Pelleg A, Hurt CM. Effects of N6-endonorbornan-2-yl-9-methyladenine, N0861, on negative chronotropic and vasodilatory actions of adenosine in the canine heart in vivo. Can J Physiol Pharmacol 1992;70:1450-56.

(157) Borbouse L, Dick GM, Asano S, Bender SB, Dincer UD, Payne GA, Neeb ZP, Bratz IN, Sturek M, Tune JD. Impaired function of coronary BK_{Ca} channels in metabolic syndrome. Am J Physiol Heart Circ Physiol 2009;297:H1629-H1637.

(158) Tune JD, Richmond KN, Gorman MW, Olsson RA, Feigl EO. Adenosine is not responsible for local metabolic control of coronary blood flow in dogs during exercise. Am J Physiol Heart Circ Physiol 2000;278:H74-H84.

(159) Tune JD, Richmond KN, Gorman MW, Feigl EO. K_{ATP}^{+} channels, nitric oxide, and adenosine are not required for local metabolic coronary vasodilation. Am J Physiol Heart Circ Physiol 2001;280:H868-H875.

(160) Tune JD, Richmond KN, Gorman MW, Feigl EO. Control of coronary blood flow during exercise. Exp Biol Med 2002;227:238-50.

(161) Laxson DD, Homans DC, Bache RJ. Inhibition of adenosine-mediated coronary vasodilation exacerbates myocardial ischemia during exercise. Am J Physiol 1993;265:H1471-H1477.

(162) Morrison RR, Tan XL, Ledent C, Mustafa SJ, Hofmann PA. Targeted deletion of A2A adenosine receptors attenuates the protective effects of myocardial postconditioning. Am J Physiol Heart Circ Physiol 2007;293:H2523-H2529.

(163) Schmieder RE, Hilgers KF, Schlaich MP, Schmidt BM. Renin-angiotensin system and cardiovascular risk. Lancet 2007;369:1208-19.

(164) Rogerson FM, Fuller PJ. Mineralocorticoid action. Steroids 2000;65:61-73.

(165) Rocha R, Martin-Berger CL, Yang P, Scherrer R, Delyani J, McMahon E. Selective aldosterone blockade prevents angiotensin II/salt-induced vascular inflammation in the rat heart. Endocrinology 2002;143:4828-36.

(166) Rocha R, Rudolph AE, Frierdich GE, Nachowiak DA, Kekec BK, Blomme EA, McMahon EG, Delyani JA. Aldosterone induces a vascular inflammatory phenotype in the rat heart. Am J Physiol Heart Circ Physiol 2002;283:H1802-H1810.

(167) Pitt B, Zannad F, Remme WJ, Cody R, Castaigne A, Perez A, Palensky J, Wittes J. The effect of spironolactone on morbidity and mortality in patients with severe heart failure. N Engl J Med 1999;341:709-17.

(168) Pitt B, Remme W, Zannad F, Neaton J, Martinez F, Roniker B, Bittman R, Hurley S, Kleiman J, Gatlin M; Eplerenone Post-Acute Myocardial Infarction Heart Failure Efficacy and Survival Study Investigators. Eplerenone, a selective aldosterone blocker, in patients with left ventricular dysfunction after myocardial infarction. N Engl J Med 2003;348:1309-21.

(169) ONTARGET Investigators, Yusuf S, Teo KK, Pogue J, Dyal L, Copland I, Schumacher H, Dagenais G, Sleight P, Anderson C. Telmisartan, ramipril, or both in patients at high risk for vascular events. N Engl J Med 2008;358:1547-59.

(170) McMurray JJV. ACE inhibitors in cardiovascular disease -- unbeatable? N Engl J Med 2008;358:1615-6.

(171) Hill BJF, Katwa LC, Wamhoff BR, Sturek M. Enhanced endothelin$_A$ receptor-mediated calcium mobilization and contraction in organ cultured porcine coronary arteries. J Pharmacol Exp Ther 2000;295:484-91.

(172) Hill BJF, Wamhoff BR, Sturek M. Functional nucleotide receptor expression and sarcoplasmic reticulum morphology in dedifferentiated porcine coronary smooth muscle cells. J Vasc Res 2001;38:432-43.

(173) Wamhoff BR, Bowles DK, Dietz NJ, Hu Q, Sturek M. Exercise training attenuates coronary smooth muscle phenotypic modulation and nuclear Ca^{2+} signaling. Am J Physiol Heart Circ Physiol 2002;283:H2397-H2410.

(174) Kumar B, Dreja K, Shah SS, Cheong A, Xu SZ, Sukumar P, Naylor J, Forte A, Cipollaro M, McHugh D, Kingston PA, Heagerty AM, Munsch CM, Bergdahl A, Hultgårdh-Nilsson A, Gomez MF, Porter KE, Hellstrand P, Beech DJ. Upregulated TRPC1 channel in vascular injury in vivo and its role in human neointimal hyperplasia. Circ Res 2006;98:557-63.

(175) George SJ, Johnson JL, Angelini GD, Jeremy JY. Short-term exposure to thapsigargin inhibits neointima formation in human saphenous vein. Arterioscler Thromb Vasc Biol 1997;17:2500-6.

(176) Otis CR, Wamhoff BR, Sturek M. Hyperglycemia-induced insulin resistance in diabetic dyslipidemic Yucatan swine. Comp Med 2003;53:53-64.

(177) Shen J, Seye CI, Wang M, Weisman GA, Wilden PA, Sturek M. Cloning, upregulation, and mitogenic role of porcine $P2Y_2$ receptor in coronary artery smooth muscle cells. Mol Pharm 2004;66:1265-74.

(178) Pratt JH, Rothrock JK, Dominguez JH. Inhibition of aldosterone production by pinacidil in vitro. Hypertension 1991;18:529-34.

(179) Liu IM, Tzeng TF, Tsai CC, Lai TY, Chang CT, Cheng JT. Increase in adenosine A1 receptor gene expression in the liver of streptozotocin-induced diabetic rat. Diabetes Metab Res Rev 2003;19:209-15.

(180) Fahim M, Mustafa SJ. Evidence for the presence of A1 adenosine receptors in the aorta of spontaneously hypertensive rats. Br J Pharmacol 2001;134:1760-6.

(181) Nie Z, Mei Y, Ford M, Rybak L, Marcuzzi A, Ren H, Stiles GL, Ramkumar V. Oxidative stress increases A1 adenosine receptor expression by activating nuclear factor κB. Mol Pharm 1998;53:663-9.

(182) Nissen SE, Nicholls SJ, Sipahi I, Libby P, Raichlen JS, Ballantyne CM, Davignon J, Erbel R, Fruchart JC, Tardif JC, Schoenhagen P, Crowe T, Cain V, Wolski K, Goormastic M, Tuzcu EM; ASTEROID Investigators. Effect of very high-intensity statin therapy on regression of coronary atherosclerosis: the ASTEROID trial. JAMA 2006;295:1556-65.

(183) Dixon JL, Stoops JD, Parker JL, Laughlin MH, Weisman GA, Sturek M. Dyslipidemia and vascular dysfunction in diabetic pigs fed an atherogenic diet. Arterioscler Thromb Vasc Biol 1999;19:2981-92.

(184) Egan BM, Stepniakowski K, Goodfriend TL. Renin and aldosterone are higher and the hyperinsulinemic effect of salt restriction greater in subjects with risk-factors clustering. Am J Hypertens 1994;7:886-93.

(185) Jaffe IZ, Mendelsohn ME. Angiotensin II and aldosterone regulate gene transcription via functional mineralocortocoid receptors in human coronary artery smooth muscle cells. Circ Res 2005;96:643-50.

(186) Sun Y, Ramires FJA, Weber KT. Fibrosis of atria and great vessels in response to angiotensin II or aldosterone infusion. Cardiov Res 1997;35:138-47.

(187) Yamashita R, Kikuchi T, Mori Y, Aoki K, Kaburagi Y, Yasuda K, Sekihara H. Aldosterone stimulates gene expression of hepatic gluconeogenic enzymes through the glucocorticoid receptor in a manner independent of the protein kinase B cascade. Endocr J 2004;51:243-51.

(188) Brown NJ. Aldosterone and vascular inflammation. Hypertension 2008;51:161-7.

(189) Caprio M, Newfell BG, la Sala A, Baur W, Fabbri A, Rosano G, Mendelsohn ME, Jaffe IZ. Functional mineralocorticoid receptors in human vascular endothelial cells regulate intercellular adhesion molecule-1 expression and promote leukocyte adhesion. Circ Res 2008;102:1359-67.

(190) Callera GE, Touyz RM, Tostes RC, Yogi A, He Y, Malkinson S, Schiffrin EL. Aldosterone activates vascular p38MAP kinase and NADPH oxidase via c-Src. Hypertension 2005;45:773-9.

(191) Gal D, Isner JM. Atherosclerotic Yucatan microswine as a model for novel cardiovascular interventions and imaging. In: Swindle MM, Moody DC, Phillips LD, editors. Swine as Models in Biomedical Research. 1 ed. Ames: Iowa State University Press; 1992;118-40.

(192) Johnson GJ, Griggs TR, Badimon L. The utility of animal models in the preclinical study of interventions to prevent human coronary artery restenosis: analysis and recommendations. Thromb Haemost 1999;81:835-43.

(193) Lowe HC, Schwartz RS, Mac Neill BD, Jang lK, Hayase M, Rogers C, Oesterle SN. The porcine coronary model of in-stent restenosis: current status in the era of drug-eluting stents. Catheterization and Cardiovascular Interventions 2003;60:515-23.

(194) Touchard AG, Schwartz RS. Preclinical restenosis models: challenges and successes. Toxicol Pathol 2006;34:11-8.

(195) Schwartz RS, Edelman ER. Drug-eluting stents in preclinical studies. Recommended evaluation from a consensus group. Circulation 2002;106:1867-73.

(196) Schwartz RS, Chronos NA, Virmani R. Preclinical restenosis models and drug-eluting stents: still important, still much to learn. J Am Coll Cardiol 2004;44:1373-85.

(197) Neely CF, DiPierro FV, Kong MH, Greelish JP, Gardner TJ. Adenosine receptor antagonists block ischemia-reperfusion injury of the heart. Circulation 1996;94 Suppl:376-80.

(198) Virmani R, Kolodgie FD, Farb A, Lafont A. Drug eluting stents: are human and animal studies comparable? Heart 2003;89:133-8.

(199) Jonas M, Edelman ER, Groothuis A, Baker AB, Seifert P, Rogers C. Vascular neointimal formation and signaling pathway activation in response to stent injury in insulin-resistant and diabetic animals. Circ Res 2005;97:725-33.

(200) Stone AA, Chambers TC. Microtubule inhibitors elicit differential effects on MAP Kinase (JNK, ERK, and p38) signaling pathways in human KB-3 carcinoma cells. Exp Cell Res 2000;254:110-9.

(201) Omura T, Yoshiyama M, Izumi Y, Kim S, Matsumoto R, Enomoto S, Kusuyama T, Nishiya D, Nakamura Y, Akioka K, Iwao H, Takeuchi K, Yoshikawa J. Involvement of c-Jun NH2 Terminal Kinase and p38MAPK in Rapamycin-Mediated Inhibition of Neointimal Formation in Rat Carotid Arteries. J Cardiovasc Pharmacol 2005;46:519-25.

(202) Christen T, Verin V, Bochaton-Piallat M, Popowski Y, Ramaekers F, Debruyne P, Camenzind E, van Eys G, Gabbiani G. Mechanisms of neointima formation and remodeling in the porcine coronary artery. Circulation 2001;103:882-8.

(203) Versluis M, van den Berge M, Timens W, Luijk B, Rutgers B, Lammers JW, Postma DS, Hylkema MN. Allergen inhalation decreases adenosine receptor expression in sputum and blood of asthma patients. Allergy 2008;63:1186-94.

(204) Nakav S, Chaimovitz C, Sufaro Y, Lewis EC, Shaked G, Czeiger D, Zlotnik M, Douvdevani A. Anti-Inflammatory preconditioning by agonists of adenosine A1 receptor. PLoS One 2008;3:e2107.

(205) Feoktistov I, Goldstein AE, Ryzhov S, Zeng D, Belardinelli L, Voyno-Yasenetskaya T, Biaggioni I. Differential expression of adenosine receptors in human endothelial cells: role of A2B receptors in angiogenic factor regulation. Circ Res 2002;90:531-8.

(206) Wyatt AW, Steinert JR, Wheeler-Jones CP, Morgan AJ, Sugden D, Pearson JD, Sobrevia L, Mann GE. Early activation of the p42/p44MAPK pathway mediates adenosine-induced nitric oxide production in human endothelial cells: a novel calcium-insensitive mechanism. FASEB J 2002;16:1584-94.

(207) Richard LF, Dahms TE, Webster RO. Adenosine prevents permeability increase in oxidant-injured endothelial monolayers. Am J Physiol Heart Circ Physiol 1998;274:H35-H42.

(208) Ryzhov S, Solenkova NV, Goldstein AE, Lamparter M, Fleenor T, Young PP, Greelish JP, Byrne JG, Vaughan DE, Biaggioni I, Hatzopoulos AK, Feoktistov I. Adenosine receptor-mediated adhesion of endothelial progenitors to cardiac microvascular endothelial cells. Circ Res 2008;102:356-63.

(209) Li J, Fenton RA, Wheeler HB, Powell CC, Peyton BD, Cutler BS, Dobson JG Jr. Adenosine A2a receptors increase arterial endothelial cell nitric oxide. J Surg Res 1998;80:357-64.

(210) Dubey RK, Gillespie DG, Jackson EK. A2B adenosine receptors stimulate growth of porcine and rat arterial endothelial cells. Hypertension 2002;39:530-5.

(211) Sexl V, Mancusi G, Baumgartner-Parzer S, Schütz W, Freissmuth M. Stimulation of human umbilical vein endothelial cell proliferation by A2-adenosine and beta 2-adrenoceptors. Br J Pharmacol 1995;114:1577-86.

(212) Kang E, Vedantham K, Long X, Dadara M, Kwon IK, Sturek M, Park K. A drug eluting stent for delivery of signal pathway-specific 1,3-dipropyl-8-cyclopentyl xanthine (DPCPX). Mol Pharm 2009;6:1110-7.

(213) Auchampach JA, Gross GJ. Adenosine A1 receptors, K_{ATP} channels, and ischemic preconditioning in dogs. Am J Physiol 1993;264:H1327-H1336.

(214) Lankford AR, Yang JN, Rose'Meyer R, French BA, Matherne GP, Fredholm BB, Yang Z. Effect of modulating cardiac A1 adenosine receptor expression on protection with ischemic preconditioning. Am J Physiol Heart Circ Physiol 2006;290:H1469-H1473.

(215) Wainwright CL, Parratt JR. Effects of R-PIA, a selective A1 adenosine agonist, on haemodynamics and ischaemic arrhythmias in pigs. Cardio Res 1993;27:84-9.

(216) Reiss AB, Rahman MM, Chan ES, Montesinos MC, Awadallah NW, Cronstein BN. Adenosine A2A receptor occupancy stimulates expression of proteins involved in reverse cholesterol transport and inhibits foam cell formation in macrophages. J Leukoc Biol 2004;76:727-34.

CURRICULUM VITAE

Xin Long

A. Education and Training

1997-2002	Degree	Bachelor of Medicine in Medicine
	Institution	Hunan Medical University. Changsha, Hunan, China
	Supervisor	Weiqiong Gu, MD
2002-2004	Degree	Master of Medicine in Medicine
	Institution	Second Xiang-Ya Hospital, Hunan Medical University. Changsha, Hunan, China
	Supervisor	Qingnan He, MD
2002-2004	Position	Research Assistant
	Institution	Institute of Endocrinology and Metabolism, Hunan Medical University. Changsha, Hunan, China
	Supervisor	Zhiguang Zhou, MD, PhD
2004-2010	Degree	PhD
	Institution	Dept of Cellular & Integrative Physiology, Indiana University. Indianapolis, IN
	Supervisor	Michael Sturek, PhD

B. Academic Activities and Honors

<u>Professional Membership</u>

2005-09	American Physiological Society
2006-09	Sigma Xi, the Scientific Research Society
2008-09	American Association of Anatomists

Poster Presentations and Talks

2006	Experimental Biology Conference SF, CA-Poster
2006	American College of Sports Medicine Conference, Indianapolis, IN-Poster
2008	Experimental Biology Conference SD, CA-Poster
2008	Annual Statewide Physiology Retreat Talk Indianapolis, IN
2009	Keystone Symposia-Dissecting the vasculature Vancouver, Canada-Poster
2009	Langman Platform Presentation Award finalist Experimental Biology Conference NO, LA
2009	Nano Drug Delivery Symposia, Indianapolis, IN-Poster

Mentorship

2008	Direct supervisor of summer undergraduate - Raven Elosiebo (M1)
2008-09	International peer mentor of new graduate students - Cong Xu, Jing Wan and Xuemei Guo

Honors

2002	First Class Prize in National Competition of Medicine, China
2004	University Fellowship, Indiana University
2006, 09	University Travel Fellowship, Indiana University
2008-09	American Heart Association Predoctoral Fellowship
2009	Education Enhancement Travel Grant, Indiana University
2009	Keystone Symposia Travel Scholarship, NIDDK
2009	Students Travel Award, American Association of Anatomists

C. Abstracts and Manuscripts

Abstracts

1. Long X, Lloyd PG, Sheehy AJ, Mokelke EA, and Sturek M. Bare metal stents increase mitogenic receptor gene expression in coronary artery of Ossabaw pig model of the metabolic syndrome. FASEB Journal 20:A699, 2006.

2. Long X, Edwards JM, Lloyd PG, Mokelke EA, and Sturek M. Activation of adenosine A1 receptors induces coronary smooth muscle cell proliferation in an in vitro model of atherosclerosis. Med Sci Sports Exercise 38:S34, 2006.

3. Long X, Edwards JM, Neeb ZP, Alloosh M, and Sturek M. Upregulation of Adenosine A1 Receptor in Coronary Atherosclerosis in the Metabolic Syndrome and in the in Vitro Organ Culture Model of Coronary Atherosclerosis. FASEB Journal, 22:924.1, 2008.

4. Kang E, Vedantham K, Long X, Dadara M, Kwon I-K, Sturek M, and Park K. Stent for delivery of 1,3-dipropyl-8-cyclopentyl xanthine (DPCPX)-a signaling pathway specific drug. J Control Release, 2008.

5. Long X, Elosiebo R, Sturek M. Importance of Adenosine A1 Receptors and ERK1/2 Signaling in Coronary Atherosclerosis and In-stent Stenosis. Keystone Symposia, 2009.

6. Neeb Z, Long X, Sturek M. Store-operated Ca^{2+} influx in coronary smooth muscle cells predicts coronary atherosclerosis in the metabolic syndrome. Keystone Symposia, 2009.

7. Long X, Elosiebo R, Sturek M. Role of Adenosine A1 Receptors and P2Y2 Receptors and ERK1/2 Activation in Coronary Atherosclerosis and In-stent Stenosis. FASEB Journal, 2009.

8. Neeb ZP*, Long X*, Mokelke EA, Edwards JM, Alloosh M, and Sturek M (*Authors equally contributed to this work). Adenosine A2a/b receptor-mediated vasodilation is antagonized by adenosine A1 receptor in coronary circulation of healthy Ossabaw swine. FASEB Journal, 2009.

9. Long X, He Y, Kitsongsermthon J, Park K, Sturek M. Novel drug-eluting stents to reduce coronary in-stent stenosis in a porcine model of metabolic syndrome. NanoDDS Symposia, 2009.

10 Long X, Alloosh M, Kitsongsermthon J, He Y, Park K, Sturek M. Adenosine A1 receptor elicits coronary in-stent stenosis in metabolic syndrome. FASEB Journal, 2010.

Manuscripts

1. Feng Q, Zhou ZG, Tang WL, Yang XL, Long X. Comparison of 3 working definitions of metabolic syndrome in male medical examinees. Zhong Nan Da Xue Xue Bao Yi Xue Ban 30:130-4, 2005.

2. Edwards JM, Alloosh MA, Long X, Dick GM, Lloyd PG, Mokelke EA, Sturek M. Adenosine A1 receptors in neointimal hyperplasia and in-stent stenosis in Ossabaw miniature swine. Coron Artery Dis 19:27-31, 2008.

3. Bender SB, Tune JD, Borbouse L, Long X, Sturek M, Laughlin MH. Altered mechanism of adenosine-induced coronary arteriolar dilation in early-stage metabolic syndrome. Exp Biol Med 234:683-692, 2009.

4. Kang E, Vedantham K, Long X, Dadara M, Kwon I-K, Sturek M, and Park K. A drug eluting stent for delivery of signal pathway-specific 1, 3-dipropyl-8-cyclopentyl xanthine (DPCPX). Mole Pharm 6:1110-7, 2009.

5. Edwards JM, Neeb ZP, Alloosh MA, Long X, Bratz IN, Peller CR, Byrd JP, Kumar S, Obukhov AG, Sturek M. Exercise training decreases store-operated Ca^{2+} entry associated with metabolic syndrome and coronary atherosclerosis. Cardiovasc Res 85:631-40, 2010.

6. Long X, Bratz IN, Edwards JM, Alloosh M, Sturek M. Short-term exercise training prevents micro- and macrovascular disease following coronary stenting. J Appl Physiol (In revision).

7. Long X, Mokelke EA, Neeb ZP, Alloosh M, Edwards JM, Sturek M. Adenosine receptor regulation of coronary blood flow in Ossabaw miniature swine (In preparation).

8. Long X, Elosiebo R, Neeb ZP, Byrd JP, Alloosh M, Sturek M. Aldosterone regulation of adenosine A1 receptors in coronary atherosclerosis in metabolic syndrome (In preparation).

9. Long X, Alloosh M, Kitsongsermthon J, He Y, Park K, Sturek M. Adenosine A1 receptor antagonism attenuates coronary in-stent stenosis in metabolic syndrome (In preparation).